Numerical Modelling of Offshore Pipeline Flotation during Sand Backfilling

Development and validation of a simplified predictive model

L.W. Stelling

MSc. Thesis Geo-Engineering
Delft University of Technology
Faculty of Civil Engineering and Geosciences

TU Delft

Van Oord
Marine ingenuity

Numerical Modelling of Offshore Pipeline Flotation during Sand Backfilling

Development and validation of a simplified predictive model

by

L.W. Stelling

to obtain the degree of Master of Science
at the Delft University of Technology,
to be defended publicly on Monday October 31, 2022.

Student number: 4491181
Date: 24-10-2022
Thesis committee:

Dr. ir. W. Broere,	TU Delft, chair
Dr. ir. F. Pisanò,	TU Delft, supervisor
Ir. W. J. Karreman,	Van Oord, supervisor
Ir. E. F. Uelman,	Van Oord, supervisor
Dr. ir. G. Della Vecchia,	Politecnico di Milano, supervisor
Dr. ir. F. Cecinato,	Università degli studi di Milano, supervisor

TU Delft

Van Oord
Marine ingenuity

Preface

This master thesis represents my final product of the master Geo-Engineering at the faculty of Civil Engineering and Geosciences at the TU Delft. This thesis has been conducted in collaboration with Van Oord and has had valuable input from the University of Milan and the Polytechnic University of Milan.

In the first week of my bachelor at Utrecht University we, the students, had to come up with a “Earth Science related” homemade experiment. At that time I decided to collect three types of sediment: small pebbles, beach sand and potting soil and pour a small hand full into a large transparent vase. I timed how long it took for all the material to settle and wrote a small report on it. I am sure it wasn’t a scientific masterpiece at the time. Little did I know that six years after, I would graduate from the TU Delft where the settling of fine sand grains would be a major part in my masters thesis.

I would like to thank my supervisors Dr. ir. Wout Broere, Dr. Federico Pisanó, Dr. ir Gabriele Della Vecchia and Dr. ir Francesco Cencinato for their time, energy, feedback and fruitful discussions. Moreover I would like to express my gratitude to Ir. Wouter Karreman and Ir. Evert Uelman from Van Oord for the delightful weekly meetings and advice during this project. Also a word of thanks to Pippi Eikhout for willing to answer all the questions regarding her work on this subject. The input of all mentioned above made this research project possible.

Last but not least, I would like to thank my friends and family for their support, interest and distraction in the sometimes lonesome research work.

Lennart Stelling
October, 2022

Abstract

Offshore pipelines are considered the arteries of the offshore oil and gas industry and transport hydrocarbon products as well as other fluids. During the installation process of an offshore pipeline, the pipeline is most often located in a trench and covered with backfill material. The burial of the pipeline ensures onbottom stability as well as mechanical protection. With a Trailer Suction Hopper Dredger (TSHD) sand can be deposited in the trench, thereby covering the pipeline in a relatively controlled manner. One major risks associated with this backfilling method is the risk of vertical upward displacement of the pipeline during the backfilling process. The vertical upward movement of the pipe is referred to as pipeline flotation and may result in unprotected or damaged pipes. With the rising use of small diameter and lighter pipelines this risk has become more prevalent.

Pipeline flotation is induced by augmented buoyancy which originates from the presence of the water-sand mixture around the pipeline. The particle concentration of the water-sand mixture and the embedment rate of the pipe are leading in the assessment of the buoyancy force acting on the pipeline. The weight of the pipeline is the major force counteracting buoyancy force. In addition, a friction force, resulting from the contact between the pipe and the new formed sand layer around the pipe, counteracts the buoyancy force.

The aim of this research is to develop and validate a simplified numerical model for the analysis of offshore pipeline flotation during sand backfilling with a TSHD. The numerical model has been validated against the small-scale physical experiments of Eikhout (2021). The small-scale physical experiments have been developed and used by Yang (2020) and Eikhout (2021) to simulate a simplified sand backfilling process.

The numerical model is developed to simulate the sedimentation process and has been developed in the finite element software COMSOL Multiphysics. The model is capable of effectively simulating the simplified backfilling process from the small-scale experiments by Eikhout (2021). Moreover, the sedimentation model is able to simulate the inflow of material over time in the physical domain. The sedimentation process has been modelled with a convection equation in which the settling velocity of the water-sand mixture is described with the hindered settling formulation proposed by Metha (1986). The hindered settling formulation describes the velocity of the suspension as a function of its local particle concentration. The numerical data has been processed and used in a force balance which is able to predict the occurrence or absence of pipeline flotation.

The parameters in the hindered settling formulation as well as the numerical settings have been described from a theoretical perspective as well as their practical impact on the numerical solution. After validation against the small-scale physical experiments the numerical model has been used to simulate a more practical scenario. In addition a simplified, spreadsheet friendly, calculation method is proposed.

Contents

List of Tables

List of Figures

Nomenclature

Abbreviations

CFL-condition	Courant, Friendrichs and Lewy condition
DP	Differential pressure sensor
PDE	Partial differential equation
RZ-exponent	Richardson-Zaki exponent
SG	Specific gravity
SOD	Stand-off distance
TP	Tuning parameter
$TSHD$	Trailing suction hopper dredger

Symbols

A_{eff}	Effective cross-sectional area of the pipe
A_{pipe}	Cross-sectional area of the pipe
A_{seg}	Area of a pipe-segment
C_1	Constant for particle settling velocity
C_2	Shape factor for particle settling velocity
C_u	Uniformity coefficient
D	Diameter of the pipe
D_f	Diffusion coefficient
F_b	Buoyancy force
$F_{b,seg}$	Buoyancy force acting on a pipe segment
H	Height physical domain
H_{res}	Reservoir height
H_{sed}	Height new formed sand layer
H_{sol}	Solid height
H_{trans}	Height transition layer

L	Length of the experimental tank
N	Normal force
M_{sol}	Mass of solids discharged
P_{atm}	Atmospheric pressure
Q_{dis}	Discharge flow rate
R	Submerged specific gravity particle
Re	Reynolds number
S	Particle flux
T	Friction force
T_{dis}	Discharge time
V	Buoyant weight of the pipe
$V(c)$	Local wave velocity
V_{dis}	Discharged volume
V_{sol}	Volume of solids discharged
V_v	Volume of voids
W	Width of the experimental tank
W_p	Weight of the pipe
Z	Characteristic curve
a	Absorption coefficient
c	Volumetric particle concentration
c_0	Initial volumetric particle concentration
c_{dis}	Discharge concentration
c_{domain}	Domain concentration
c_{max}	Maximum domain concentration
c_{phase}	Phase transition concentration from fluid to soil
d	Diameter particle
d_{10}	Cumulative 10% of the diameter of the sand particles
d_{50}	Median diameter of the sand particle

d_{60}	Cumulative 60% of the diameter of the sand particles
d_a	Damping coefficient
e	Void ratio
f	Source term
g	Gravitational acceleration
n	Exponent hindered settlement formulation
n_{mix}	Porosity of the water-sand mixture
t	Time
vs	Terminal settling velocity
$v(c)$	Hindered settling velocity
z	Height dimension
w	Embedment rate
α	Empirical parameter
α_c	Conservative flux convection coefficient
β	Semi-angle subtended by the contact surface of the sedimentation front
β_c	Convection coefficient
θ	Inclination from vertical
μ	Friction coefficient
μ_{dyn}	Dynamic viscosity
ρ_f	Density fluid
ρ_m	Density water-sand mixture
ρ_p	Density pipe
ρ_s	Density sand grain
ρ_w	Density water
σ_r'	Normal effective stress on the pipe-soil contact surface
υ	Kinematic viscosity
ξ	Total number of particles

1 Introduction

1.1. Background

Pipelines are the arteries of the offshore oil and gas industry. The offshore pipelines transport the hydrocarbon product and other fluids between wells and in-field processing facilities, as well as transporting the product to the shore (Randolph and Gourvenec, 2011). A pipeline is a fixed asset with large capital costs. Once the pipeline is in place, however, the operation and maintenance costs are relatively small, and the pipeline has an operating life of 40 years or more (Palmer and King, 2008). This makes offshore pipelines a safe, fast and economically convenient connection between offshore and onshore facilities (Bizzotto et al., 2017).

Trenching and backfilling of pipelines and cables is required to provide mechanical protection in regions where fishing and ship anchoring operations are present (Bizzotto et al., 2017). Moreover, burial of the pipeline ensures onbottom stability against environmental forces (Finch and Machin, 2001). In addition, the burial contributes to the pipeline's thermal insulation which is mainly relevant in cold regions and for pipelines that transport oil or other hot products (Finch, 1999).

In recent years small diameter, steel pipelines, linking remote subsea fields to existing infrastructure have become increasingly common. These pipelines are often relatively light due to significant insulation systems and are required to transport hydrocarbons under very high temperature and pressure (Finch and Machin, 2001). Another reason for the decrease in weight of the pipelines is that less raw materials are needed in the production of the pipeline. This makes lighter pipelines economically viable.

1.2. Problem description

With the rise of the small diameter and lighter pipelines the, relatively new, phenomenon of pipeline flotation during the installation process has become more prevalent. Pipeline flotation during backfilling is the vertical displacement of a pipeline which may occur during the backfilling process. Excessive vertical displacements can lead to unprotected or damaged pipes (Figure 1.1). The costs and time needed to restore and re-cover the pipeline are often significant and is something that is to be avoided. With a Trailer Suction Hopper Dredger (TSHD) sand can be deposited in the trench, thereby covering the pipeline in a relatively controlled manner. Common practice is to backfill the trench in layers at a time in order to minimize the risk of pipeline flotation. However, little is known about the optimal way of backfilling in layers and its relationship with the flotation risk.

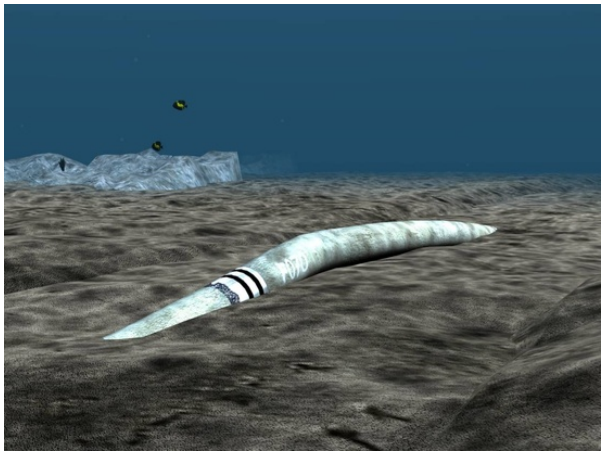

Figure 1.1: Pipeline resurfacing

1.3. Objective and research questions

The aim of this research is to develop and validate a simplified numerical model for the analysis of offshore pipeline flotation during sand backfilling with a Trailer Suction Hopper Dredger. In order to develop the model, a good understanding of the mechanism of pipeline flotation is necessary as well as good understanding on the influence of different variables and assumptions implemented in the numerical model. The numerical model will be validated against experimental data. The experimental data concern the simulation of a simplified backfilling process in a small-scale experimental set-up, developed and used by Yang (2020) and Eikhout (2021). This thesis will describe the set-up of a simplified numerical pipeline flotation model and describe it's potential as well as its uncertainties and limitations.

In order to reach the objective the following research questions need to be addressed:

1. What forces can be identified which contribute to the force balance of the pipeline?
2. How can the sedimentation process of sand particles in a dispersion best be modelled?
3. What is the influence of different variables in the hindered settlement formulation on the sedimentation process as well as on the buoyancy development?
4. How can the transition from a water-sand mixture to a solid sandy soil best be modelled?
5. How can the inflow of sediment, both uniform and non-uniform, best be modelled?

1.4. Research outline

- In Chapter 2 the engineering background will be provided. In this chapter, the backfilling process with a TSHD and the forces acting on the pipeline during this process will be discussed.
- In Chapter 3 the sedimentation theory will be described in detail. Moreover, a sedimentation problem from the literature has been validated analytically.
- In Chapter 4 more theoretical background will be provided on the numerical modelling and the finite element program COMSOL Multiphysics. Two sedimentation models from the literature have been validated numerically and the outline of the sedimentation model used to simulate the simplified backfilling experiments will be provided.
- In Chapter 5 background regarding the small-scale experiments will be provided first, which will also be linked to the implementation in the numerical model. This chapter also includes the results and analyses.
- In Chapter 6 uncertainties and limitations of the proposed numerical model will be highlighted.
- The conclusions and recommendations are given in chapter 7

2

Engineering Background

In Section 2.1 the process of backfilling a subsea trench with a Trailer Suction Hopper Dredger will be discussed. In Section 2.2 the theory behind the force balance of the pipe during the backfilling process will be covered.

2.1. Backfilling process with a Trailer Suction Hopper Dredger

When the pipeline is placed, the subsea trench can be backfilled with sand with different methods, one of the methods being with a TSHD. This technique allows for the controlled release of the material and limits the turbidity of the surrounding waters. Before discharging, pumps and water jets will liquefy the sandy material present in the vessels hold. The water-sand mixture will be pumped through the suction pipe to drag head, from where the sediment mixture is discharged. A schematized figure of a TSHD from Van Oord is displayed in figure 2.1. The process of discharging the sediment mixture is schematized in figure 2.2.

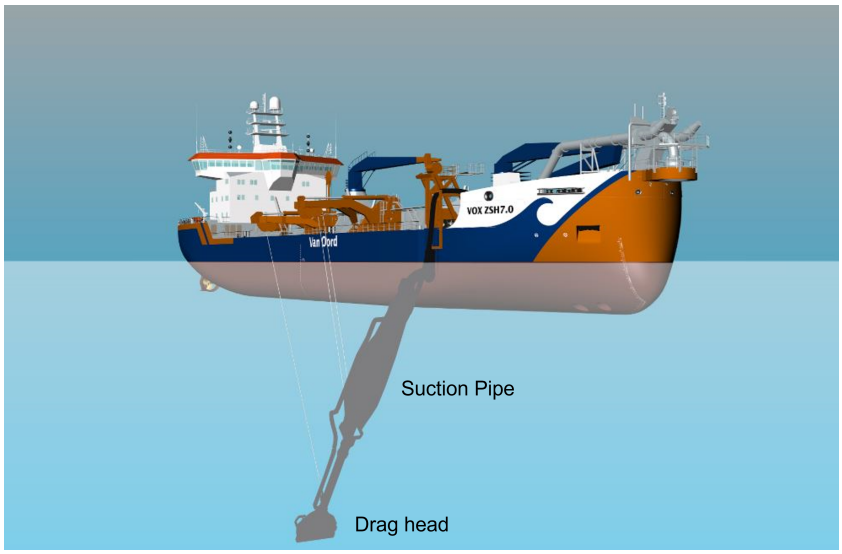

Figure 2.1: TSHD from Van Oord and its primary components

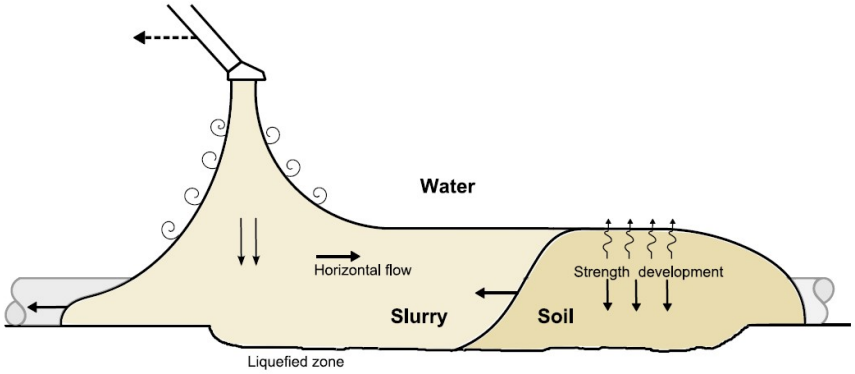

Figure 2.2: Schematic illustration of the backfilling along the pipe. The vessel in this illustration is moving from right to left (after Biemans, 2012)

Different kind of fluxes determine the behaviour of the sediment plume after leaving the suction head. This behaviour has been described with two different fluxes by de Nijs (2009): the momentum flux and the buoyancy flux. A discharge with no buoyancy is referred to as a ”non-buoyant jet” or ”jet”. A release of buoyancy only (no initial momentum) is called a ”plume”. The jet characteristics are schematized in figure 2.3. A discharge with both momentum and buoyancy is called a ”buoyant jet” or ”forced plume”. The buoyant discharge is diluted due to entrainment of surrounding ambient fluid into the discharge plume (de Nijs et al., 2009).

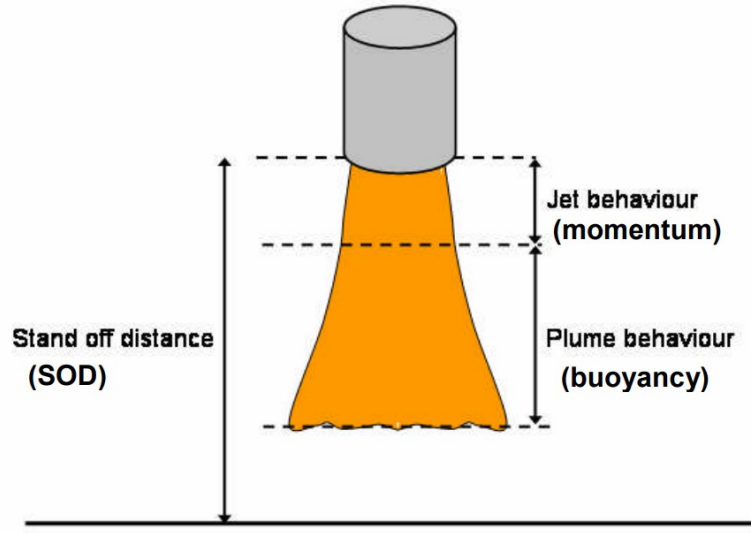

Figure 2.3: Graphical illustration of the jet characteristics (after de Nijs et al., 2009)

In order to limit the risk of pipeline flotation the trench is not backfilled at once, but is instead backfilled in layers. This means that multiple passages are required by the vessel to cover the pipeline. Logically, the backfilling process takes longer when the height of each backfilled layer is small and hence more passages are required to fully cover the pipe.

During the process the first backfill layers are deemed critical because the effective area on which the buoyancy force acts is largest. As the pipe is increasingly embedded the effective area decreases and thereby the risk of flotation is expected to reduce.

In practice, several parameters influence the backfilling process. The discharge concentration and discharge velocity will be kept constant as much as possible. The trailing speed of the vessel then determines the thickness of the new sediment layer. Another influential parameter is the stand off dis-

tance (SOD); the distance between the suction head and the seabed. A too small SOD can result in erosion around the pipeline as well as possible damaging the pipe. A too large SOD, however, may result in sediment losses as a result of currents. From the experience of several marine contractors, a SOD of approximately 5 meter was found to be optimal (Burgmans, 2005).

2.2. Force balance of the pipeline

The forces and processes acting on the pipe which are discussed in this section are based on a one-dimensional force balance. Additional effects and forces which might be relevant in assessing three-dimensional, more realistic scenarios, are shortly listed at the end of this section but not included in the numerical flotation model.

2.2.1. Selfweight of the pipe

The main downward force is the self weight of the pipe. This force ensures that the pipe will remain on the seafloor if the conditions are at rest (Eikhout, 2021). As mentioned in the introduction, reduction of the pipe diameter and thermal isolation around the pipeline drastically lowered the weight of the pipe over the past decades. In this study the length-dimension is not taken into account, therefore it is convenient to express all forces considered as the force per unit length. Moreover, the negative direction of forces is considered to be downwards. For the self weight of the pipe this force can be determined with equation 2.1:

$$W_p = -A_{pipe} * \rho_p * g \tag{2.1}$$

where A_{pipe} is the cross-sectional area of the pipe, ρ_p is the average density of the pipe and g is the gravitational acceleration. Note that this force thus has the unit [N/m].

2.2.2. Buoyancy force

The submerged pipe is subjected to the buoyancy force induced by the water. During the backfilling process, the suspended sand particles in the domain induce additional buoyancy as the density of the soil-water mixture has increased with respect to the density of water. Moreover, the discharge rate exceeds the sedimentation rate; resulting in concentration building up around the pipeline (Eikhout, 2021). The density of the water-sand mixture thus depends on the density of water (fresh- or saltwater), the density of the sand grains and the particle concentration. The particle concentration of the mixture is presented as the volume fraction of the solids (the volume of solids per total volume of the water-sand mixture $= \frac{V_{sol}}{V_{mix}}$) or as volume percent (equals volume fraction x100%). The volume fraction can be related to the void ratio and porosity of the water-sand mixture:

$$e = \frac{V_v}{V_{sol}} \tag{2.2}$$

$$c = \frac{1}{1+e} \tag{2.3}$$

$$c = 1 - n_{mix} \tag{2.4}$$

in equation Eq.2.2, Eq.2.3 and Eq.2.4; V_v is the volume of voids, V_{sol} is the volume of solids, e is the void ratio of the mixture [-], c is the volume concentration [-] and n_{mix} is the porosity water-sand mixture [-].

Based on the above mentioned variables an equivalent fluid density of the water-sand mixture can be expressed as:

$$\rho_m = \rho_w * (1-c) + \rho_s * c \tag{2.5}$$

where ρ_m is the density of the water-sand mixture, ρ_w is the density water and ρ_s is the density of the sand grains. The buoyant force per unit length is expressed in equation 2.6:

$$F_b = A_{pipe} * \rho_m * g \tag{2.6}$$

Besides the density of the water-sand mixture the area on which the buoyancy force acts is of importance in assessing this force. This area reduces as the embedment of the pipe increases. During the backfilling process, sedimentation takes place. The sedimentation causes the pipeline to become embedded in the new formed sand layer around the pipe, of which the top is called the sedimentation front. The consolidation period of the new sand layer is expected to very small. As a result no excess pore water pressures are expected in the new sand layer and therefore the assumption that this new formed layer only exerts buoyancy induced by water, can be justified. The additional buoyancy force, induced by the suspension, now only works on the part of the pipe that is above the sedimentation front; this is called the effective area of the pipeline (Figure 2.4).

The equation to calculate the buoyancy force for a partly embedded pipe thus becomes:

$$F_b = A_{eff} * \rho_m * g + (A_{pipe} - A_{eff}) * \rho_w * g \tag{2.7}$$

where A_{eff} is the effective cross-sectional area of the pipe, which will decrease over time as the sedimentation front moves upward.

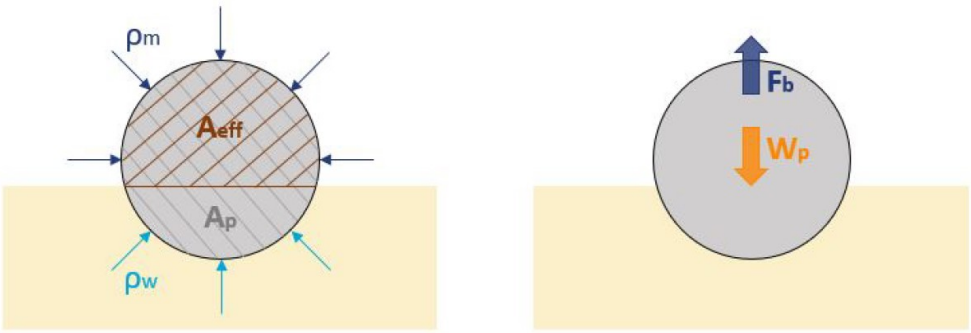

Figure 2.4: Schematic drawing of a one-dimensional section of the pipeline, which is partially embedded and fully surrounded by the sand-water mixture above the sedimentation front (after Eikhout, 2021)

2.2.3. Friction induced by the new formed sand layer

As the pipeline gets embedded, interaction forces will be present between the pipeline and the soil. One of the interaction forces assessed to be potentially relevant is the friction force induced by the new formed sand layer. According to White and Randolph (2007), the assumption can be made that the normal effective stress on the pipe-soil contact depends on the amount of embedment of the pipe. The normal effective stress on the pipe-soil contact surface (σ_r') can be approximated following the elastic solution for a line load acting on a half-space (White and Randolph, 2007) (Eq.2.8).

$$\sigma_r' = \frac{V}{D} * \frac{2\cos\theta}{\beta + \sin\beta + \cos\beta} \tag{2.8}$$

where V is the buoyant weight of the pipe, D is the diameter of the pipe, θ is the inclination form the vertical, β is the semi-angle subtended by the contact surface of the sedimentation front (Figure 2.5) (Eikhout, 2021).

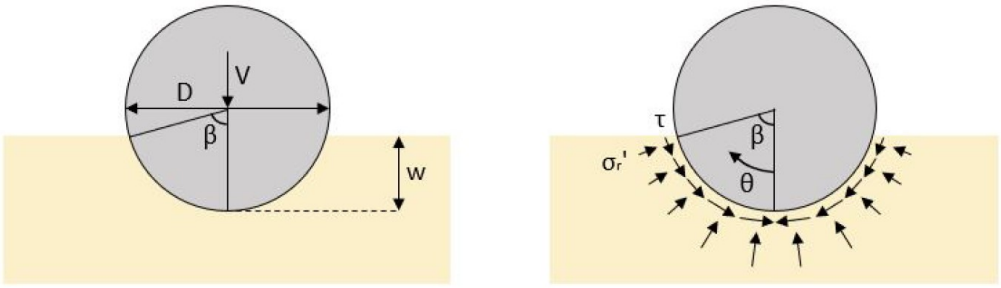

Figure 2.5: Schematisation of the pipe-soil contact stresses (after Eikhout, 2021)

The resulting buoyant weight of the pipe (V) is a function of the weight of the pipe and the buoyancy force acting on the pipe (Eq.2.10). The buoyant weight of the pipe (V) thus varies over time.

$$V = W_p + F_b \tag{2.9}$$

In order to calculate the friction force, the normal force (N) should be derived from the vertical force (V). Due to the curved surface, the normal force is enhanced as the embedment increases. The formula suggested by White and Randolph (2007), is:

$$N = V * \frac{2 * \sin\beta}{\beta + \sin\beta + \cos\beta} \tag{2.10}$$

where

$$\beta = \arccos\left(1 - \frac{w}{D}\right) \tag{2.11}$$

in which w is the height of the new formed sand layer around the soil and D the diameter of the pipeline.

The friction force (T) can be calculated with the pipe-soil friction coefficient (μ) and the normal force N.

$$T = -\mu * N \tag{2.12}$$

The effective stresses present are much lower compared to typical geotechnical stress-values. White and Randolph (2007) suggested a formulation for the residual friction coefficient for low normal effective stress levels (2 to 5kPa); a trend which has been obtained from ring shear test data of West African clay (Equation 2.13). According to White and Randolph (2007), the friction coefficient at these low stress levels is significantly larger compared to typical geotechnical values.

$$\mu = 0.25 - 0.30 * \log\left(\frac{\sigma_r'}{P_{atm}}\right) \tag{2.13}$$

In this equation, the normal effective stress (σ_r') is normalised by the atmospheric pressure (P_{atm}). Because this formulation was derived from data regarding clay it was chosen to retain a more 'regular' pipe-soil friction coefficient; a friction coefficient independent of the normal effective stress for sand-steel is approximately 0.60 (Uesugi et al., 1988). An analysis, presented in Chapter 6, further elaborates on this subject.

2.2.4. Other identified forces

When assessing more realistic, three dimensional cases, the force balance is expected to entail more forces. Forces which might contribute to the flotation of the pipeline are:

- Currents: exerting a force mainly in lateral direction;
- (Local) turbulence, which might be induced by the geometry of the trench: exerting a force in upward direction;
- Inflow of additional material: this could result in an additional increase in the particle concentration around the pipe and therefore induce additional buoyancy.

Forces which may be present and counteract the upward movement of the pipe are:

- Structural restoring forces which are associated with the continuity of the three-dimensional pipe. In reality a vessel is trailing over the full length of the pipe, thereby discharging only locally. When the buoyancy induces local upward movement, this movement is expected to be restricted by the bending moment;
- Suction force: when the upward motion starts, the pipe looses contact with the soil and a small area between the soil and the pipe will develop. Initially this space is a vacuum, however, pore water will flow towards this space. For a brief moment negative pore water pressures might hinder the upward movement of the pipe. Whether or not this force might be present depends on a number of factors such as the permeability of the seabed and fill-material as well as the velocity with which the pipeline moves in upward direction. Moreover, this force is expected to be more relevant as the embedment rate increases and thus the contact area between the pipe and the soil increases.

3

Sedimentation

In this chapter the theory behind sedimentation will be discussed. As discussed in Chapter 2, the buoyancy force is to a large extent dependent on the particle concentration of the mixture; which varies over time and space. Therefore, a good understanding and mathematical description of the sedimentation process is necessary to assess the concentration development around the pipe and thereby evaluate the buoyancy force acting on the pipeline over time.

First, single particle settling will be discussed, after which the settling of a dispersion will be elaborated upon. The basis of the sedimentation theory for particles in a dispersion comes from Kynch (1951). In more recent years, different researchers suggested slightly modified hindered settling formulations and different optimal parameters for different cases. In this Chapter information will be provided on Kynch's theory, modified versions of the hindered settling formulation and the physical meaning of the parameters parameters in the hindered settling formulation. Moreover, the analytical solution of a sedimentation sedimentation problem from the literature will be presented.

3.1. Settling velocity of a single particle

The settling velocity of a single particle is given by its terminal velocity (vs). In this section two widely used and accepted mathematical formulations are presented with which the terminal velocity of a single particle can be calculated. For spherical, massive particles like sand, Stokes found that:

$$vs = \frac{(\rho_s - \rho_f) g * d^2}{18 * \mu_{dyn}} \tag{3.1}$$

where ρ_s is the density of a sand particle, ρ_f the density of the fluid, μ_{dyn} the dynamic viscosity of the fluid, d the particle diameter and g the acceleration of gravity.

Ferguson and Church, 2004, suggested a different equation for the particle's fall velocity:

$$vs = \frac{R * g * d^2}{C_1 * \upsilon + \sqrt{0.75 * C_2 * R * g * d^3}} \tag{3.2}$$

where υ is the kinematic viscosity of the liquid, C_1 and C_2 are constants with values 18 and 1 respectively and R denotes the submerged specific gravity of the particle:

$$R = \frac{(\rho_s - \rho_f)}{\rho_f} \tag{3.3}$$

For small particle diameters the solution of Ferguson and Church converges to Stokes' law. For particle sizes in the particle size range of fine sand and medium sand, both solutions diverge as can be seen in figure3.1.

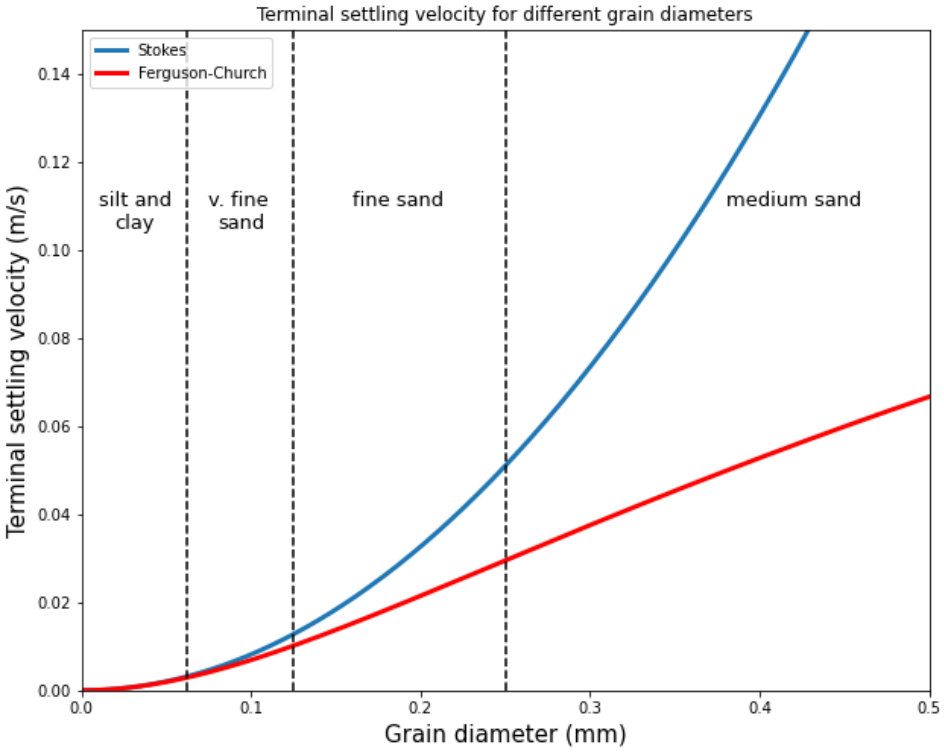

Figure 3.1: Settling velocity depending on grain size and calculation method

3.2. Speed of fall of particles in a dispersion

Kynch (1951) derived a theory of sedimentation based on the fundamental assumption that the speed of fall of particles in a dispersion is determined by the local concentration of particles. This kind of settling is known as hindered settling. Hindered settling is thus caused by the influence of neighbouring particles on the settling velocity of an individual particle within a suspension (Winterwerp, 2002).

Kynch assumed that a first order partial differential equation controlled the entire sedimentation process. His equation is based on a continuity balance and a sedimentation velocity being a unique function of solid particulate concentration (Tiller, 1981). The hindered settling formulation assumes that the settling velocity is a decreasing function of the local sediment concentration. The suggested hindered settling formulation by Kynch is:

$$v(c) = vs * (1 - \alpha * c) \tag{3.4}$$

where $v(c)$ is the hindered settling velocity depending on the local sediment concentration, c is the particle concentration as volume fraction, vs is the terminal velocity of a single particle and α is an empirical parameter with a suggested value of 2.5 for hard spheres.

Together with a hindered settlement formulation Kynch introduced the particle flux S, which is the number of particles crossing a horizontal section per unit area per unit of time (Kynch, 1951). The particle flux is equal to the settling velocity $v(c)$ times the local concentration (Eq.3.5).

$$S = v(c) * c \tag{3.5}$$

The particle flux is thus a function of the local concentration as well as the local velocity of the particles, which in itself is a function of the local concentration. Since along a horizontal layer, the concentration is assumed the same, the particle flux does not vary along this horizontal layer. However, if the concentration in a column (where the vertical position is indicated with z) is not constant, the particle flux

(S) also varies along the height of this column. Considering a segment in this column where there is a difference between the inflow of particles and the outflow of particles then accumulation of particles is present within this segment. Put differently; the concentration of particles will built up over time in the segment. With the particle flux, the continuity equation can be written as:

$$\frac{\partial c}{\partial t} = \frac{\partial S}{\partial z} \tag{3.6}$$

where t is time and z is the vertical coordinate, positive in downward direction.

The derivative of the particle flux over the concentration (Eq. 3.7) provides the local wave speed ($V(c)$), which should not to be confused with the settling velocity ($v(c)$). The wave velocity is useful for obtaining the solution analytically since it represents lines of equal concentration in the ($z-t$)-space. This will be discussed in more detail in Section 3.2.1.

$$V(c) = -\frac{dS}{dc} \tag{3.7}$$

In a different form the equation governing hindered settlement can thus be written as:

$$V(c) * \frac{\partial c}{\partial z} + \frac{\partial c}{\partial t} = 0 \tag{3.8}$$

Critical assumptions in Kynch' theory are:

- The particle concentration is uniform across any horizontal layer;
- The initial concentration increases towards the bottom of the dispersion;
- The settling velocity tends to zero as the concentration goes to its maximum value.

Kynch (1951) analysed several modes of sedimentation depending on the flux function (S) and therefore depending on the hindered settlement formulation ($v(c)$). In particular, the theory shows that layers may exist in the dispersion where the value of the concentration changes abruptly and that these discontinuities are responsible for linear and non-linear settling modes (Pane and Schiffman, 1985). The focus is on three different modes of sedimentation as are described by Bustos et al. (1999). Definition sketches of the three modes are displayed in Figure3.2 and described in more detail below ((Biemans, 2012), (Bustos et al., 1999), (Bürger and Tory, 2000), (Dankers, 2006), (Minico, 2020)).

- MS1: This is a pure hypothetical sedimentation mode which describes a concentration jump from zero concentration to c_0 (the initial particle concentration) and another concentration jump from c_0 to c_{max}, the maximum volumetric concentration of a consolidated soil (Dankers, 2006).
- MS2: A concentration jump from a zero concentration to c_0 is followed by a sudden change from c_0 and then increases gradually to c_{max}.
- MS3: The concentration jumps to c_0 after which it gradually increases to c_{max}.

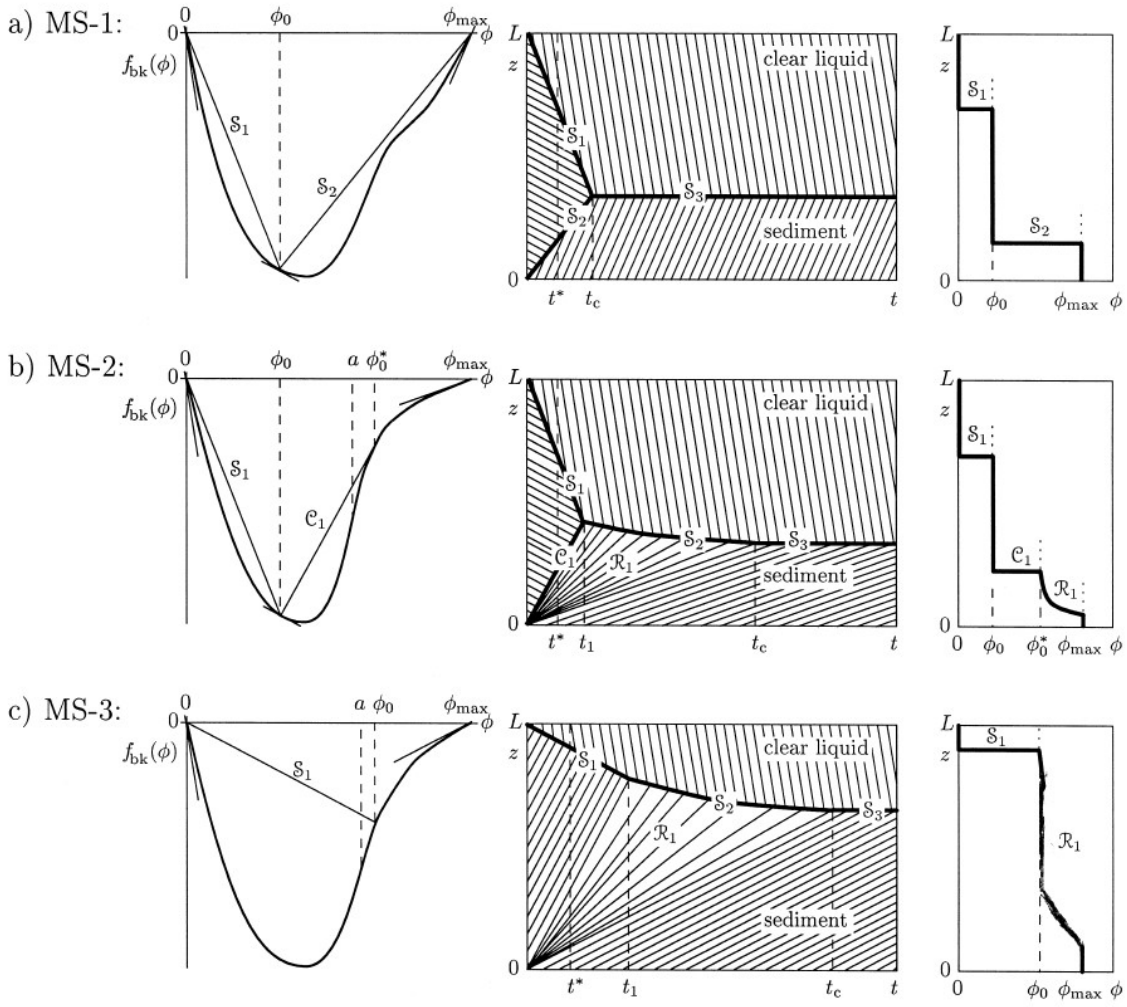

Figure 3.2: Modes of sedimentation MS-1 to MS-3. From the left to the right, the flux plot, the settling plot showing characteristics and shock lines, and a representative concentration profile at a certain time (after Bürger and Tory, 2000).

3.2.1. Method of characteristics

The sedimentation problem as described in the previous section can, in some cases (i.e., in absence of in-outflow of material), be solved analytically. Equation 3.6 is a one dimensional wave equation which can be solved analytically by means of the method of characteristics (Salsa, 2008).

In the method of characteristics, one makes use of characteristics curves. Characteristics curves are lines along which the concentration is constant and are therefore also called iso-concentration lines. Characteristics are curves $Z = z_c(t)$ in the space of independent variables (z, t), the so-called $(z - t)$-plane, on which the solution c is constant (Zijlema, 2015).

One can verify that c on these curves is constant by differentiating $c(z_c(t), t)$ with respect to t as follows:

$$\frac{dc}{dt} = \frac{\partial c}{\partial z} * \frac{dz_c}{dt} + \frac{\partial c}{\partial t} = V(c) * \frac{\partial c}{\partial z} + \frac{\partial c}{\partial t} = 0 \tag{3.9}$$

On a graph where position z is plotted against time t, curves can be drawn through points with the same value of concentration (Kynch, 1951). The coordinates (z, t) and $(z + dz, t + dt)$ of two adjacent points on such a curve are related by the equation:

$$\frac{\partial c}{\partial z} * dz + \frac{\partial c}{\partial t} * dt = 0 \tag{3.10}$$

Combining equation3.8 and equation3.10 the slope of such a curve is :

$$V(c) = \frac{dz}{dt} \tag{3.11}$$

This equation provides a unique value for each concentration; thus, as c and therefore $V(c)$ is constant, it must be a straight line. On a $(z-t)$-diagram, the concentration is constant along straight lines whose slope $V(c)$ only depends on the value of the concentration (Kynch, 1951):

$$Z = z_0 + V(c) * t \tag{3.12}$$

In order to calculate the analytical solution we now have the wave velocity $V(c)$ of a level in the $z-t$ plane, across which particles with concentration c fall with the velocity $v(c)$ downwards. In time t from the start, the number of particles which have crossed this level (ξ) is:

$$\xi = c * (V(c) + v(c)) * t \tag{3.13}$$

The total number of particles initially in the dispersion is:

$$\xi = \int_0^H (c)dz \tag{3.14}$$

The water-slurry interface is dictated by the number of particles crossed by each level of constant concentration. The sum of the particles crossing all the constant concentration levels is constant over time and is equal to the total number of particles initially present in the dispersion.

3.2.2. Different hindered settlement formulations

As noted in the introduction of this chapter, different forms of hindered settlement formulations exist. Kynch initially suggested the formulation mentioned in Equation 3.4. In the same publication, Kynch suggested one other hindered settlement formulation (Eq. 3.15). Kynch however, stated this formulation was not in full agreement with experimental results.

$$v(c) = vs * (1 - \frac{c}{c_{max}}) \tag{3.15}$$

Another widely used equation to represent the fall velocity of particles in a suspension comes from Richardson and Zaki, 1954. In this formulation the empirical α-parameter was left out of the equation and an exponent was introduced to the hindered settling formulation (Eq 3.16). This n-parameter is also known as the RZ-exponent.

$$v(c) = vs * (1 - c)^n \tag{3.16}$$

For hindered settling of mud flocs, Mehta, 1986, suggested a modified form of the Richardson and Zaki formula (Eq 3.17).

$$v(c) = vs * (1 - \alpha * c)^n \tag{3.17}$$

this equation consists of both an empirical α-parameter as present in the original formulation of Kynch (Eq.3.4) as well as the exponent (n) introduced by Richardson and Zaki (Eq.3.16).

3.2.3. The Richardson-Zaki exponent

The exponent (n), in the hindered settling formulation of Richardson and Zaki has been subject to discussion. According to the original experiments by Richardson and Zaki, n should have a value between 2.5 and 5.5, depending on the particles' Reynolds number ((Richardson and Zaki, 1954), (Dankers, 2006)) . Similar research of Tomkins et al., 2005 and Spearman and Manning, 2017 confirm this view, providing formulations to calculate the exact value of n based on Reynolds number. In these formulations the n-value increases as Reynolds number decreases. A widely accepted approximation of the n-value comes from Rowe, 1987:

$$n = \frac{4.7 + 0.41 * Re^{0.75}}{1 + 0.175 * Re^{0.75}} \tag{3.18}$$

where Re is Reynolds number. Reynolds number is a function of the terminal velocity of a particle, the fluid density, the dynamic viscosity of the fluid and the diameter of the particle (Eq.3.19).

$$Re = \frac{vs * \rho_f * d}{\mu_{dyn}} \tag{3.19}$$

where ρ_f is the density of the fluid, vs is the terminal velocity based on Stokes' equation (Eq. 3.1), d is the diameter of the particle and μ_{dyn} is the dynamic viscosity.

As the diameter of the particle increases, the terminal velocity of a single particle increases and the particles' Reynolds number increases. This results in a decrease of the RZ-exponent. This is illustrated for a range of particle diameters in figure 3.3, where the RZ-exponent has been calculated as suggested by Rowe (1987) in equation 3.18.

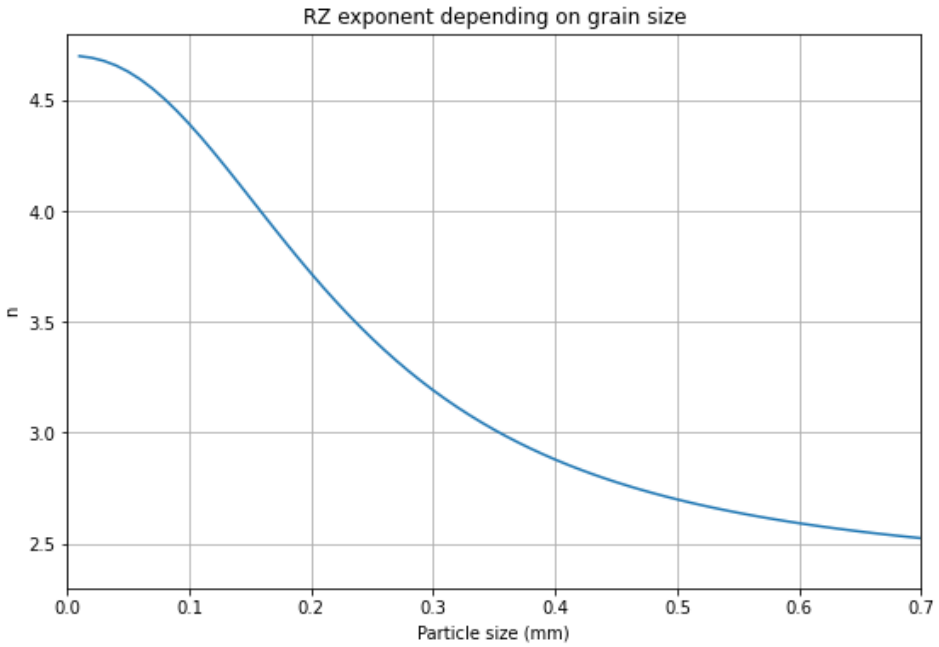

Figure 3.3: Predicted relationship between n and grain size based on Rowe (1987)

The range of n-values for natural sands are roughly similar to the values following from Richardison and Zaki (1954) and the other authors mentioned previously in this section. Baldock et al., 2004, suggested a different relationship for n which narrows down the range of n for natural and filtered sands to between 3.0 and 4.5.

The effect of the RZ-exponent on the hindered settling velocity is illustrated in figure 3.4. An exponent equal to 1.0 represents the original Kynch formulation. It can be noticed that an increase in the

RZ-exponent results in a more rapid decrease of the hindered settling velocity as the particle concentration of the sediment mixture increases. The effect of the RZ-exponent on the concentration profiles and buoyancy development will be illustrated and discussed in Chapter 5.

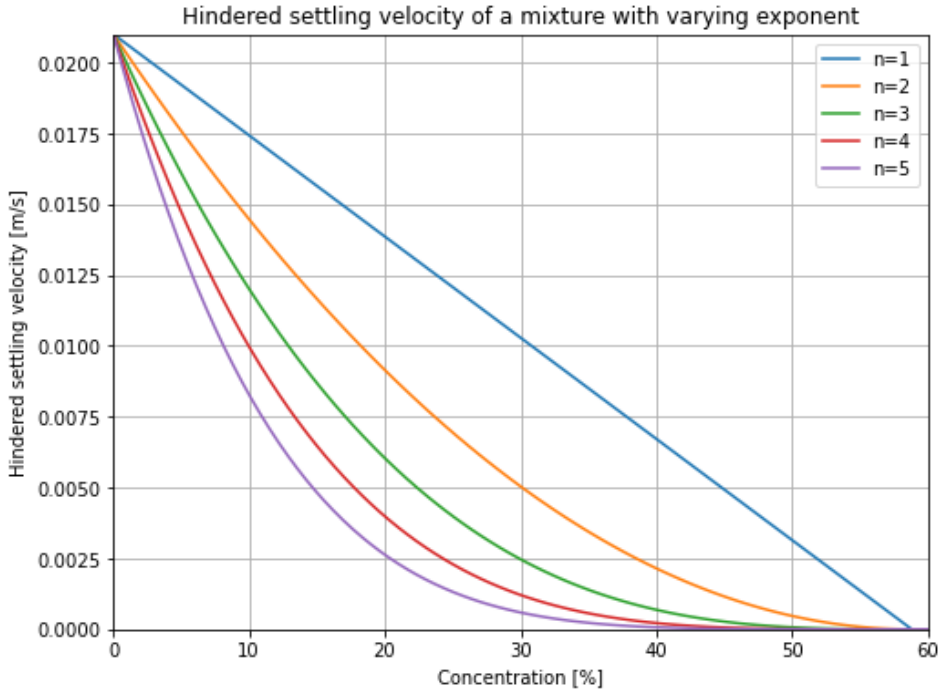

Figure 3.4: Settling velocity of a suspension with different concentrations.

3.2.4. Limiting the concentration with Kynch' alpha- parameter

The α-parameter in the hindered settling formulations of Kynch (1951) and Metha (1986), is an empirical parameter which was found useful to limit the maximum concentration. When the term inside the brackets in Eq.3.4, Eq.3.16 and Eq.3.17 vanishes, the settling velocity will also reach zero. The maximum particle concentration can be calculated as:

$$c_{max} = \frac{100\%}{\alpha} \tag{3.20}$$

Besides limiting the maximum concentration, the α- parameter also influences the speed at which the hindered settling velocity reduces as the concentration increases. An increase in the α- parameter reduces the hindered settling velocity (Figure 3.5).

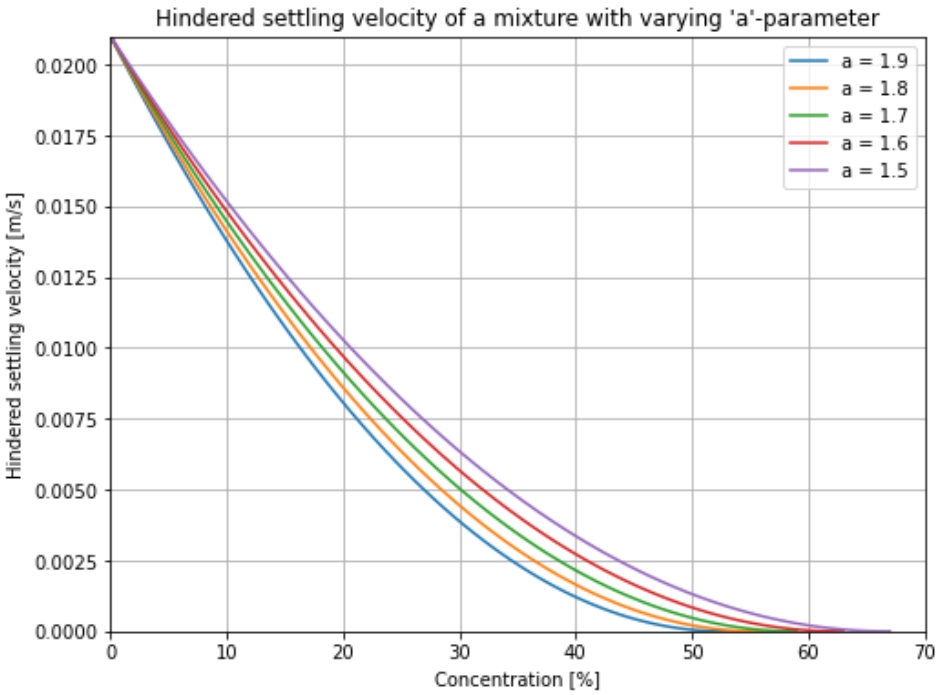

Figure 3.5: Settling velocity depending α- parameter. Analysis based on the formula: $v(c) = 0.021 * (1 - \alpha * c)^2$

How the maximum concentration is influenced by this empirical parameter is illustrated in figure 3.6.

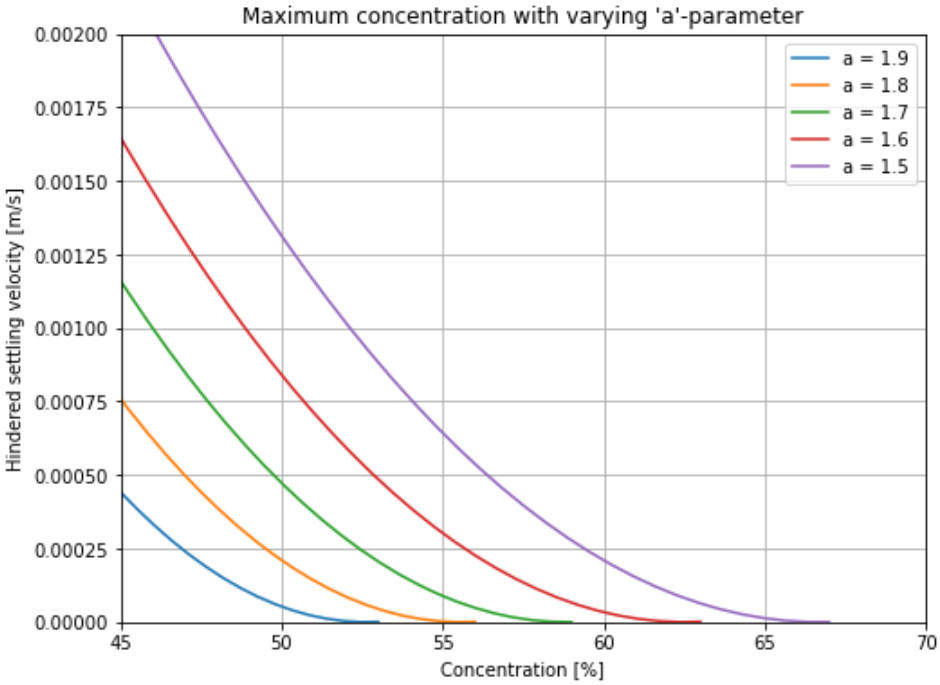

Figure 3.6: Maximum concentration variying with the α-parameter. Analysis based on the formula: $v(c) = 0.021 * (1 - \alpha * c)^2$

3.3. Analytical solution of a sedimentation model

In this section the results are presented to prove the ability of solving simple sedimentation problems analytically with the method of characteristics. The case tested is based on an initially homogeneous suspension in a confined domain.

In the paper of Bürger et al. (2000), the settling of a flocculated suspension has been simulated. This simulation considers Chilean copper ore tailings. A settling column with the height of 6.0 meter is closed at the bottom and filled with a suspension with an initially homogeneous concentration of 12.3%. A Kynch particle flux function of the Maude and Withmore type (Maude and Whitmore, 1958), which is a generalization of the flux density function proposed by Richardison and Zaki, has been proposed ((Bürger et al., 2000), (Bürger et al., 1999)). This batch flux density function [m/s] has the mathematical form:

$$S = -vs * c * (1 - c)^n \tag{3.21}$$

This particle flux function follows from the hindered settling velocity formulation which has the form:

$$v(c) = -vs * (1 - c)^n \tag{3.22}$$

The hindered settlement equation, with v(c) in [m/s] as proposed by Bürger et al. (2000) follows:

$$v(c) = -6.05 * 10^{-}5 * (1 - c)^{12.59} \tag{3.23}$$

The analytical solution obtained with the method of characteristics was found to be in good agreement with the results of Bürger et al. (2000). Figure 3.7 indicates the iso-concentration lines together with the water-slurry interface. Figure 3.8 depicts the concentration profiles for batch settling of an ideal suspension described by the Kynch theory.

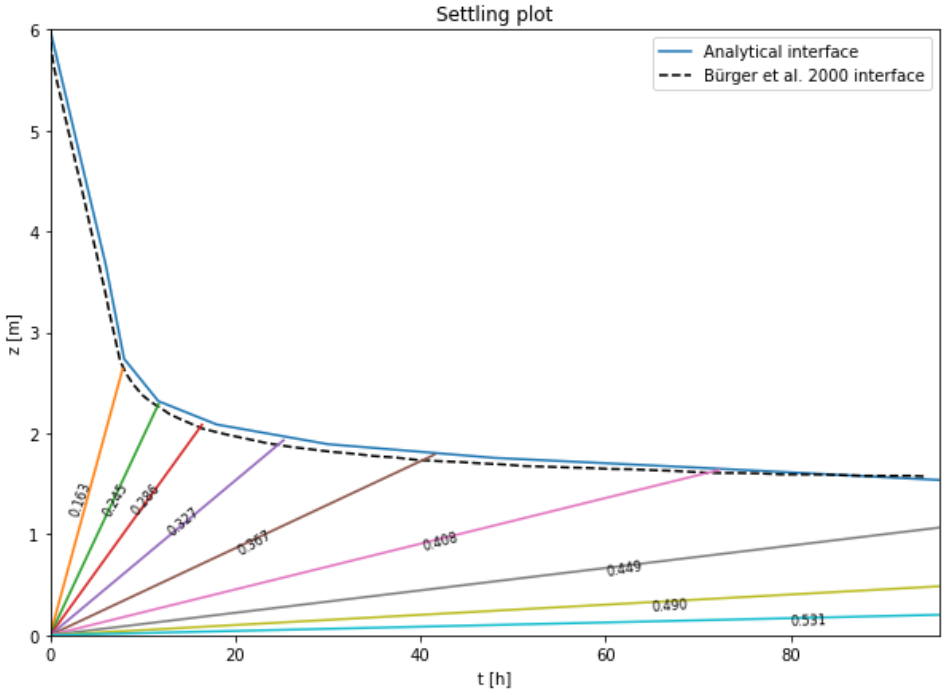

Figure 3.7: Comparison between the analytically obtained water-slurry interface and interface from Bürger et al. (2000)

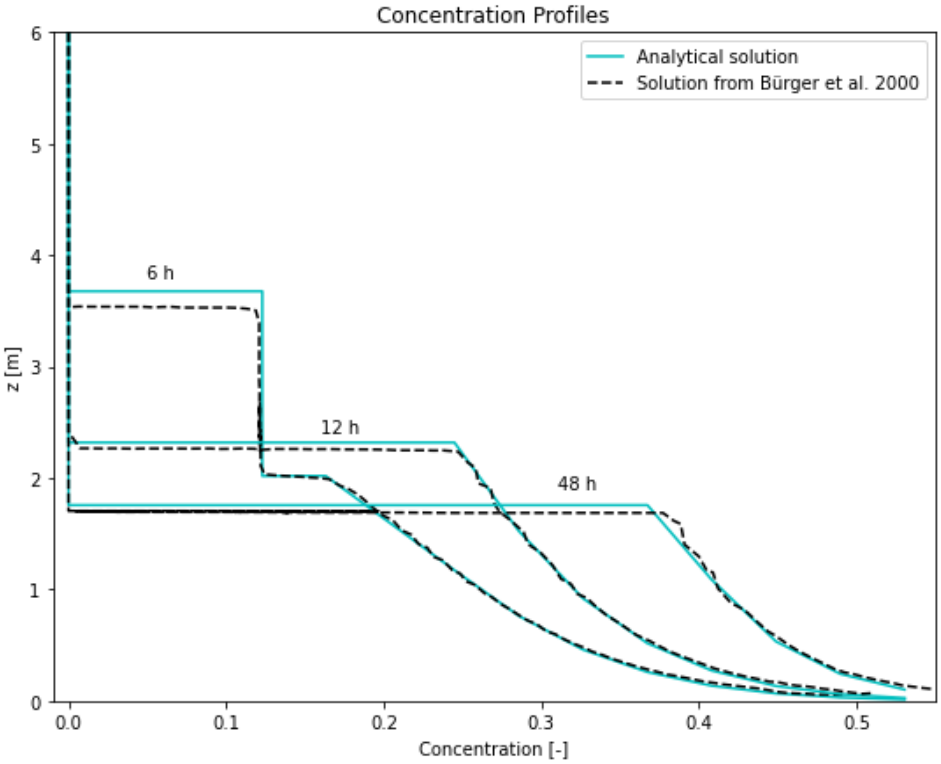

Figure 3.8: Comparison between the analytically obtained concentration profiles and concentration profiles from Bürger et al. (2000)

The particle size of the copper ore tailings is not specified in the paper of Bürger et al. (2000). Considering the terminal velocity of a single particle, a mean particle size of 28μm is expected; this is in correspondence with particle sizes of copper ore tailings reported in literature ((Shamsai et al., 2007), (Li et al., 2022)). According to the literature discussed in section 3.2.3 a RZ-exponent between 4.5 and 5.5 would be expected. The RZ-exponent considered by Bürger et al. (2000) is based on empirical findings and was not elaborated on in the physical context of this parameter.

4

Numerical Modelling

In this chapter, the theory regarding the implementation of a sedimentation problem in a numerical model will be provided. In section 4.3, two sedimentation problems from literature, with an initially homogeneous concentration and without inflow or outflow of material, will be solved using the developed numerical model. In section 4.4, the numerical model will be extended with a 'dummy reservoir', which regulates the inflow of material.

In chapter 3 the theory of sedimentation has been elaborated, where the hindered settlement of particles in suspension can be modelled as a pure convection equation as displayed in equation 3.8. Equation 3.8 is an one-dimensional convection equation in which the propagation speed of the water-sand mixture is dependent on the local particle concentration (c) in the suspension at a certain location in the domain (z) at a certain moment in time (t). Moreover, it has been illustrated that a simple sedimentation case, with an initial homogeneous suspension present in the domain and without inflow and outflow, can be solved analytically with the method of characteristics. When simulating the sedimentation process during the backfilling of a trench, the inflow of particles into a domain with an initial 0% particle concentration needs to be considered. The best strategy to solve this sedimentation problem was considered by means of numerical approximation. The numerical sedimentation model was developed in the finite element program COMSOL Multiphysics.

4.1. Stabilized convection-diffusion equation in COMSOL Multiphysics

A convection equation, as equation 3.8, classifies as a first order partial differential equation (PDE). A PDE permits one to describe solutions that depend on more than one independent variable. Often these independent variables are time and one or more spatial dimensions (Zijlema, 2015).

The sedimentation problems of Latsa et al. (1999), Bürger et al. (2000) and the small-scale physical experiments by Eikhout (2021) have been modelled by using the finite element program COMSOL Multiphysics. A Stabilized Convection-diffusion Equation interface has been used to simulate this problem. This interface allows to reduce numerical instabilities by Streamline diffusion and Crosswind diffusion which are automatically implemented in the interface (COMSOL-Multiphysics, 2019). The convection-diffusion equation has the standard form of:

$$f = d_a * \frac{\partial c}{\partial t} + \nabla * (-D_f * \nabla c + \alpha_c * c) + \beta_c \nabla c + a * c \tag{4.1}$$

where c is the particle concentration, d_a is a damping coefficient, D_f is the diffusion coefficient, α_c is the conservative flux convection coefficient, β_c is the convection coefficient and a is an absorption coefficient.

This equation reduces to a pure convection equation (Eq.4.2) in the case of sedimentation, for which the diffusion-, absorption- and conservative flux convection coefficient are zero. Moreover, the source term is zero and the damping coefficient is 1.0.

$$\frac{\partial c}{\partial t} = -V(c)\nabla c \tag{4.2}$$

In one dimension, equation 4.2 is the same as equation 3.8.

In addition to the partial differential equations, some boundary conditions and initial data must be provided to uniquely specify a solution. Solving the equations means finding the dependent variable or variables as function of the independent variables such that they fulfill the PDE and the boundary conditions are satisfied (Zijlema, 2015). This is called the boundary value problem.

When solving a sedimentation problem without inflow and outflow, only the no-flux boundary condition is needed. The no-flux boundary condition, functions as an impervious boundary. This condition is applied at the top- and bottom boundary.

4.2. Stabilization Methods

It is well known that for convective dominated PDE's significant stability problems arise. The properties of these systems of equations, in particular the lack of sufficient physical diffusion, cause the appearance of violent and non-physical oscillations, even for the single equation case (Hernández et al., 2018). In order to obtain a physical solution and to reduce the magnitude of the oscillations numerical stabilization techniques are needed. The automatically implemented Streamline diffusion and Crosswind diffusion were found insufficient.

4.2.1. CFL condition for numerical modelling

A condition essential for stability of the solution is the CFL condition. Satisfying the CFL condition is necessary for the convergence of a finite difference scheme to a (non)linear hyperbolic PDE (Zijlema, 2015). This condition is named after Courant, Friedrichs and Lewy who published the result in 1928. It is one of the most important results − historically and practically − in numerical solutions of PDEs (Zijlema, 2015).

The CFL condition states that a necessary condition of a numerical scheme to converge is, that the numerical domain of dependence must contain the analytical domain of dependence (Zijlema, 2015). Put differently; the distance covered during a numerical timestep (dt) with speed $v(c)$ must be smaller than or equal to the distance between the nodes (dz): $v * dt \leq dz$.

$$\frac{v(c) * dt}{dz} \leq 1.0 \tag{4.3}$$

4.2.2. Isotropic diffusion in COMSOL Multiphysics

In order to stabilize the numerical model an isotropic diffusion term, the so called 'tuning parameter', should be added. This inconsistent stabilization method adds a certain amount of numerical diffusion, independently of how close the numerical solution is to the exact solution (COMSOL-Multiphysics, 2019). Thus, adding isotropic diffusion is equivalent to adding a term to the physical diffusion coefficient. The implementation and correct setting of the isotropic diffusion limits the oscillations which tend to occur close the impervious bottom boundary.

The correct setting of the tuning parameter was found to be of great importance: the value should be large enough to dampen the effects of oscillations and impede their propagation to other parts of the system, but still low enough not to dampen the convective motion too significantly.

4.3. Numerical validation of sedimentation models

With the theory regarding sedimentation together with the theory on the numerical modelling in COMSOL Multiphysics the sedimentation problems of Latsa et al. (1999) and Bürger et al. (2000) can be solved numerically.

4.3.1. Numerical solution sedimentation problem Bürger et al. (2000)

The sedimentation problem presented in Bürger et al. (2000) has been described in chapter 3.3. The same sedimentation problem has also been modelled numerically with COMSOL Multiphysics: the results are displayed in figure 4.1 and figure 4.2. The tuning parameter, depicting the amount of numerical diffusion, was set at a value of 1.4[-]. The consequence of this, relatively high, value is clearly visible; in particular when comparing the concentration profiles. The artificial diffusion smoothens the transition between the slurry and the clear liquid. As a consequence the interface is not sharp but a gradual transition, which explains the rounded corners in figure 4.2. Overall however, the agreement between the numerical model in COMSOL Multiphysics and the solution of Bürger et al (2000) was found to be good.

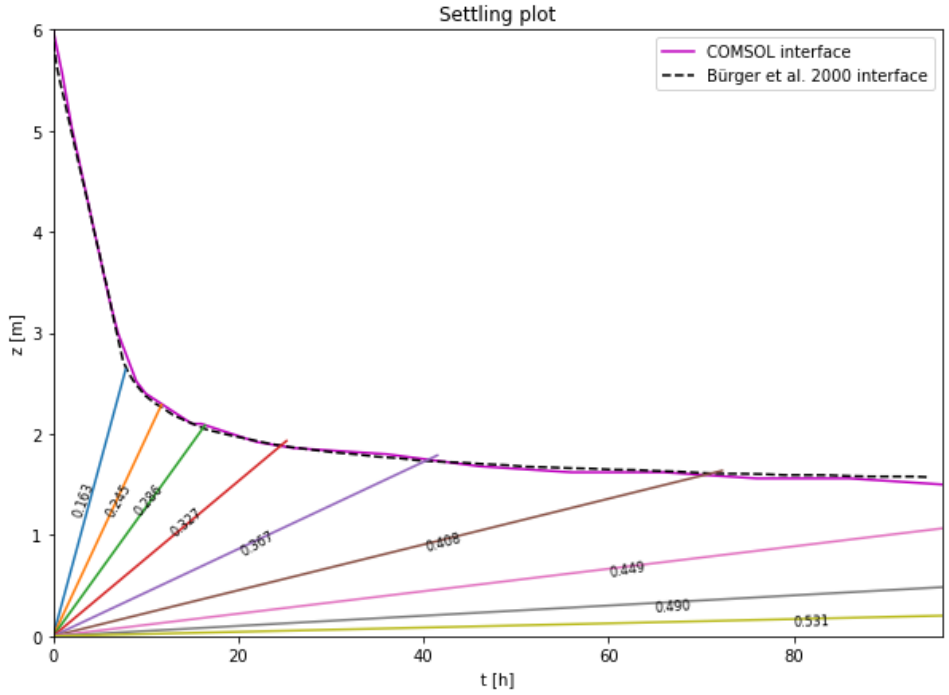

Figure 4.1: Comparison between the water-slurry interface modelled in COMSOL Multiphysics and interface from Bürger et al. 2000

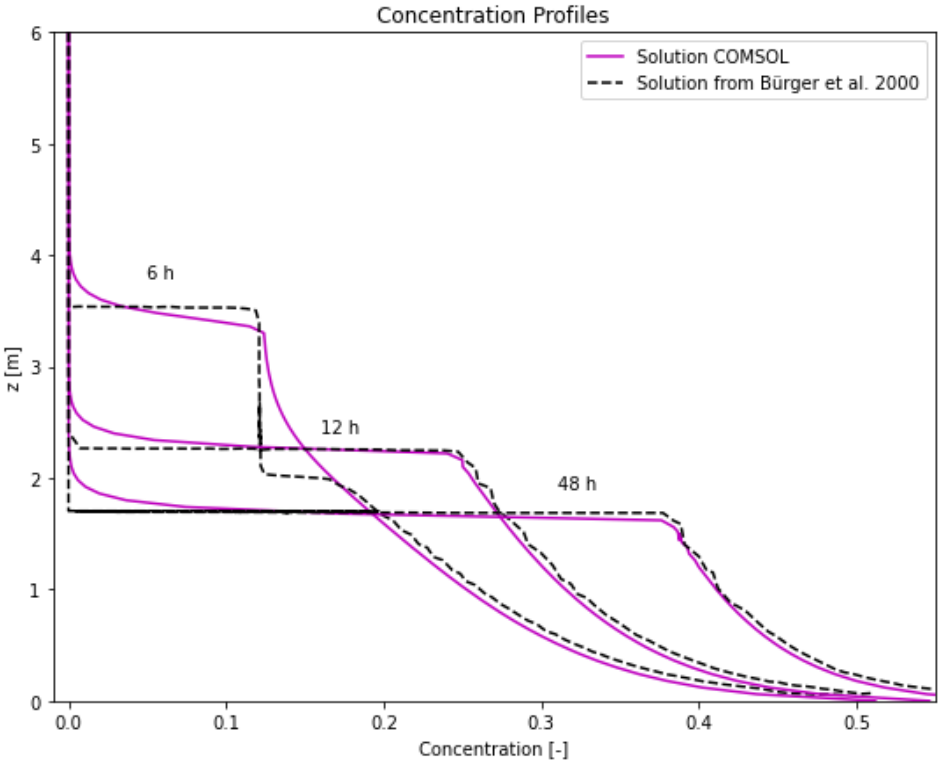

Figure 4.2: Comparison between the concentration profiles modelled in COMSOL Multiphysics and concentration profiles from Bürger et al. 2000

4.3.2. Numerical solution sedimentation problem Latsa et al. (1999)

The paper of Latsa et al. (1999) considers batch sedimentation of monodispersed particles with sludge thickening. The sedimentation model in COMSOL Multiphysics was tested against the numerical model developed by Latsa et al. (1999), which was computed in TFLOW-2D. The numerical model of Latsa et al., 1999 has been verified against the model predictions of Stamatakis and Tien, 1992.

The case tested considers a suspension of monodispersed particles with a diameter of 75μm and an initial volume fraction of 0.2[m^3_{sol}/m^3_{mixt}]. The density of the liquid is 1000[kg/m^3], whereas the particles have a density of 2500[kg/m^3]. The mixture is contained in a two dimensional tank with a height of 1.0[m] and a width of 0.3[m]. As the particles settle, a sludge layer forms which increases over time until it reaches a constant height. During settling, three distinct layers are formed which vary in thickness over time; the clear liquid, the suspension layer and the sludge layer (Latsa et al., 1999).

The hindered settling formulation used in the COMSOL model has been derived empirically and has the form as the equation suggested by Metha (1986) (Eq.3.17). The terminal velocity of a single grain, $vs[m/s]$, has been calculated with both the Stokes equation (Eq.3.1) as well as with the equation proposed by Ferguson and Church (Eq.3.2). The terminal velocity obtained with the equation from Ferguson and Church provided the best correlation with the model of Latsa et al. (1999). In order to limit the concentration of the sludge layer to 55.6% the α- parameter in the hindered settling formulation has the value of 1.8. Moreover, a value of 2.0 for the RZ-exponent was found to correspond best with the numerical solution of Latsa et al. (1999). Based on the theory discussed in chapter 3.2.3 this value was expected to be higher. The value for the tuning parameter needed to stabilize the solution was 0.3[-]. This yields the hindered settling formulation for this specific problem:

$$v(c) = -0.0041 * (1 - 1.8c)^2 \tag{4.4}$$

The numerical solutions are in good agreement with the results of the model predictions by Latsa et al. (1999) and Stamatakis and Tien (1992) (Figure 4.3 and 4.4).

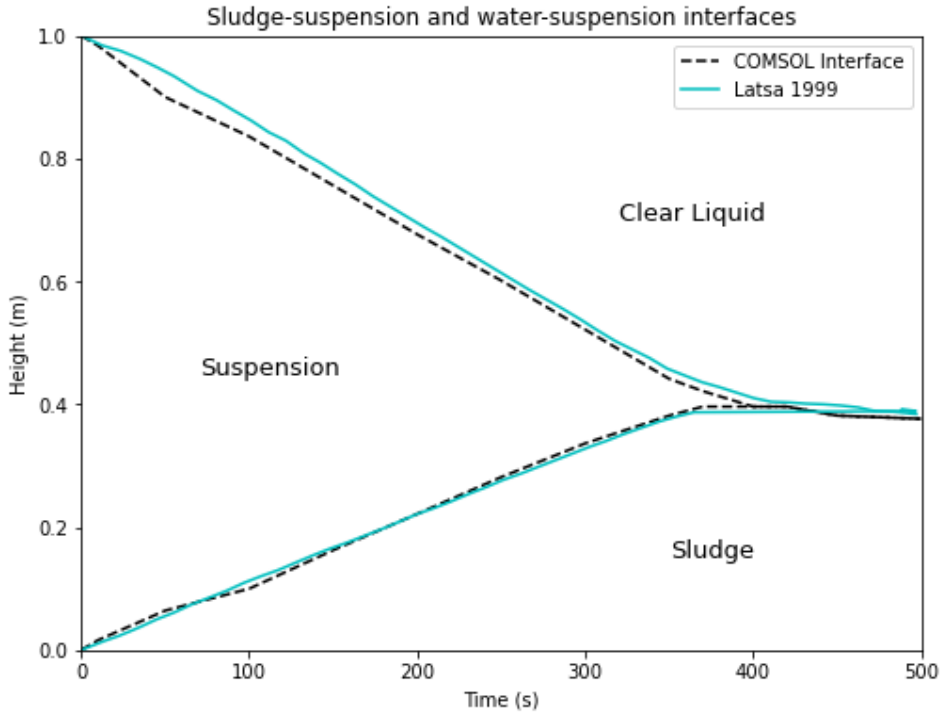

Figure 4.3: Comparison between the water-slurry interface modelled in COMSOL Multiphysics and interface from Latsa et al. (1999)

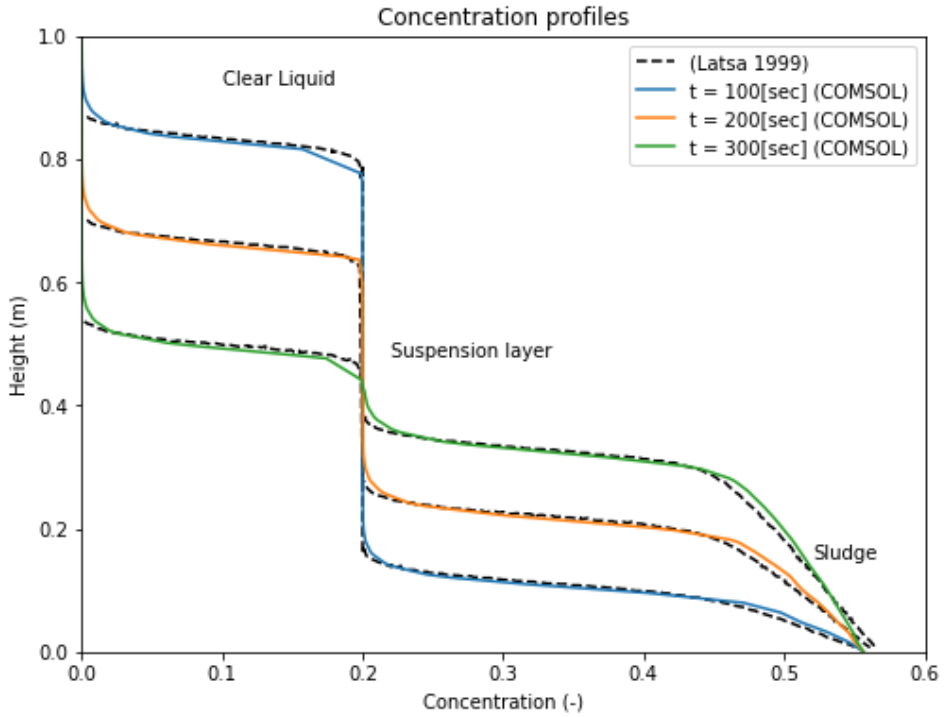

Figure 4.4: Comparison between the concentration profiles modelled in COMSOL Multiphysics and concentration profiles from Latsa et al. 1999

4.4. Small-scale physical model to 1D numerical model

The numerical sedimentation model thus far is in good agreement with the sedimentation models presented in literature. The numerical model is extended in order to simulate a simplified sand backfilling process. First, background regarding the small-scale experimental model from Yang (2020) and Eikhout (2021) will be provided after which the implementation of the inflow of sediment in the numerical model will be explained.

4.4.1. Background on the physical modelling of pipe flotation

Due to the lack of available field data regarding the mechanisms of pipeline flotation during sand backfilling, Yang (2020) designed an experimental set-up simulating a simplified sand backfilling process. This set-up has been used and improved by Eikhout (2021). A schematic overview of the laboratory set-up and the experimental tank are provided in figure 4.5 and 4.6 respectively.

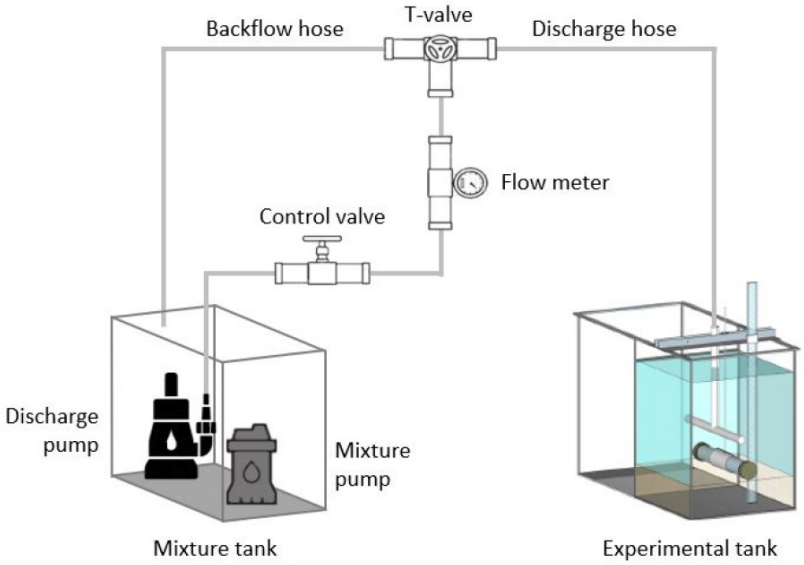

Figure 4.5: Laboratory set-up (after Eikhout (2021))

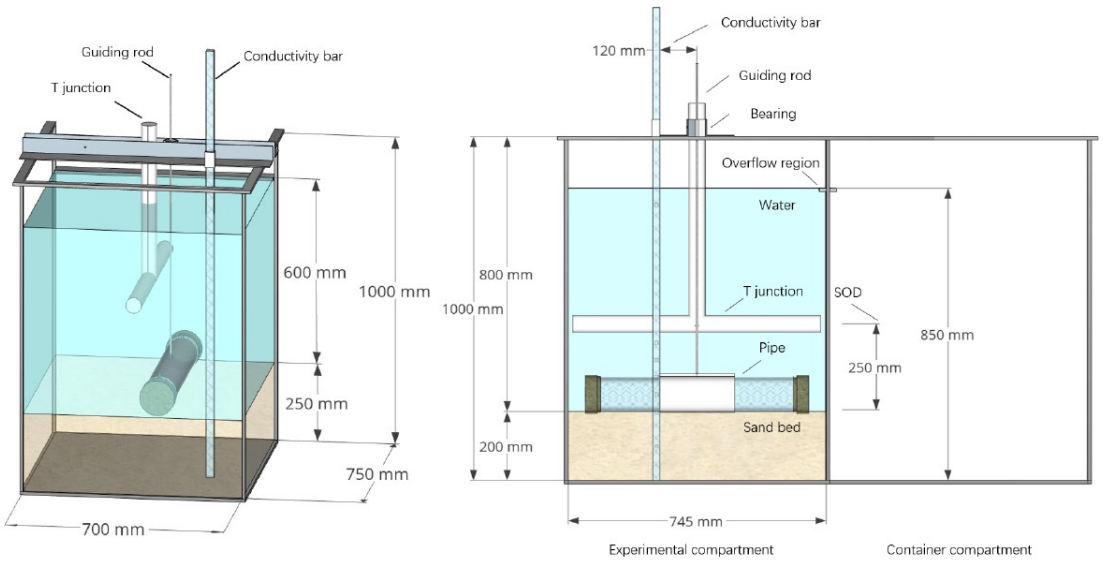

Figure 4.6: Set-up experimental tank (after Yang (2020))

During the physical experiments a water-sand mixture has been discharged from the T-junction. The discharge parameters were controlled and the potential displacement of the pipe, as well as the concentration development in the domain have been measured over the course of the experiment. The variables controlling the discharge of material in the small-scale physical experiments are:

- Direction of discharge: either downwards, horizontal or vertically upward;
- Discharge flow rate [L/s]: measured before the T-valve;
- Discharge concentration;
- Duration of the discharge period.

Yang (2020) and Eikhout (2021) together produced a substantial amount of data. This study proposes a numerical sedimentation model which is tested against the experimental data of Eikhout (2021).

4.4.2. Sediment inflow in the numerical model with a 'Dummy Reservoir'

The inflow of solids has been modelled with the use of a dummy reservoir; which has the function to regulate the inflow of solids. During the discharge period solids enter the domain. Important for the correct modelling of the sedimentation process is that the total amount of solids discharged in the model coincides with the amount of solids discharged during the experiments. The discharge parameters, provided from the experimental data, are: the volumetric flow rate (Q_{dis}) [L/s], the discharge concentration (c_{dis}) [-] and the discharge time (T_{dis}) [sec]. The total discharged volume (V_{dis}) [L], the volume of solids discharged (V_{sol}) [m^3] and the mass of the discharged solids (M_{sol}) [kg] can be calculated:

$$V_{dis} = Q_{dis} * T_{dis} \tag{4.5}$$

$$V_{sol} = \frac{(V_{dis} * c_{dis})}{1000} \tag{4.6}$$

$$M_{sol} = V_{sol} * \rho_s \tag{4.7}$$

The COMSOL model is one-dimensional which means that the amount of solids is not expressed in cubic meters nor kilograms, but in solid height (H_{sol}) [m]. The model only considers the height dimension and therefore the volume of solids calculated should be divided by the base area ($L * W$) of the experimental tank Eq.4.8. The solid height should not be mistaken for the new formed sediment height. The solid height refers to a theoretical height of pure solids (100% particle concentration), whereas the sediment formed from these solids has a certain porosity.

$$H_{sol} = \frac{V_{sol}[m^3]}{L * W[m^2]} \tag{4.8}$$

In order to ensure that the same total amount of particles have flowed in the numerical model as have been calculated with equation 4.8, the concentration should be integrated over the physical domain height in the numerical model (Eq.4.9). This integration provides the solid height in meters in the domain. Overall this calculation method was found to be reasonably well in line with the experimental data.

$$H_{sol} = \int_0^H (c) dz \tag{4.9}$$

where H is the height of the physical domain [m] and does not include the height of the dummy reservoir.

A second boundary condition is introduced in the dummy reservoir: the Dirichlet boundary condition. The Dirichlet boundary condition is imposed as the top boundary of the Dummy reservoir and specifies a concentration value on the boundary of the domain. By default, this is a unidirectional condition (COMSOL-Multiphysics, 2019).

5

From theory to implementation

Before considering the parameter selection and presenting the results of this research, a discussion on the uncertainties arising from the small-scale physical experiments was considered necessary. A good understanding of the experimental data is considered to be beneficial for the optimization of the numerical model. Moreover, it is important to identify the uncertainties arising from the small-scale physical experiments because it helps to explain the results obtained with the numerical model. With several analyses on different parameters regarding the hindered settlement formulation as well as in the force balance and the numerical settings the optimal settings and parameters have been selected. In addition, the numerical model, validated on the small-scale physical experiments, has been scaled to a more realistic practical case. Also an attempt has been made to further simplify the numerical model.

5.1. Interpretation of the small-scale physical experiments

The aim of the research of Yang (2020) and Eikhout (2021) was to develop a better understanding of the mechanism of pipeline flotation during sand backfilling. Of particular interest in the experiments were the buoyancy development and sedimentation during and after the discharge period. The concentration measurements were done with electrodes on the conductivity bar as well as with differential pressure sensor's (DPs) (Figure 5.1). Together, Yang (2020) and Eikhout (2021) produced a substantial amount of data. A total of six experiments have been modelled numerically; an overview of the experimental data of the selected experiments is listed in table 5.1.

Table 5.1: Overview of the experiments considered in this research

Overview experimental data					
Experiment	Discharge direction	Actual discharge time	Height new sand layer	Specific gravity pipe	Flotation
VNL12	Upward	60[s]	6.6[cm]	1.03[-]	Yes
VML30	Upward	49[s]	7.7[cm]	1.03[-]	Yes
VML33	Upward	38[s]	7.0[cm]	1.03[-]	Yes
VVL39	Upward	67[s]	7.3[cm]	1.03[-]	Yes
VNH47	Upward	26[s]	4.6[cm]	1.12[-]	No
VNH50	Upward	44[s]	5.1[cm]	1.12[-]	No

Several difficulties emerged when simulating the three-dimensional small-scale experiments with an one-dimensional numerical model. The first difficulty comes from the vertical upward discharge, the discharge method preferred by Eikhout (2020) (Figure 5.2). The upward discharge method reduces the erosive effect at the sand bed (which was present when discharging directly towards the sandbed) as well as limits the turbulence due to the influence of the sidewalls of the experimental tank (as was the case when discharging horizontally).

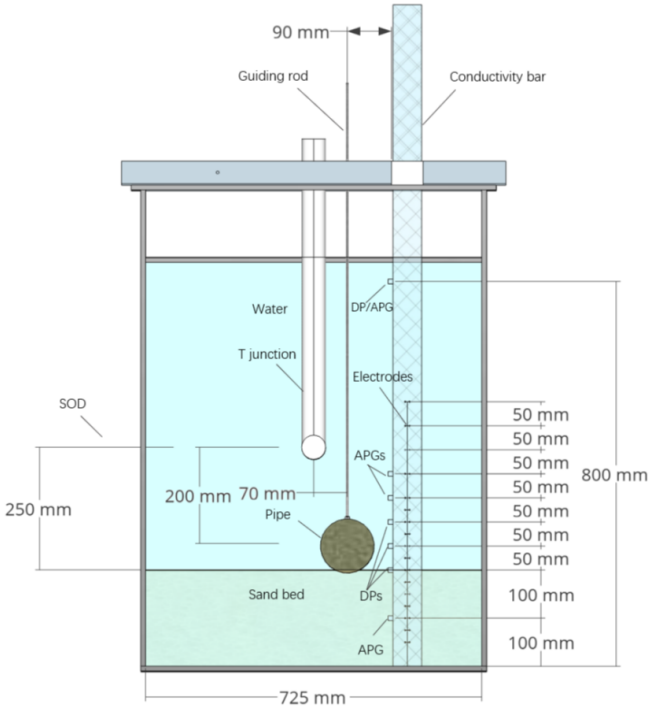

Figure 5.1: Experimental set-up with the location of the measurement devices (after Yang (2020))

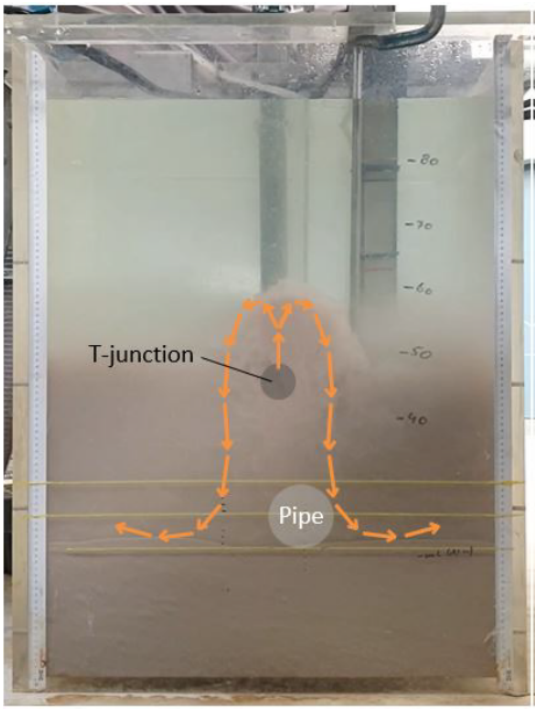

Figure 5.2: Upward discharge from T-junction during the experiments of Eikhout (2020)

The first difficulty regarding the upward discharge method is the difference between the actual- and apparent discharge time. The actual discharge time is the time during which the water-sand mixture comes out of the T-junction. In figure 5.3 the concentration development over time is displayed for test VML30. The measurements have been conducted at a height of 25[cm] above the sand bed, which is the height of the centre of the T-junction. It can be noticed that at the start of the discharge period ($t = 0[sec]$) little particle concentrations were measured at this location. In this experiment, significant particle concentrations have been measured 25[sec] after the start of the upward discharge period. Moreover, it is noticed that for a long time after the end of the discharge period ($t = 49[sec]$) (indicated with the black dotted line) solids enter the domain, this is referred to as the apparent discharge time.

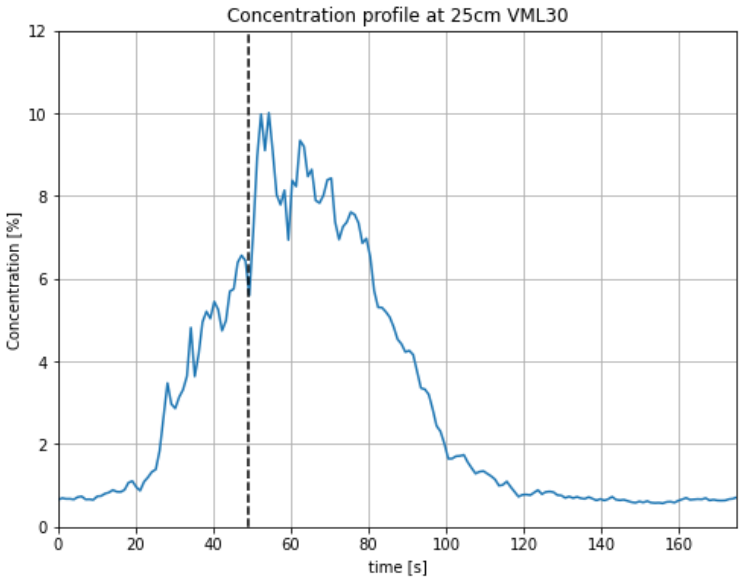

Figure 5.3: Concentration profile at height of the centre of T-junction test VML30

Moreover, no direct link was found between the discharge concentration measured in the discharge hose and the discharge concentration measured in the domain at the height of the T-junction. During the upward discharge several processes may play a role, which are difficult to quantify:

- The travel path of a single particle is not constant over time nor equal for every discharged particle;
- In the region above the T-junction, both upward mass movement as well as downward mass movement are present at the same time;
- Dispersion and turbulence are present;
- The discharge flow rate and discharge concentration vary significantly over the course of the experiment due to difficulties controlling these parameters (Eikhout, 2021).

Other difficulties and uncertainties arise with the experimental set-up. The conductivity bar was placed, for practical reasons, at a lateral distance of $16[cm]$ from the centre of the T-junction. The consequence is that the measurements might not represent the exact same concentrations as are present around the pipeline. Moreover, the pipeline (with it's centre not directly underneath the T-junction) forms a ridge, dividing the discharged material unevenly. In addition, the electrodes provide measurements every $2.5[cm]$ on the conductivity probe. This has the following consequences:

- The exact location of the sedimentation front has a theoretical uncertainty of $2.49[cm]$;
- Transition layers and concentration jumps can not be defined exactly in terms of their thickness nor their exact location; for both the uncertainty is again $2.49[cm]$.

5.2. Numerical settings

In this section the experimental-specific settings of the numerical model will be discussed. In addition, the implementation of both constant and inconsistent sediment inflow with the dummy reservoir will be considered.

5.2.1. Numerical domain and stabilization methods

The physical domain in the numerical model represents the tank in the small-scale physical experiments. The bottom of the numerical domain is considered the top of the sand bed. In the numerical model, the material enters the physical domain at a height of 25[cm] above the sand bed, which is the distance from the centre of the T-junction to the initial height of the sandbed in the experimental set-up. The mesh is refined with respect to the standard COMSOL settings to a mesh with a node every 0.4[mm] ($= dz$). The numerical time step equals 0.01[sec] ($= dt$).

In the physical domain, the convection equation with the hindered settlement formulation dictate movement of the water-sand mixture. The CFL condition (Eq.4.3) must be satisfied for the highest settling velocity, which is equal to the terminal settling velocity (vs) in case the particle concentration approaches zero.

$$\frac{0.019[m/s] * 0.01[sec]}{0.4 * 10^{-}3[m]} = 0.475 \leq 1.0 \tag{5.1}$$

As discussed in chapter 4.2.2, artificial diffusion needs to be added in order to obtain a physical solution and reduce the non-physical oscillations. In COMSOL this has been done with the tuning parameter (TP), where an increasing the TP, increases the amount of artificial diffusion. With the standard setting of the tuning parameter in COMSOL (TP = 0.25[-]) no physical solution was obtained. The effect of the TP on the concentration profiles is depicted in figure 5.4 to figure 5.7.

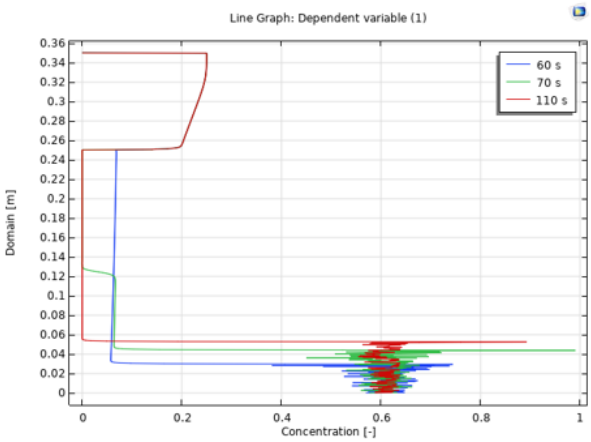

Figure 5.4: Concentration profiles; TP = 0.5

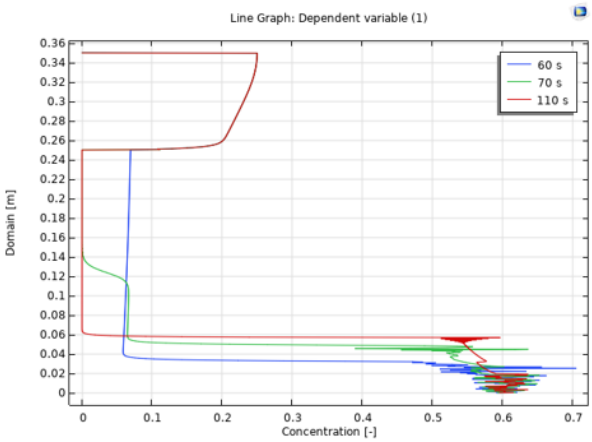

Figure 5.5: Concentration profiles; TP = 2.0

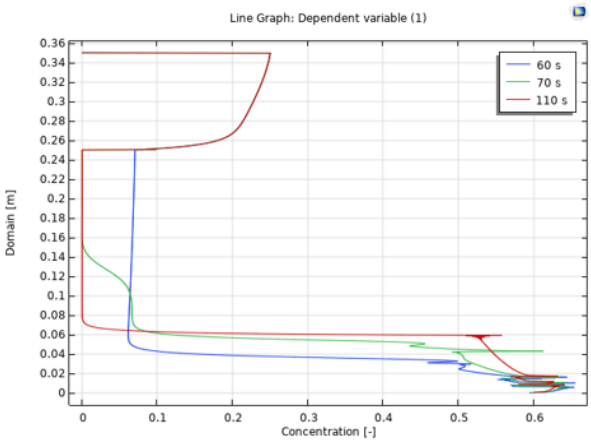

Figure 5.6: Concentration profiles; TP = 6.0

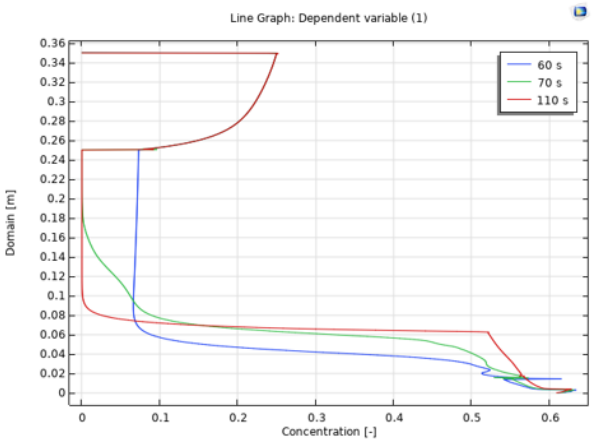

Figure 5.7: Concentration profiles; TP = 14.0

It can be noticed that an increase of the tuning parameter results in:

- A reduction of the oscillations;
- Less abrupt concentration changes which can be noticed from the corners of the concentration profile;
- A less sharp concentration jump: which is defined as the thin layer over which the concentration increases from the maximum domain concentration (approximately 8% in this case) to a significantly higher particle concentration (45%).

In order to reduce the oscillations but limit the effect of the artificial diffusion on the convective nature of the equation, the optimal value of the tuning parameter was found to be 6.0[-].

5.2.2. Dummy reservoir and amount of solids discharged

The dummy reservoir has the function to regulate the inflow of solids. Inside the dummy reservoir one formulation dictates the outflow velocity and regulates the outflow concentration over time. It was found practical choosing a formulation for the dummy reservoir in the same or similar form as the hindered settling formulation in the physical domain (Eq.3.17). Thus linking the outflow concentration to the outflow velocity. Moreover, the hindered settling formulation in the actual domain still has to be able to cope with the implied particle inflow. In case the discharge velocity is significantly larger compared to the hindered settling velocity, concentration will built up at the top of the actual domain. This triggers a spiral where, when the concentration increases the hindered settling velocity will further decrease, resulting in a further built-up of concentration and so on. Only the artificial diffusion counteracts

on this negative spiral. The dummy reservoir and the actual domain thus can not be completely uncoupled. After all, during the discharge period solids should pass from one domain into the other. If the discharge concentration is expected to be constant, the simplest approach of implementing this in the numerical model in COMSOL would be:

- Defining a small dummy reservoir ($> 1cm$);
- The top boundary of the dummy reservoir is a Dirichlet boundary condition which is equal to the (constant) discharge concentration;
- The formulation in the dummy reservoir is equal to the hindered settling formulation in the domain.

One could also disregard the dummy reservoir completely in this case and could imply the Dirichlet boundary conditions to the top node of the physical domain.

In the experiments however, the inflow concentrations are not constant over the apparent discharge time. The dummy reservoir can in this case be useful to match the inflow concentrations over time in the model with the measurements in the experiments. During the modelling of the experiments the inflow concentrations in the numerical model have been calibrated against the concentrations measured around the T-junction.

The way this has been implemented in the COMSOL model is by adjusting the parameters in the formulation of the dummy reservoir together with adjusting the reservoir height and the Dirichlet top boundary condition. How these parameters influence the maximum inflow concentration, the time needed for the first particles to flow in the physical domain and the time to reach the maximum inflow concentration is summarized in the table below (Table 5.2) .

Table 5.2: Parameters in the dummy reservoir regulating the inflow of material

Regulating the inflow			
Parameter	Maximum inflow concentration	Time to reach first inflow	Time to built up to max inflow
Increase vs	Increases	Decreases	Decreases
Increase α	Increases	No change	Decreases
Increase n	Decreases	No change	Increases
Increase H_{res}	Decreases	Decreases	Increases
Increase boundary concentration	Increases	Decreases	Decreases

Finetuning the dummy reservoir with these parameters will provide an inflow with varying concentration and varying inflow velocity over time into the domain.

5.3. Parameter selection hindered settlement formulation

The hindered settling formulation proposed by Metha (1986) was identified the most suitable formulation for the simulation of the small-scale physical experiments: $v(c) = vs * (1 - \alpha * c)^n$.

5.3.1. Grainsize distribution and terminal velocity

The sand used in the backfilling experiments by Yang (2020) and Eikhout (2021) is Geba Weiss sand. Yang (2020) performed multiple soil tests in order to obtain an overview of the acquired sand properties. The particle size distribution is displayed in figure 5.8. The narrow grain size distribution, together with the uniformity coefficient, $C_u = d60/d10$ equal to 1.45, indicate a well sorted sand.

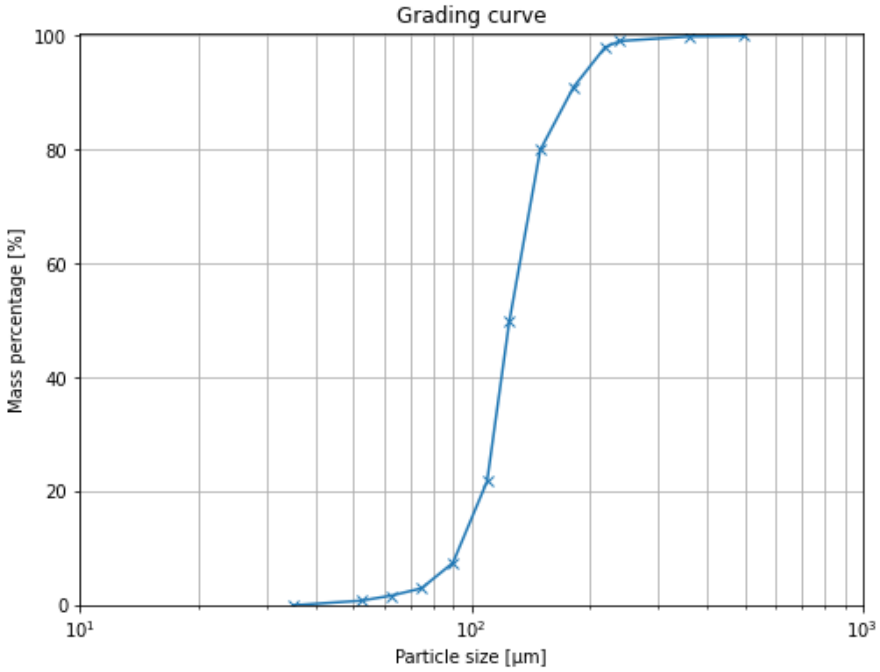

Figure 5.8: Grainsize distribution Geba Weiss sand used for experimental modelling (after Yang (2020)

Despite the sand being well sorted, the settling velocity of a single particle in water varies within the mixture due to the variation in particle size. The velocity with which the smallest 10% grains settle is at least a factor 3 to 4 lower compared to the settling velocity of the largest 10% particles as illustrated in figure 5.9. The dependence of terminal settling velocity on particle size leads to vertical size sorting when grains settle in standing water (Ferguson and Church, 2004)(Biemans, 2012).

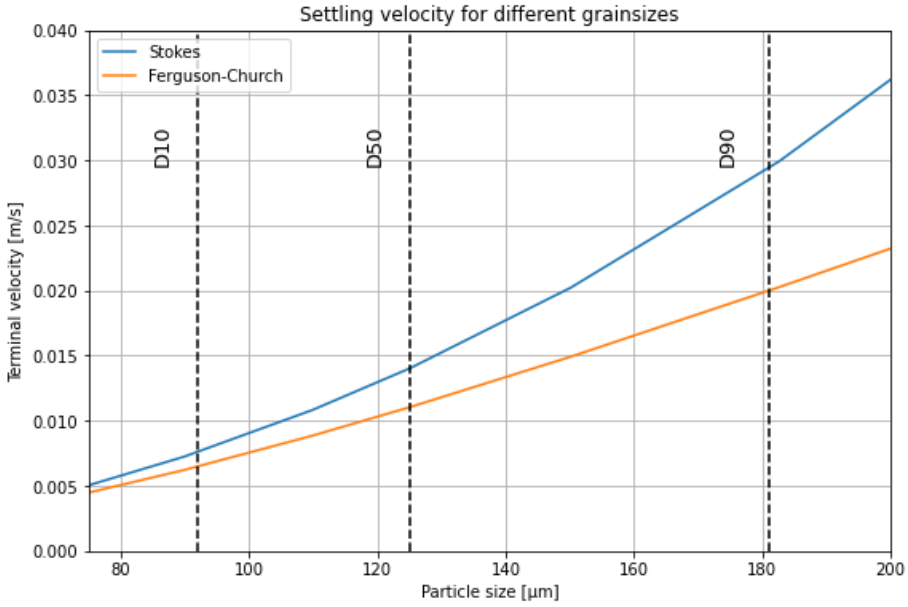

Figure 5.9: Terminal velocity of particles within the particle size distribution range

The the median diameter of the sand fraction (D50) is 125[μm]. The terminal settling velocity of a single grain corresponding to the D50 is 0.011[m/s] or 0.014[m/s] depending on the calculation method. A terminal settling velocity of 0.019[m/s] was found optimal for accurate modelling. This would correspond to the D75 or D88 mass percentage depending on the calculation method.

5.3.2. RZ exponent

The choice of the correct exponent, n, in the hindered settling formulation was found to be crucial in the numerical model. The theory behind this exponent has been elaborated in chapter 3.2.3. This parameter is also dependent on the grain size and therefore is not equal for every particle in the water-sand mixture considering the particle size distribution of the Geba Weiss sand (Figure 5.10). An exponent of 4.23 corresponds to the median grain diameter.

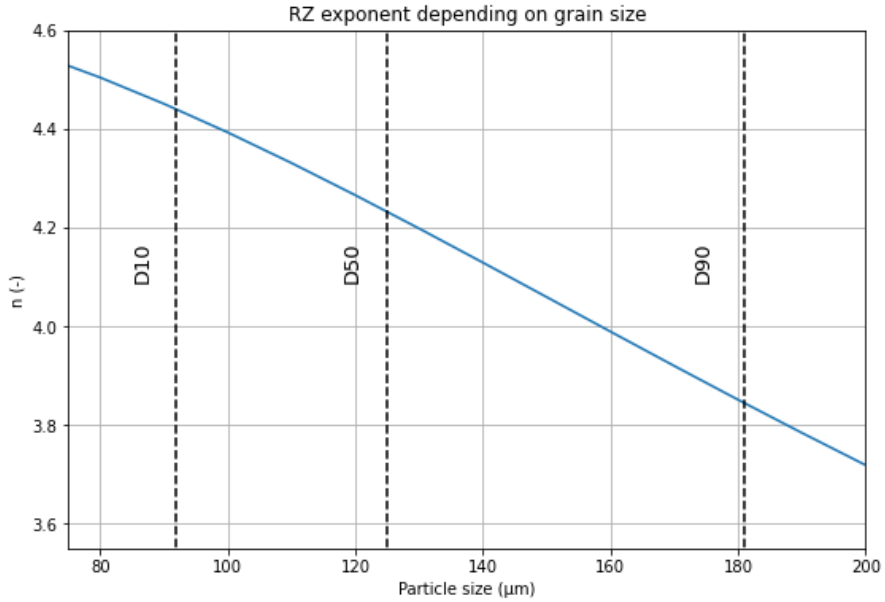

Figure 5.10: Variation of RZ-exponent in the range of the particle size distribution of the Geba Weiss sand

The exponent was found to have interesting results on the concentration profiles as well as on the buoyancy development. Simulations with a different exponent have been projected on the data of the experiment VML30. In the simulations the same amount of solids have been discharged in the same time span. The concentration profiles at 73[sec] are displayed in figure 5.11.

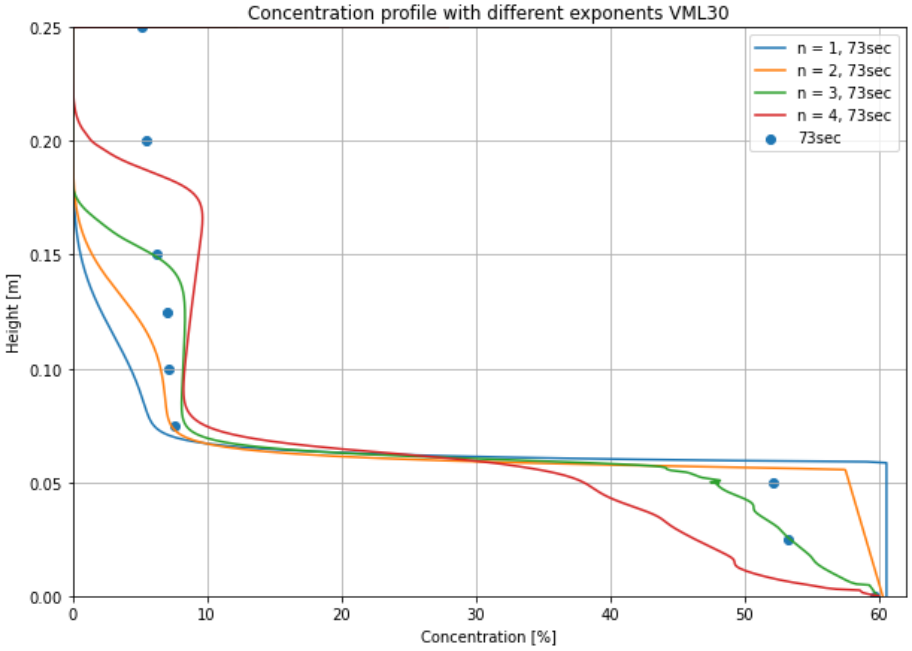

Figure 5.11: Concentration profiles with different RZ exponent at 73 seconds

All the concentration profiles regarding this analysis can be found in Appendix B. It can be noticed that for the case where $n = 1$ the concentration built up from below is a vertical line. This indicates that once the sand grains have settled no more densification takes place; it is an instant process. As the exponent increases, the concentration built up from below is elongated. This is the result of the hindered settling velocity getting close to zero at lower concentrations as the exponent increases. Moreover, the concentration jump, from the max domain concentration $(+/-9\%)$ to the phase transition concentration (40%), is significantly less sharp for the case of $n = 4$. The consequence is that the thin layer over which the concentration jump occurs is thicker for the $n = 4$ case. In addition, the maximum domain concentration slightly increases as the exponent increases.

The exponent also influences the buoyancy built-up (Figure 5.12). As the exponent decreases, the maximum average specific gravity of the water-sand mixture around the pipe decreases. Moreover, the maximum buoyancy force appears earlier as the value of the RZ-exponent decreases. The significantly larger average specific gravity around the pipe in the case of $n = 4$, can be explained with the concentration profiles. The first reason is the slight increase of the concentration of the mixture around the pipe as the exponent increases. The second reason is that, as the thickness of layer over which the concentration jump occurs, increases, the average specific gravity around the pipe increases.

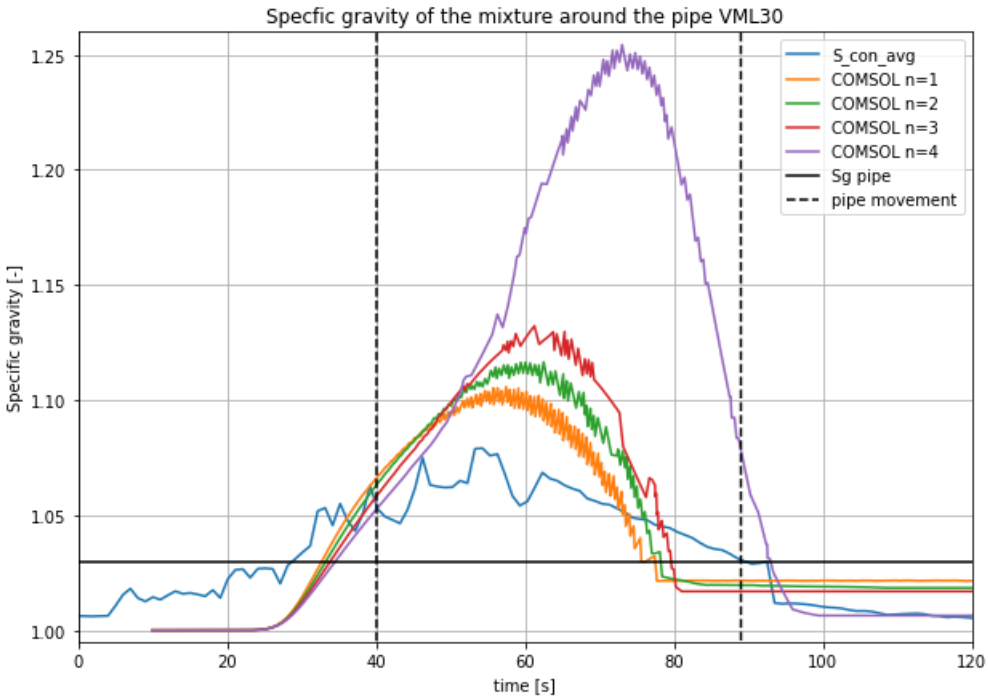

Figure 5.12: Specific gravity development with different exponents in the hindered settling formulation

Considering the concentration profiles, the best agreement between the numerical model and experimental data was obtained with a RZ-exponent of 3.0. It must be noticed however, that no physical solution was obtained when the exponent was a decimal number.

5.3.3. Alpha-parameter

Tests on the sand bed underneath the pipeline, performed by Yang (2020), indicate a porosity of approximately 0.4[-]. This is equal to a particle volume concentration of 60%. Measurements from Eikhout (2021) confirm this particle concentration. In the numerical model, the α-parameter was set at 1.65 to ensure a maximum particle concentration of 60.6%.

5.3.4. Results: concentration profiles

With the numerical settings discussed as well as the most optimal parameter selection for the hindered settling formulation the concentration profiles can be obtained from the numerical model. In the concen-

tration profiles the experimental data is displayed as dots, whereas the modelling results are displayed as solid lines (Figure 5.13). All the modelling results regarding the experiments, including experiment- and model specifications, can be found in Appendix A. For test VML33, of which the concentration profiles are displayed in figure 5.13, the experiment- and model specifications are displayed in table 5.3. With respect to the experimental data: the discharge time is the actual discharge time (T_{dis}), the solid height (H_{sol}) is calculated with the method elaborated in chapter 4.4.2. and the sediment height (H_{sed}) is a range since the sedimentation front is located somewhere in between the two measurement points. With respect to the numerical implementation: the discharge time is the time during which inflow from the dummy reservoir in the physical domain occurs, the discharge concentration (c_{dis} is the maximum particle concentration of the mixture flowing into the physical domain and the solid height is by obtained by integration over the physical domain (Eq.4.9).

Table 5.3: Experimental- and numerical data Test VML33

Test VML33		
Parameter	Experimental data	Numerical implementation
Flotation	Yes	Yes
T_{dis}	38[s]	68[s]
c_{dis}	27.0%	7.5%
H_{sol}	0.0361[m]	0.0462[m]
H_{sed}	7.5-10[cm]	8.4[cm]

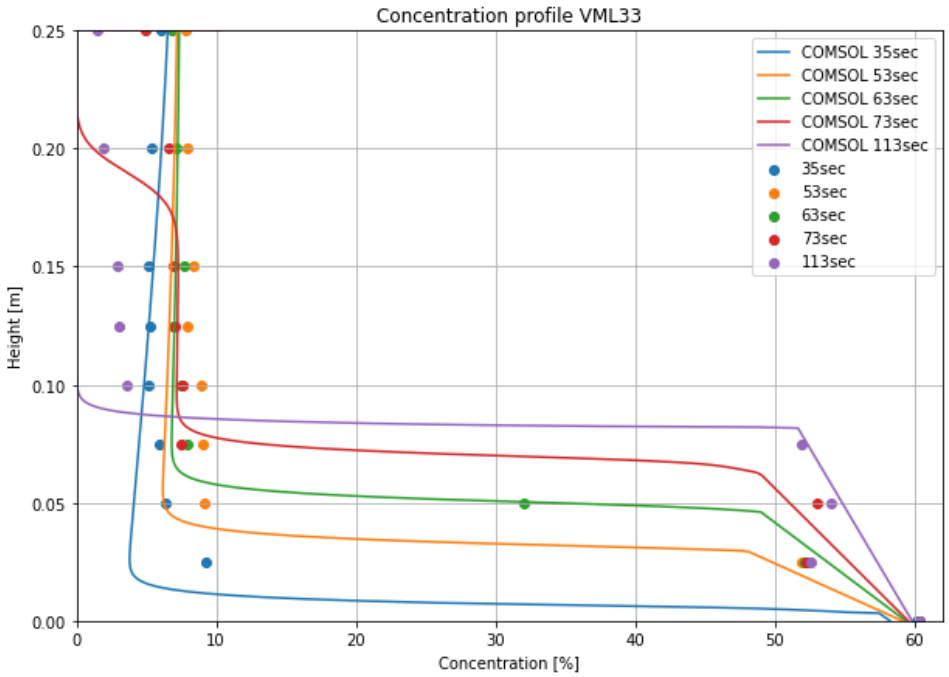

Figure 5.13: Concentration profile test VML33

Overall, the exact inflow concentrations, as extracted in similar manner as figure 5.3 were found difficult to reconstruct. The increasing trend can captured reasonably well by the dummy reservoir. The decreasing trend however, can not be captured with the use of the same dummy reservoir specifications. From the experimental data of test VML33 (Figure 5.13) it can be noticed that after 113[sec] still particles flow in from a height of 25[cm] into the physical domain. In the numerical model however, the inflow stops at 68[sec], when the inflow concentration is still at its maximum.

Despite difficulties regarding the regulation of the material inflow, the concentration profiles depict the general concentration development over time reasonably well. Because the distance between two measurement points in the experimental data is 2.5[cm] the exact height at which the concentration

jump occurs in practice is unknown. From the experimental data we can only conclude that the thickness of the layer over which this jump occurs is less than 2.5[cm]. From the data of the numerical model it can be noticed that this layer has a thickness varying from 0.5[cm] to 2.0[cm]. As explained in chapter 5.2.1., the thickness of this layer is to a large extended influenced by the artificial diffusion added to the, theoretically, pure convection equation. The exact thickness of this layer, together with its positioning in respect to the pipeline is important for calculating the buoyancy force.

5.4. Force balance

For the force balance the cross-sectional area of the pipe has been divided into 100 segments. The data extracted from the numerical model thus provides the concentration every millimeter along the height of the pipe over the selected time frame.

5.4.1. Phase transition concentration

Describing the transition from a sand-water mixture to a solid sandy soil was found crucial in determining the buoyancy force. For the tests VNH50 and VNH47 (both experiments where no flotation occurred), the effect of the exact phase transition concentration on the average specific gravity around the pipe has been analyzed. It can be noticed from figure 5.14 and figure 5.15 that an increase in the phase transition concentration results in an increase in the average SG around the pipe.

From the concentration profiles a deflection point can be identified; this is the point where the sharp concentration jump bends towards its maximum concentration. The concentration at which this deflection occurs varies over time and per experiment (figure 5.13). The deflection point is most often somewhere between 40% and 52%. The large difference in the maximum SG in figure 5.14 between a phase transition concentration between 40% and 45% indicates that the inflection point was passed. Whether the layer over which the concentration jump occurs does not, does partly or does fully contribute to the buoyancy force is of great importance in assessing the buoyancy force exerted on the pipe as illustrated in figure 5.14 and figure 5.15. In the first case every particle concentration above the maximum domain concentration (8%), is completely ascribed to the consolidation process and therefore assessed as sandy soil; not exerting an additional buoyancy force to the pipe. This method has been suggested by Yang, 2020 and Eikhout, 2021. For the final case, the whole transition layer contributes to the specific gravity of the mixture around the pipe: the phase transition concentration is between 40% and 45%.

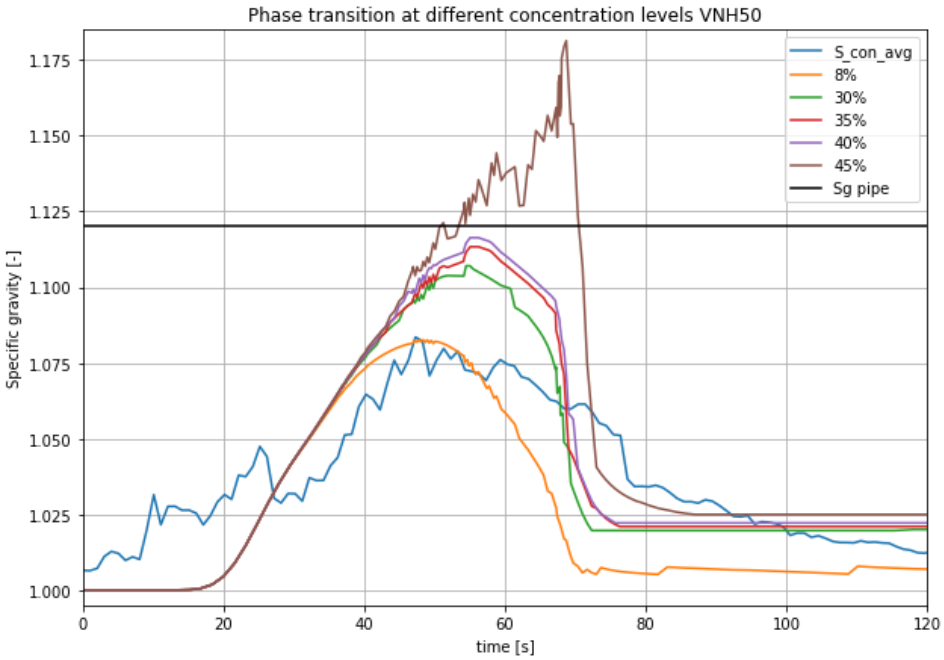

Figure 5.14: Effect of different phase transition concentrations on the specific gravity around the pipe for test VNH50

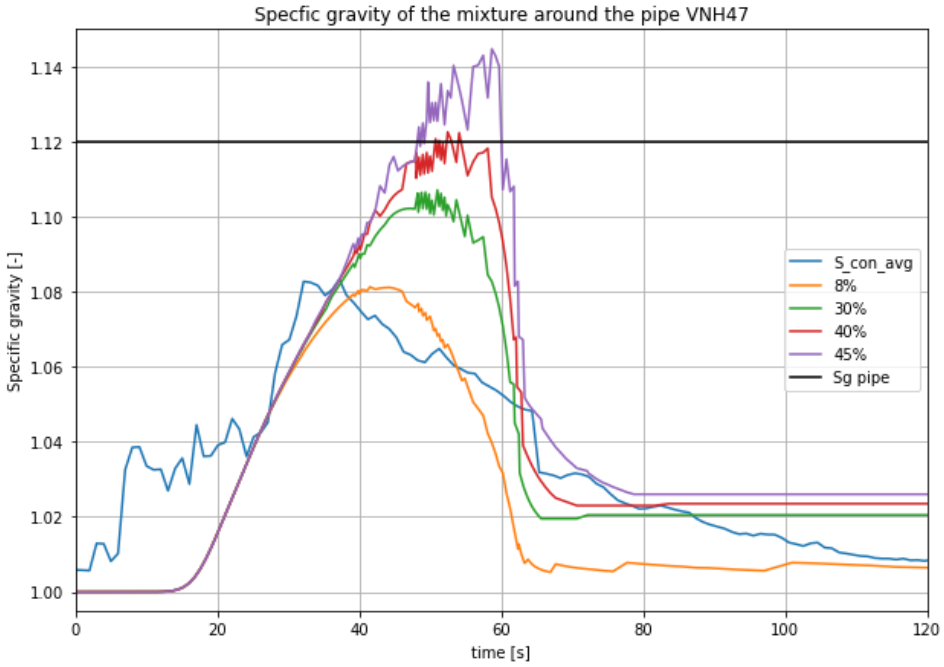

Figure 5.15: Effect of different phase transition concentrations on the specific gravity around the pipe for test VNH47

The thickness of the concentration jump-layer and its position with respect to the pipe is of particular relevance for pipe's with a relative small diameter. The area of a 1[cm] thick segment will contribute significantly to a pipe with a diameter of 10[cm]: in example when this segment is located at the centre of the pipe, the segment corresponds to 19.9% of the pipe's total area. In case of a 2[cm] thick transition layer at the same location, this will correspond to 38.7% of the total area of the small-diameter pipe. In the case where the pipe diameter is larger, the contribution of this transition layer to the total buoyancy will reduce. When in practice the pipe has a diameter of 1.0[m], the transition layer of 1.0[cm] to 2.0[cm] at the centre of the pipe, corresponds to only 2.0% respectively 3.9% to the total area of the pipe.

The transition concentration, logically, also depicts the sediment built up. As the water-sand mixture exceeds a particle concentration equal to phase transition concentration of 40%, the new sand layer forms. It can be noticed that the new formed sand layer increases with a constant rate (Figure 5.16).

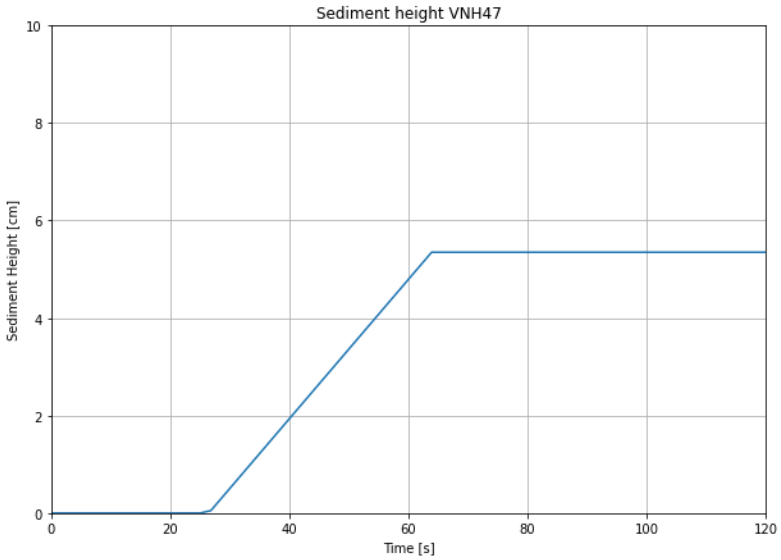

Figure 5.16: Height new formed sand layer over time (Test VNH47)

5.4.2. Buoyancy force and specific gravity

The buoyancy force has been displayed as the average specific gravity of the water-sand mixture around the pipe. In order to assess the the total average specific gravity around the pipe first the buoyancy force acting on each pipe segment is assessed. The new formed soil does not exert an additional buoyancy force on the pipe. In the case of water with a zero particle concentration and in case of a the new formed soil, the buoyancy force acting on a pipe segment is:

$$F_{b,seg} = A_{seg} * \rho_w * g \tag{5.2}$$

where $F_{b,seg}$ is the buoyancy force acting on the pipe segment considered, A_{seg} is the area of the pipe segment, ρ_w is the density of water and g is the gravitational acceleration. In case the water-sand mixture is present at the location of the segment, the buoyancy force of this segment is:

$$F_{b,seg} = A_{seg} * \rho_m * g \tag{5.3}$$

where ρ_m is the density of the water-sand mixture (Eq.2.5). The sum of the buoyancy forces acting on each segment at one moment in time provides the total buoyancy force acting on the pipe at that moment in time:

$$\sum F_{b,seg} = F_b \tag{5.4}$$

The total specific gravity of the mixture around the pipe at one moment in time can now be calculated with equation 5.5.

$$SG = \frac{F_b}{A_{pipe} * \rho_w * g} \tag{5.5}$$

The specific gravity built up of test VNL12 has been displayed in figure 5.17. The difference in magnitude of the maximum specific gravity resulting from the experimental data in compression with the processed numerical data can be explained due to the different phase transition concentrations. The phase transition used by Eikhout (2021) for this test was 7.8% against 40% used in this study.

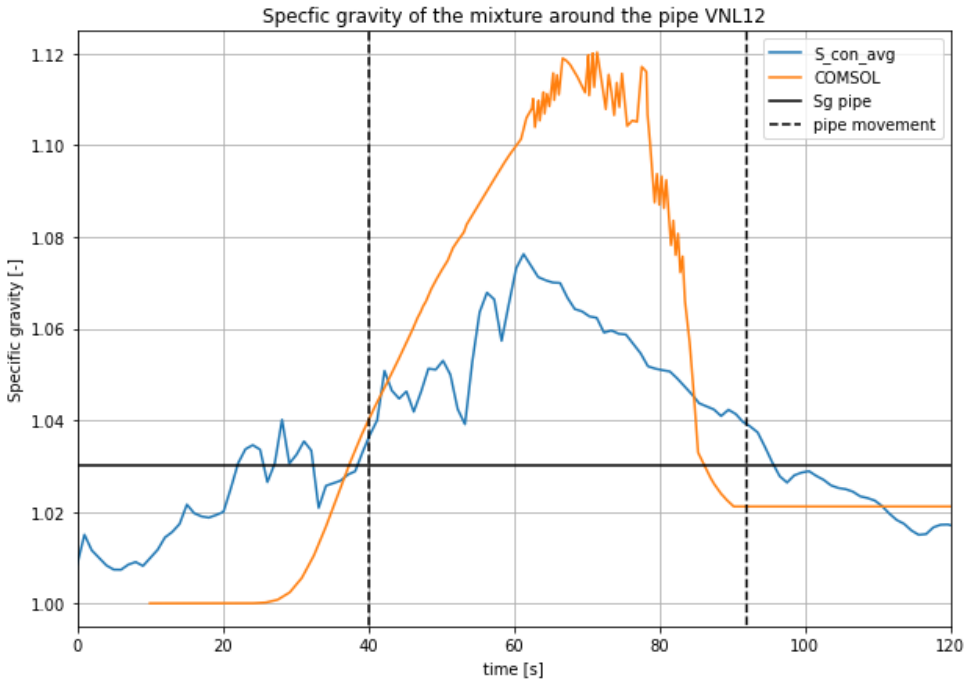

Figure 5.17: Specific gravity built up VNL12

5.4.3. Friction force

The friction force is present during the formation of the new sand layer and only when the pipe is in contact with the soil and thus is not (yet) floating. The friction coefficient (μ) for a sand-steel interface is approximately 0.6[-] under normal stress conditions. Eikhout (2021) calculated the friction coefficient based on the calculation method (Eq.2.13) suggested by (White and Randolph, 2007). Based on this method, Eikhout (2021) calculated for the small-scale experiments a friction coefficient between 1.20 and 1.45[-].

For most experiments where pipeline flotation has been observed, the time span during which friction is relevant, is relatively short. An example of this can be found in the numerical simulation of experiment VVL39. Depicted below is the resulting force balance for test VVL39 (Figure 5.18). For this case, the new formed sand layer builds up after 31[sec] whereas pipe movement was recorded at 45[sec]. Moreover, the sedimentation front, at the moment of flotation, is at a height of only 1[cm] (embedment rate of the pipe of 10%), which indicates that the friction force can not yet be very extensive. Even extreme friction forces (where μ = 2.4) cannot fully explain the time delay between the expected and actual flotation moment.

A friction force resulting from the new formed sand layer has to be added to the force balance. A constant friction coefficient between 0.6 and 0.9 seems reasonable from a theoretical perspective. Because this friction force develops as the pipe embedment increases and stops at the moment of flotation, this force on itself does not completely explain the time delay between the expected and actual flotation moment. For the experiments VML33 and VVL39 significant other forces might be considered to explain this difference.

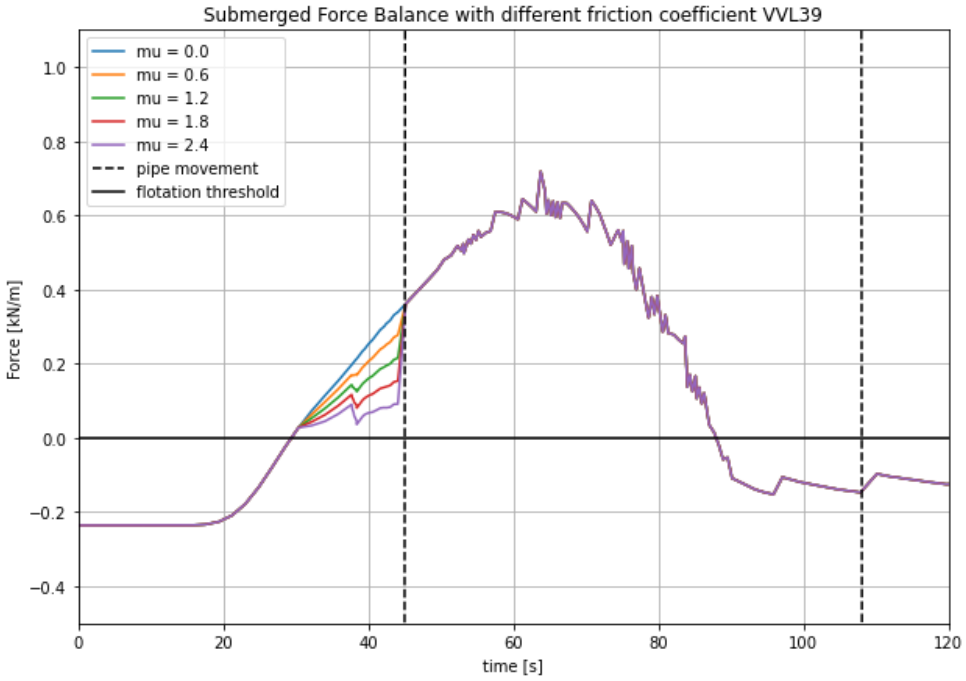

Figure 5.18: Influence of the friction coefficient on the resulting force balance for test VVL39

5.4.4. Possible additional downward force(s)

As discussed, the friction resulting from the new formed sand layer can not explain the time delay between the expected and actual flotation moment in test VVL39 (Figure 5.18). In order for the force balance to exceed the flotation threshold at the moment of actual pipe movement, a constant force (depicted as constant friction force) with a magnitude of $0.35kN/m$ has to be added to the force balance for this specific case (Figure 5.19).

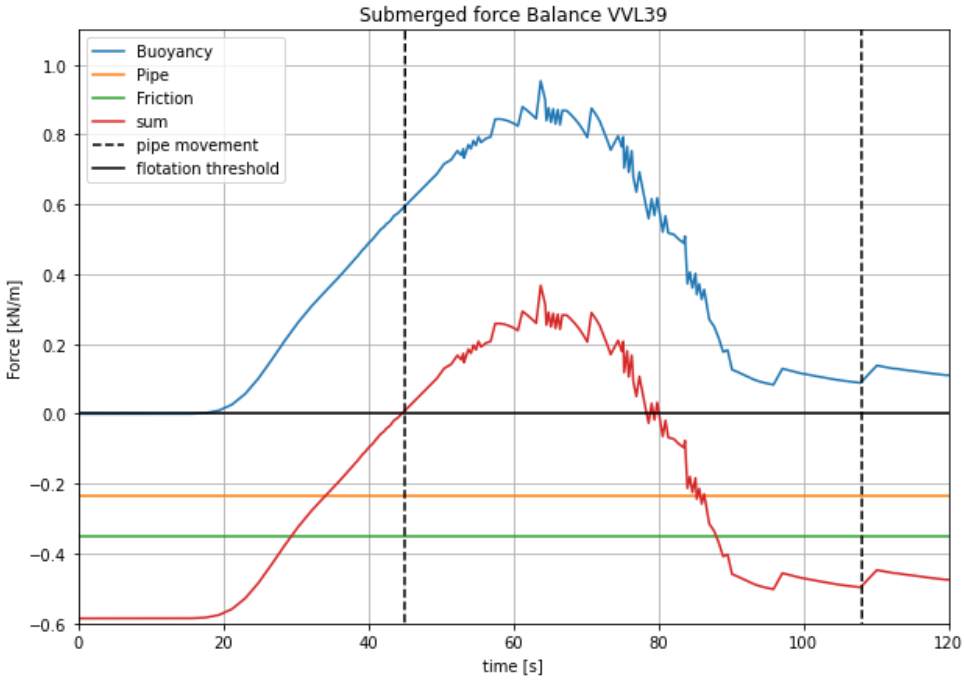

Figure 5.19: Constant additional downward force in the force balance of VVL39

Not only at test VVL39 but also at tests VML30 and VML33 a significant offset between the actual and predicted flotation moment are present. In these cases the actual flotation occurs approximately 5-15[sec] after exceeding the theoretical flotation threshold. A small additional downward force with the order of magnitude of 0.1-0.5[kN/m] could be added to the force balance in order to reduce the offset between the theoretical- and actual moment of flotation. This additional force may result from friction in the connection of guiding rod (Figure 4.6) or result from negative pore pressures when the pipe is on the verge of moving upwards. The magnitude of this force(s), however, is very speculative since the experimental data do not directly indicate on a constant additional force present during every experiment. Moreover, literature on these low stress conditions is limited.

In case additional downward forces are considered, the phase transition concentration can be increased. An example is provided with the numerical results from a simulation of test VNH47. During the test VNH47 the pipeline did not float. When the transition concentration is 40% the maximum buoyancy force generated by the mixture is close to equal to the self weight of the pipe (Figure 5.15). The friction force from the contact of the pipe with the new formed sand layer ensures the force balance to remain negative (Figure 5.20). In the case the transition concentration is 50%, the maximum buoyancy force increases significantly. The friction force in this case, cannot explain the absence of actual pipe flotation. With an additional downward force, equal to -0.65[kN/m], the resulting force does not exceed the flotation threshold (Figure 5.21).

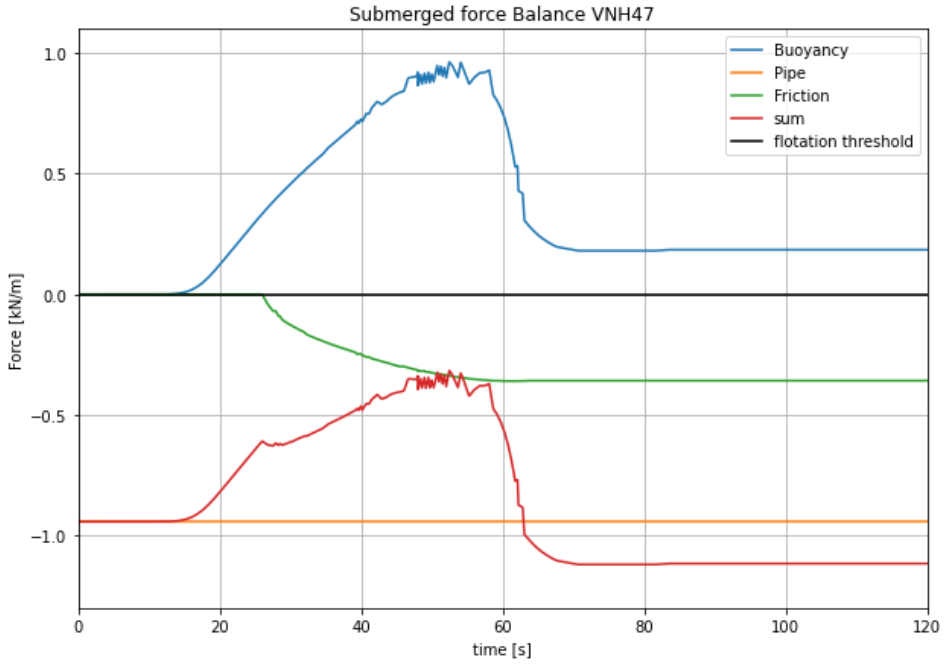

Figure 5.20: Force balance VNH47 phase transition concentration = 40%

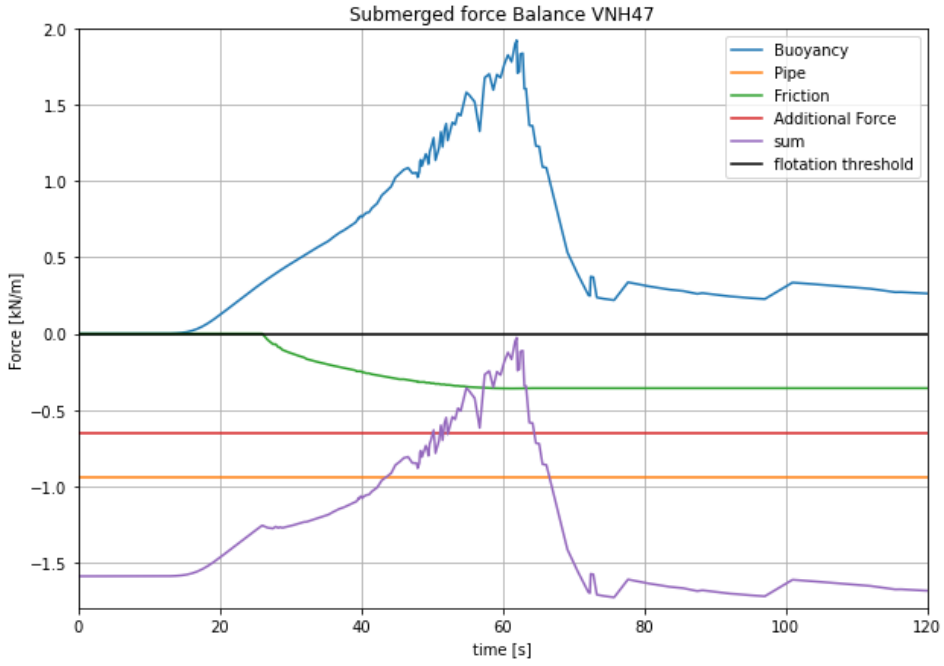

Figure 5.21: Force balance VNH47 in case the phase transition concentration is 50% with additional negative force

5.4.5. Results: force balance

From the modelling results of test VNL12, no additional downward force is needed since the offset between the expected and actual flotation moment is limited (Figure 5.22). The friction force in figure 5.22 has been added for illustrative purposes only as the pipe already started its movement at the time the new formed sand layer is developing.

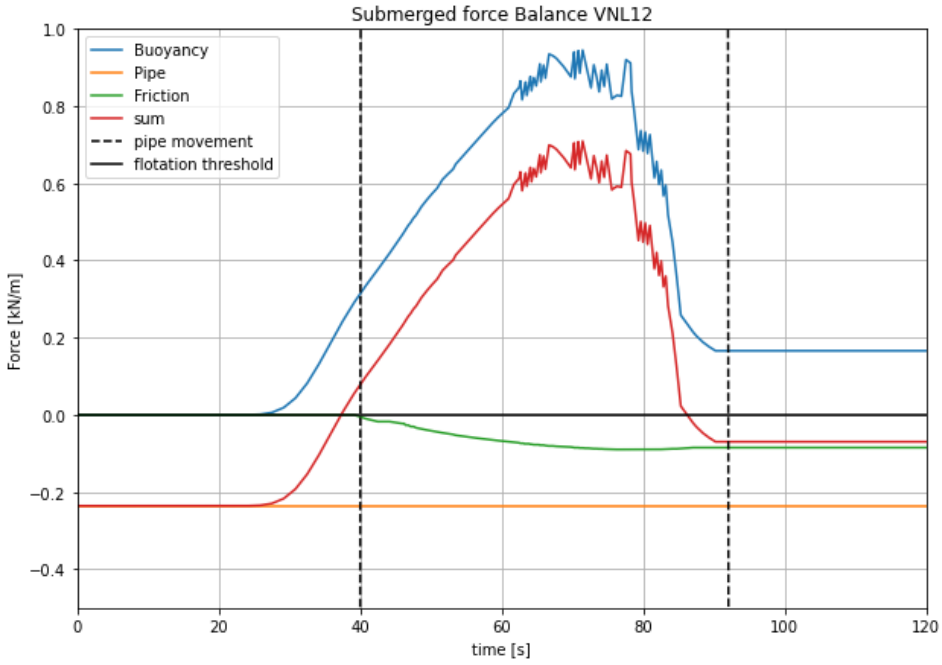

Figure 5.22: Force balance VNL12

Concluding, the buoyancy force acting on the pipe is based on a phase transition concentration of 40%. The thickness of the transition layer is to a large extend influenced by the artificial diffusion added to the numerical model. The exact thickness of this layer is important in assessing the buoyancy force acting on the pipe. From the numerical results, the thickness of this layer varies between 0.5[cm] and 2.0[cm], however if less diffusion is added the thickness of this layer reduces significantly. A friction force following from the embedment of the pipe is added to the force balance. A friction coefficient of 0.6[-] has been used in the calculations regarding this force. Little literature is currently available on the low stress conditions as present during the small-scale experiments. It has been pointed out that additional downward forces might be present. However, there are large uncertainties regarding the actual presence and potential magnitude of these force(s).

5.5. Real application

An attempt has been made in order to simulate a more realistic scenario. The numerical model has been validated against the small-scale experiments. Thus far, it can be concluded that the numerical model is able to solve buoyant driven sedimentation and is reasonably well in line with the small-scale physical experiments.

In the more realistic scenario a trench with a 1.0[m] diameter pipe has been backfilled. The specific gravity of the pipeline is 1.184[-]. The SOD is 5.0[m] and the transition from a momentum flux to a buoyancy flux is estimated to be at an elevation of 4.5[m]. Moreover, the material will be discharged with a constant particle concentration over time (c_{dis}= 25%). The analyses presented in this section have the objective to answer the following questions:

- How does the model cope with large inflow concentrations?
- Will the thickness of the transition layer change as the domain is enlarged?
- Is a large diameter pipe indeed less susceptible for the phase transition concentration?
- How does the maximum specific gravity change as more sand is discharged?

This analyses consists of six simulations; three simulations with an exponent in the hindered settling formulation of 1.0 (n = 1), and three simulations where the exponent is 3.0 (n = 3). The same terminal velocity and -parameter have been used as in the small-scale experiments. The hindered settling

formulation is: $v(c) = 0.019 * (1 - 1.65 * c)^n$ [m/s]. Moreover, the same numerical settings have been used in terms of mesh density, time step and tuning parameter. The reasoning behind the two different exponent-cases is to identify how the inflow concentration and the SG development are affected by the exponent when the discharge concentration has significantly increased.

Moreover, for each case three scenarios were tested; where respectively 25[cm], 50[cm] and 75[cm] of sediment has been deposited. In addition, the hypothesis that the phase transition concentration is less relevant in the case of larger pipe diameter has been tested.

5.5.1. Hindered settlement exponent equals 1.0

The concentration profiles for the case where n=1 and a total of 50[cm] sediment has been discharged, is displayed in the figure below (Figure 5.23). The concentration profiles for the cases where 25[cm] and 75[cm] have been discharged can be found in Appendix C.

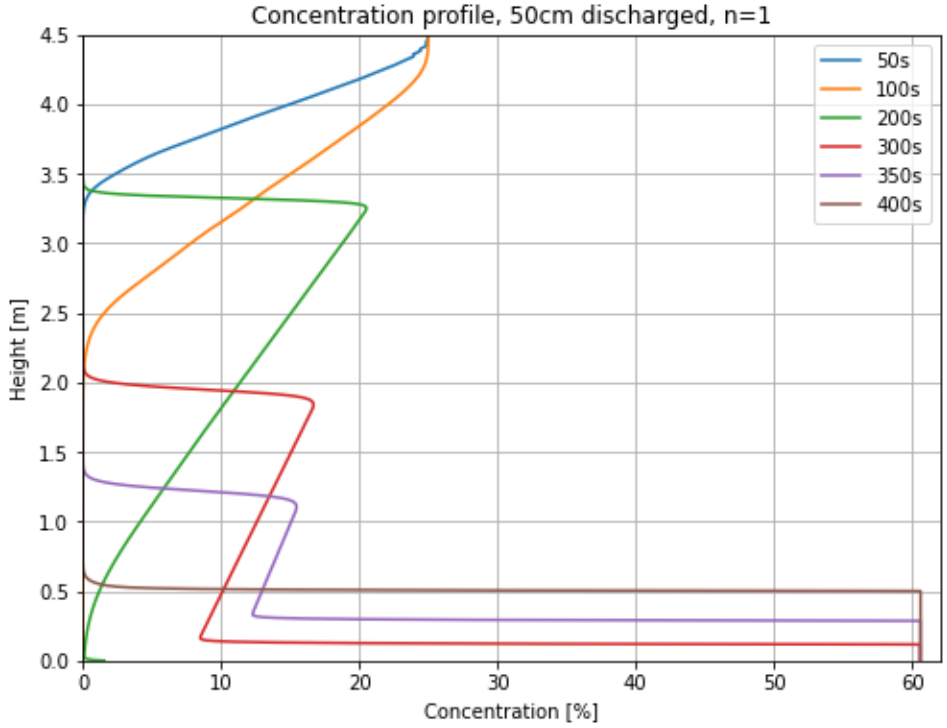

Figure 5.23: Concentration profiles, 50[cm] discharged, n = 1.0

The development of the specific gravity for this case is displayed in figure 5.24. The average SG around the pipe has been calculated based on three different phase transition concentrations: 30%, 40% and 50%. As expected, the maximum SG around the pipe as well as the development of the specific gravity around the pipe are not significantly influenced by the phase transition concentration.

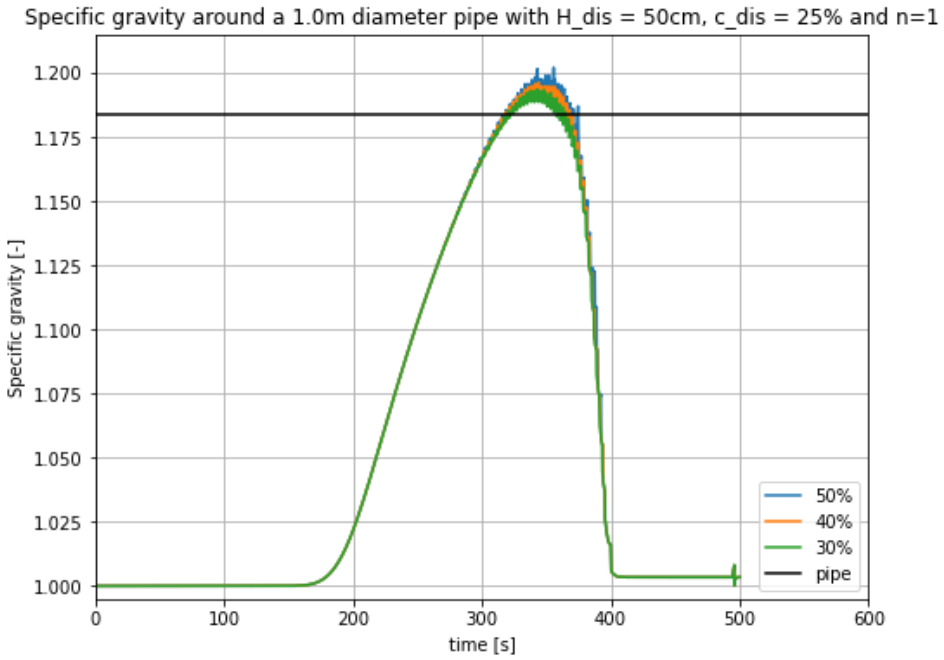

Figure 5.24: Specific gravity around a 1.0m diameter pipe with a discharge concentration of 25% (n = 1.0)

The SG development for the three scenarios (25[cm], 50[cm] and 75[cm]) have been displayed in figure 5.25. Interestingly, the maximum specific gravity around the pipe has not increased in the case where 75[cm] sand has been discharged compared to the case where 50[cm] sand has been discharged.

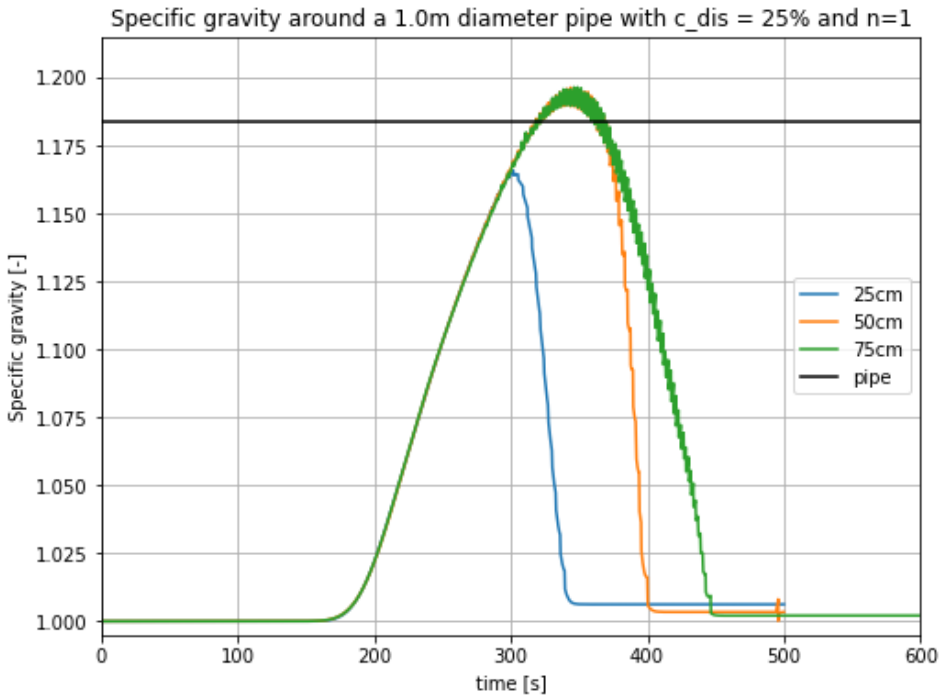

Figure 5.25: Specific gravity development around a 1.0m diameter pipe with a discharge concentration of 25% with deposition of 25[cm], 50[cm] and 75[cm] sand (n = 1.0)

5.5.2. Hindered settlement exponent equals 3.0

The concentration profiles for the case where n=3 and a total of 50[cm] sediment has been discharged, is displayed in the figure below (Figure 5.26). The concentration profiles for the cases where 25[cm] and 75[cm] have been discharged can be found in Appendix C.

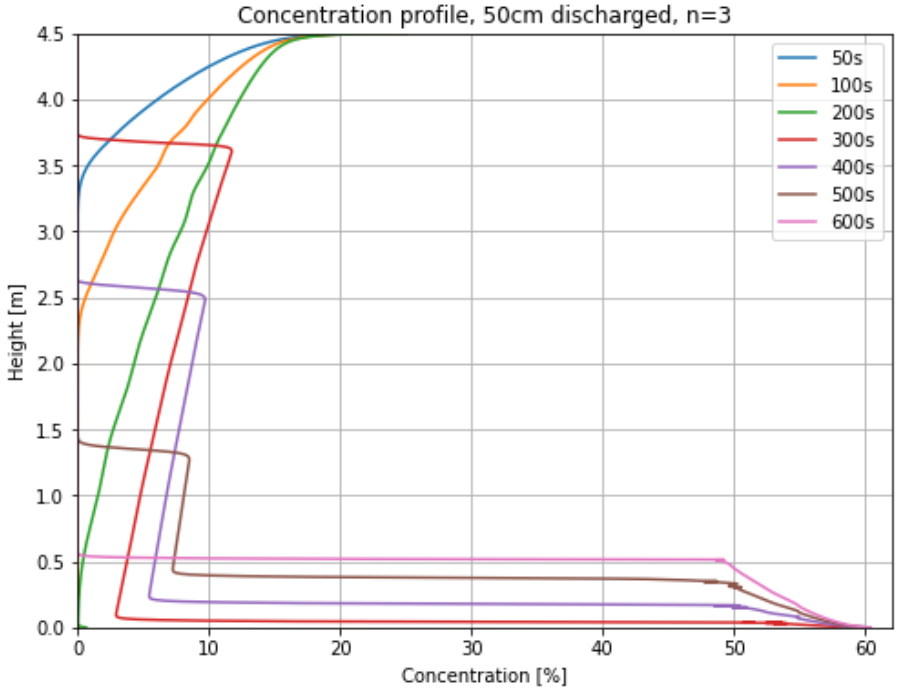

Figure 5.26: Concentration profiles, 50[cm] discharged, n = 3.0

The development of the specific gravity for this case is displayed in figure 5.27. The average SG of the water-sand mixture around the pipe has been calculated based on three different phase transition concentrations: 30%, 40% and 45%. The maximum specific gravity in the scenario where the phase transition concentration is 45%, is slightly higher compared to the two other phase transitions.

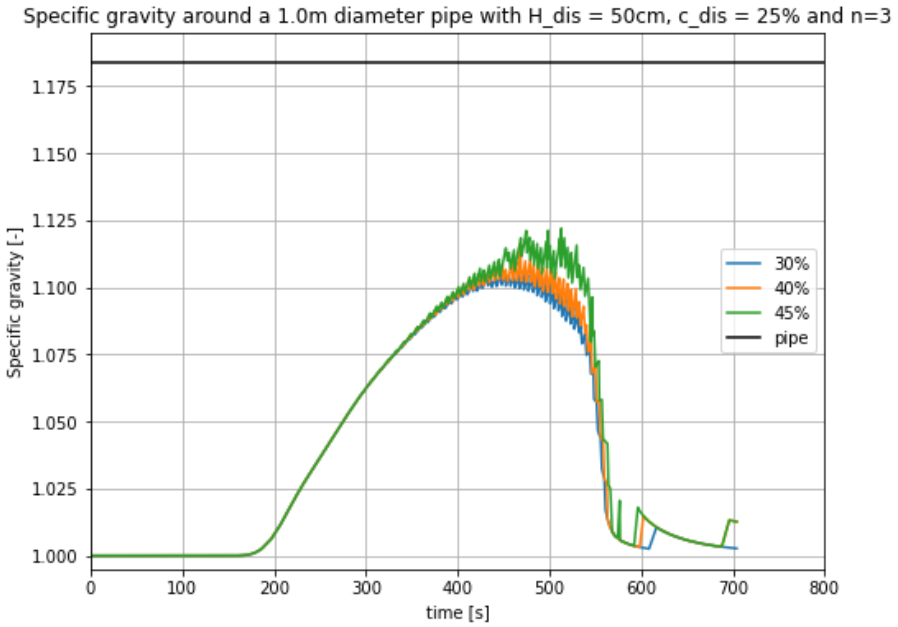

Figure 5.27: Specific gravity around a 1.0m diameter pipe with a discharge concentration of 25% (n = 3.0)

The SG development for the three scenarios (25[cm], 50[cm] and 75[cm]) have been displayed in figure 5.28. Again, the maximum specific gravity has not increased in the case where 75[cm] of soil has been discharged compared to the case where 50[cm] has been discharged.

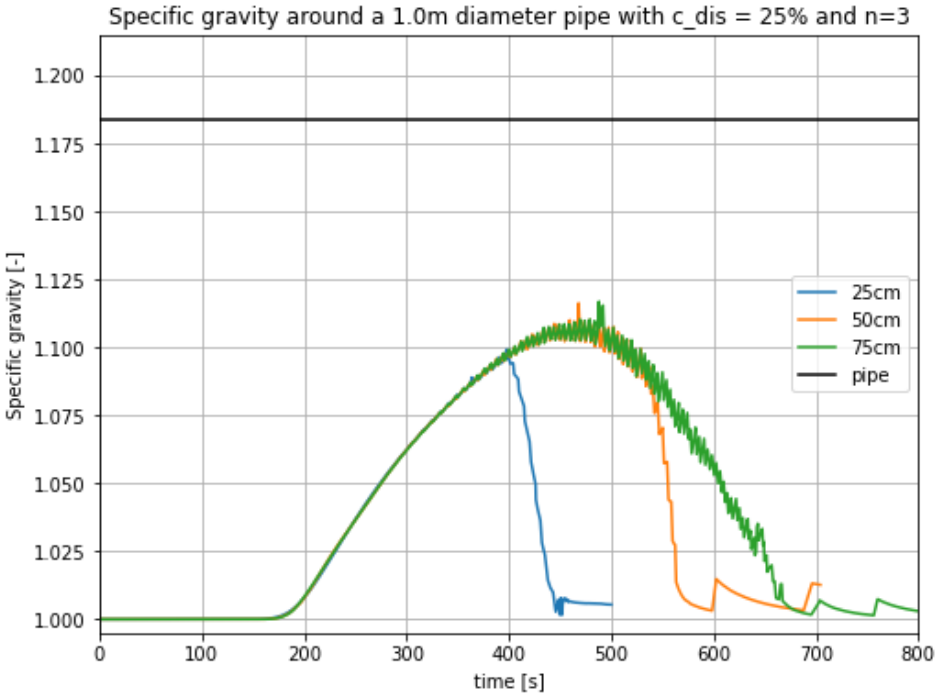

Figure 5.28: Specific gravity development around a 1.0m diameter pipe with a discharge concentration of 25% with deposition of 25[cm], 50[cm] and 75[cm] sand (n = 3.0)

5.5.3. Comparison and conclusions

The questions stated at the beginning of this section can be answered:

- How does the model cope with large inflow concentrations?

  In the modelling cases where n=1.0, the inflow concentration in the domain is equal to the discharge concentration ($c_{dis} = 25\%$).
  The modelling cases where n=3.0 however, the inflow concentration is significantly less than the discharge concentration (+/- 18%).

- Will the thickness of the transition layer change as the domain is enlarged?

  From the concentration profiles it can be noticed that the layer thickness over which the concentration jump occurs remains between 0.5[cm] and 2.0[cm]. This is despite the enlargement of the domain and increase in domain concentrations.

- Is a large diameter pipe indeed less susceptible for the phase transition concentration?

  Yes. In particular for the case where n=1.0 the differences in the maximum SG and built up of the SG are minor when considering different phase transition concentrations.
  In the modelling case where n=3.0, the maximum specific gravity and the development of the specific gravity over time are noticeable different when the phase transition concentration is 45%. This is due to the fact that the deflection point of some of the concentration profiles is at a concentration less than 45%.

- How does the maximum specific gravity change as more sand is discharged?

The maximum specific gravity increases as more sand is being discharged. However, this increase is finite; it has been noticed that the maximum SG has not increased when 75[cm] sand has been discharged compared to 50[cm]. The maximum SG can be related to embedment rate; from the modelling data of more realistic scenarios it can be noticed that the SG peak is present when approximately 30-40% of the pipeline is embedded. From the experimental data of Eikhout (2021) it can be noticed that the maximum SG has been reached when 20-40% of the pipe is embedded.

Another interesting observation from these analyses is that the maximum specific gravity of the modelling cases where n =1.0 is structurally and significantly larger compared to the cases where n=3.0 (Figure 5.29).

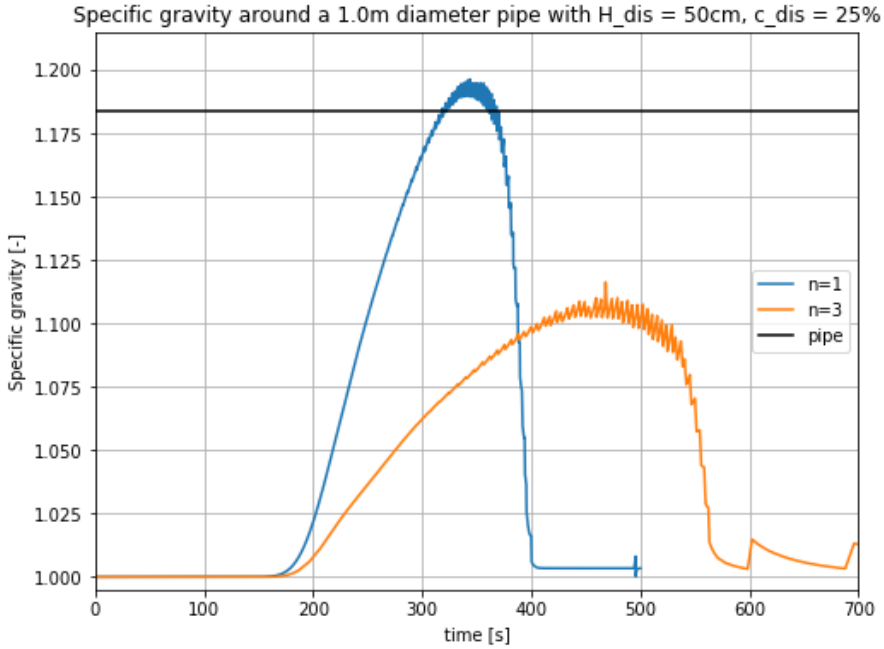

Figure 5.29: SG development when 50[cm] sand is discharged

The maximum SG is larger because as the exponent decreases, the particles are less hindered in their downward movement at higher concentrations; the velocity of the water-sand mixture is larger for the case where $n = 1$ compared to the case where $n = 3$, in particular at high particle concentrations. This results in a larger discharge flow rate and higher domain concentration around the pipe for the case where the exponent equals 1.0.

5.6. Simplified calculation method

In this section a simplified, spreadsheet friendly model is proposed. The model assesses the average specific gravity around the pipe at every embedment rate (Figure 5.30). The simplified model is based on the following assumptions:

- The transition layer is always directly above the sedimentation front;
- The average particle concentration of the transition layer is the average between the domain concentration and the phase transition concentration;
- The domain concentration is constant over time.

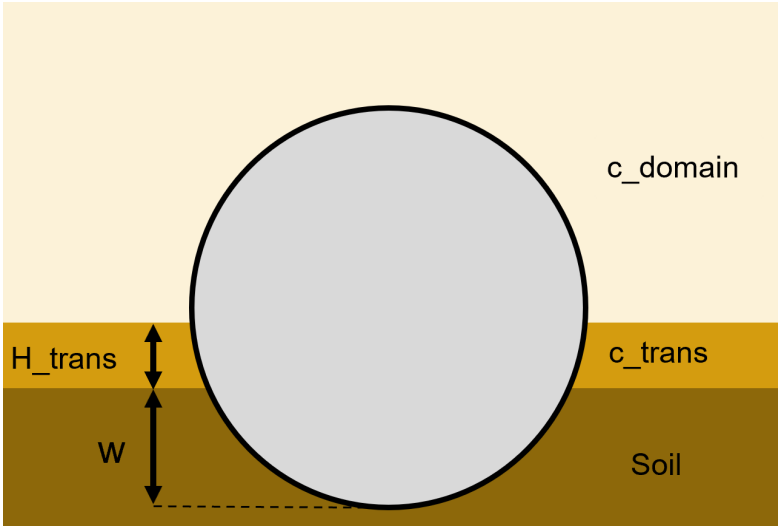

Figure 5.30: Schematization simplified model

In the model, among others, the following parameters can be adjusted:

- The phase transition concentration;
- The domain concentration;
- The thickness of the transition layer;
- The diameter of the pipe.

The average domain concentration is fairly arbitrary since in reality the domain concentration varies over time and space. Considering this parameter as a constant over time and space thus is an important assumption and results in a significant uncertainty in the model. In the results depicted below, the average domain concentration is equal to 50% of the maximum inflow concentration. Moreover, uncertainties remain regarding the thickness of the transition layer. The thickness of the layer over which the concentration jump occurs is assumed to be constant over time in this model. However, from the numerical simulations it was noticed that the thickness of this layer is not constant over time and is, to a large extent, dependent on the artificial diffusion added in the numerical model. The set of input parameters used for verification against the numerical model and experimental data is listed in the table below (Table 5.4).

Table 5.4: Model input for validation against numerical model and experimental data

Model input		
Parameter	Input value	Explanation
D	0.1 [m]	Diameter of the pipe
H_{trans}	0.02[m]	Thickness transition layer
c_{domain}	4%	Constant domain concentration
c_{phase}	40%	Phase transition concentration
ρ_p	2650 [kg/m^3]	Density sand grains
ρ_w	1000 [kg/m^3]	Density water
z	0.25[m]	Domain height (from discharge point to top sand bed)

The average specific gravity of the water-sand mixture around the pipe is plotted against the embedment rate of the pipe (Figure 5.31). It can be noticed that the agreement between the simplified calculation method and numerical model is limited for the case of test VVL39.

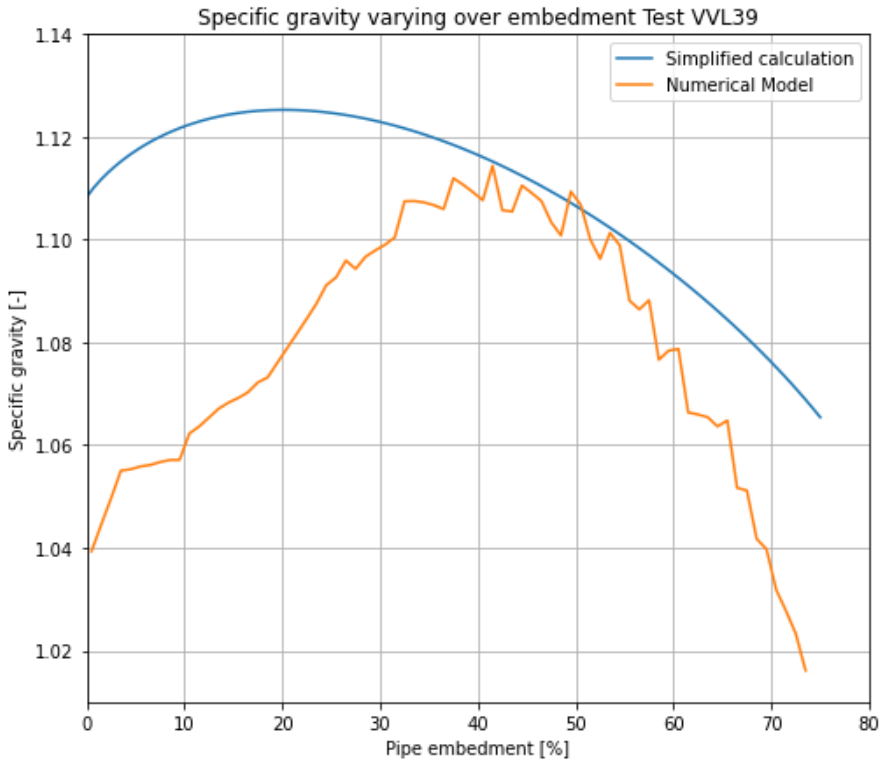

Figure 5.31: SG development when 75cm discharged

The simplified model is not able to directly provide an estimation of the specific gravity of the sediment mixture over time. Based on certain distinct moments in time, the simplified calculation method has been projected on the experimental- and numerical data for test VML33 (Figure 5.32). The solid black lines depict the specific gravity calculated with the simplified model whereas the dotted black lines interpolate between the calculation points. With red numbers four distinct moments in time have been annotated:

- 1. The discharged mixture reaches the top of the pipeline. From this moment in time, as the sediment mixture moves downward along the pipe, the average specific gravity around the pipe will increase;
- 2. At this moment in time the sediment mixture reaches the top of the sand bed. The pipeline is now completely submerged in the water-sand mixture (the particle concentration of the mixture is equal to the predefined domain concentration);
- 3. At this moment in time the formation of the new sand layer starts. The particle concentration around the bottom of the pipe has exceeded the phase transition concentration. Between time instant two and time instant three the transition layer develops. Thus at the end of time instant two, no transition layer is yet present above the sedimentation front, whereas at time moment three the 2[cm] thick transition layer has been formed and the built-up of the new sand layer starts;
- At time instant four the pipe is for 75% embedded. The transition layer and water-sand mixture are still present but will vanish over time, which has been indicated with the black dotted line.

It can be noticed that the agreement between SG development estimated with the simplified calculation and the SG development resulting from the numerical model is decent for this test case.

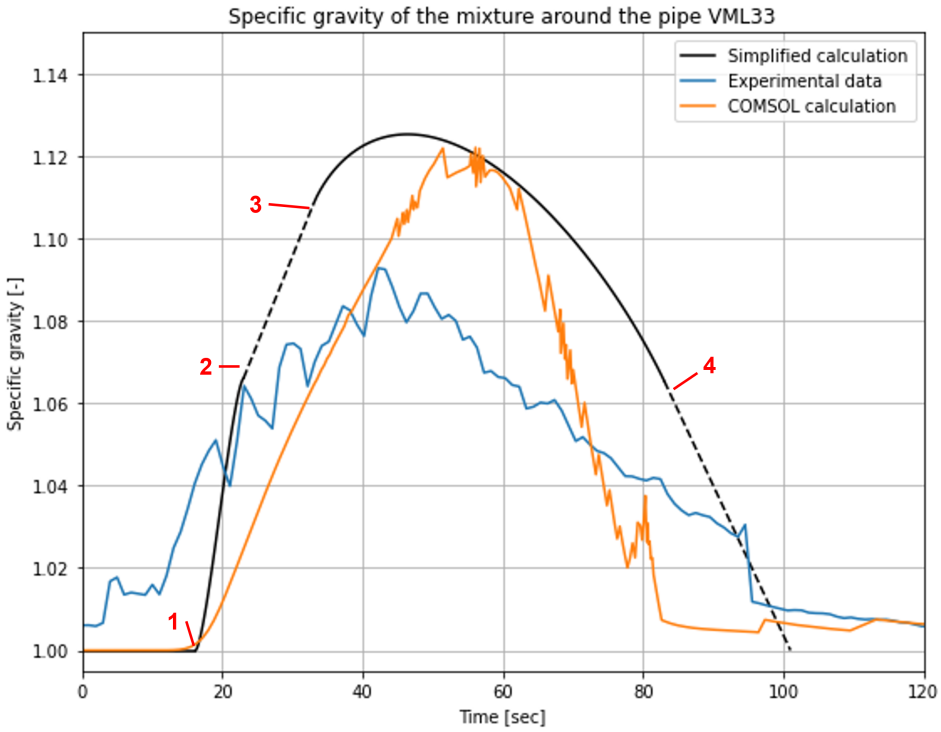

Figure 5.32: SG development when 75cm discharged

The python script of this simplified model can be found in Appendix D.

6

Discussion

In this chapter the results of this study will be discussed. The sedimentation problems have been modelled as a convection problem in which the hindered settlement velocity describes the movement of the water-sand mixture. The hindered settling formulation of Metha (1986) was found to be most suitable for the modelling of the fine grained sand-water mixture.

6.1. Numerical modelling of small-scale physical experiments

The numerical model suggested in this research project is able to predict the concentration development of the water-sand mixture over time and space. The concentration profiles obtained with the numerical simulations are well in line with the concentration measurements from the small-scale experiments. Moreover, the inflow of material can be modelled with the implementation of the dummy reservoir. The particle concentration of the discharged mixture can be constant over time as well as increasing over time.

Some of the parameters in the hindered settling formulation deviate slightly from literature. In this respect, a terminal settling velocity (vs) corresponding to the D75 grain size percentile was found optimal for modelling instead of the terminal corresponding to the median grain size. In addition, the RZ-exponent expected based on the grain size of the Geba Weiss sand is in the range of 3.8-4.4. The numerical results were found to be in better agreement with the experimental data with a RZ-exponent of 3.0.

The empirical α-parameter in the hindered settlement formulation was found useful to limit the maximum concentration. Soil tests and experimental data suggest a porosity of the loose sand bed of approximately 0.4[-]. This corresponds to a particle concentration of 60% and therefore the α-parameter of 1.65 has been suggested.

It is important to highlight that Geba Weiss sand used in the small-scale physical experiments is not completely uniform. Small deviations in particle size result in significant deviations in settling velocities and vertical size sorting is expected. The numerical model considers a uniform grain size and therefore only a single terminal settling velocity and RZ-exponent. It was found that, when considering inflow of material in the model, the model was not able to produce physical results in case the RZ-exponent was a decimal number.

When modelling the inflow of water-sand mixture it was not found possible to model the exact concentration development at the height of inflow. In particular the period where the inflow concentration decreases over time, could not be implemented using the same discharge-formulation in the dummy reservoir. The result is that, later in time, the experimental measurements indicate that there are particles present in the domain above the sedimentation front whereas this inflow is absent in the numerical model.

Simplifying a dynamic three-dimensional process into a one-dimensional model comes with certain assumptions and difficulties. During the experiments the solids have been discharged upwards. The result of this discharge method is that the predefined discharge- period and concentration are not directly relatable to the measurements at the height of the T-junction. In addition, the total volume of solids measured at the height of the T-junction does not necessarily correspond with the amount of solids deposited at the location of the measurement device.

Artificial diffusion needs to be added to the convection equation in order to obtain a physical solution and reduce the non-physical oscillations. One of the main consequences of the artificial diffusion is that the concentration jump (from the maximum domain concentration to the phase transition concentration) becomes less sharp. Whether this is inaccurate from a physical perspective is not clear. Due to the distance between the measurement points in the physical experiments it can only be concluded that the height over which this jump occurs is less than 2.5[cm]. The distance between the measurement points in the physical experiments also results in an uncertainty of the exact location of this concentration jump with respect to the pipe. It has however been reasoned and shown that the location and thickness of this thin layer has a severe effect on the buoyancy force acting on the small diameter pipeline.

The particle concentration over time and space resulting from the numerical model has been processed in a force balance of the pipeline over time. The force balance is able to predict whether or not flotation of the pipe in the small-scale experiments will occur. The forces present in the force balance are: the selfweight of the pipeline, the buoyancy force and the friction between the new-formed sand layer around the pipe and the pipeline. The friction force is a function of the embedment rate and the friction coefficient. Little is known about the effect of the low stress state in the physical experiments on the friction coefficient between sand and steel. The numerical data indicates that little embedment is present at the moment the theoretical flotation threshold is exceeded and movement of the pipe has been recorded during the small-scale experiments. The limited embedment of the pipeline results in a small effect of the friction force on the force balance. The particle concentration at which the phase transition from a water-sand mixture to a sandy soil occurs, is suggested to be 40%. Theoretically, the soil gains instant strength as the sand grains form a connecting network. The concentration at which the sludge can be classified as a soil is not exactly clear; this point however, is expected to be at a particle concentration somewhere in the range between 35% and 55%.

It has been stated that additional downward forces might be present in the small-scale physical experiments. These forces however, remain speculative since little data and information is present on the exact origin and magnitude of these potential forces.

6.2. Real application

A more realistic hypothetical backfilling scenario has been tested with the numerical model. From the cases tested, several important conclusions can be drawn as well as some limitations of the numerical model emerge.

The model has been set-up to simulate the buoyant driven behaviour as present in the small-scale experiments. The numerical model therefore, is not able to model the inflow of material with a large initial velocity. In this respect, it is not possible to model a discharge velocity of 2.0[m/s] in case the settling velocity in the domain is over 100 times less ($v(c) < 0.020[m/s]$). The physical domain in this case is not able to cope with the large amount of solid inflow. This was found especially relevant in modelling the more realistic case since the large discharge concentration results in a very low discharge velocity.

Moreover, the RZ-exponent was found to have a severe effect on the volume of solids entering the physical domain over time when considering high inflow concentrations. This also translates to significant differences in the SG development.

6.3. Simplified calculation method

With the simplified calculation method an attempt has been made to further simplify the determination of the buoyancy force acting on a pipe. This calculation method also considers the diameter of the pipe. This is an advantage of this method since it has been concluded that effect of the phase transition layer on the buoyancy force acting on the pipe reduces as the diameter of the pipe increases.

The accuracy of this model depends primarily on the chosen domain concentration and the thickness of the phase transition layer. The determination of a constant domain concentration over time and space is difficult and results in a significant uncertainty in this model. From the experimental data and numerical results it can be noticed that the concentration is not constant over time and space. How the concentration develops in the domain when the discharge concentration is high, is not yet fully understood. From the models concerning the more realistic scenario it has been noticed that the domain concentration over time and space is significantly lower than the discharge concentration. Further research might be able to clarify on the relation between the discharge concentration and the domain concentration and propose a method to convert this to a constant concentration estimation. Despite the uncertainties, this calculation method might be a good starting point to assess the buoyancy force acting on the pipe without the use of a numerical model.

7

Conclusions and recommendations

This chapter concludes this research. First, the sub-questions will be answered after which some general conclusions will be presented. Moreover, recommendations for future work are provided in section 7.2.

7.1. Conclusion

7.1.1. Sub-questions

1. What forces can be identified which contribute to the force balance of the pipeline?

   The force driving the potential upward movement of the pipeline is the buoyancy force which is enhanced by the sand concentration of the mixture. The main downward force is caused by the self weight of the pipe. The sedimentation will result in the embedment of the pipe. The embedment has two main consequences: it will reduce the effective area over which the buoyancy force acts and will induce friction between the new formed sand layer and the pipeline. At this moment in time, no literature exists on friction forces present between sand and steel interface at very low stress levels. Additional downward forces might be present. The exact origin of this force/these forces is unknown, however expected is that it might result from negative pore pressures as the pipe moves upward and/ or friction from the guiding rod mechanism in the experimental set-up. The magnitude of this potential force(s) in the order of $0.05 - 0.50[kN/m]$.

2. Which formulation, regarding the hindered settlement of the water-sand mixture matches best with the experimental data?

   The formulation of Mehta (1986) (Eq.3.17), which was originally proposed for the settling of mud flocs, was identified most suitable for modelling the sedimentation process of water-sand mixture. The α- parameter was found useful in order to limit the concentration. The RZ exponent in this formulation increases the hindered settlement as its value increases. The terminal settling velocity corresponding to the D75-D90 particle size (depending on the preferred calculation method) has been suggested. For the modelling of the physical small-scale experiments by Eikhout (2021) the following hindered settlement formulation is proposed: $v(c) = -0.019 * (1 - 1.65 * c)^3$.

3. What is the influence of different variables in the hindered settlement formulation on the sedimentation process as well as on the buoyancy development?

   The α-parameter determines the maximum particle concentration. This parameter is related to the porosity of the loose sand layer. Moreover, a decrease in this parameter results in an increase in the hindered settlement velocity.

   According to literature the RZ-exponent is related to the particle Reynolds number, which is related to the particles diameter. An increase in the diameter of the particle results in a decrease of the RZ-exponent. Moreover, the RZ-exponent significantly influences the hindered settlement

velocity; an increase in the exponent results in a decrease in the velocity, especially at higher concentrations. Moreover, an increase in the exponent results in a change in the form of the concentration profiles. In particular the concentration built-up from below is influenced. This built-up is vertical in case the exponent equals 1.0 (corresponding to Kynch' initially suggested hindered settling formulation) and will get more gradual as the exponent increases. Moreover, the concentration jump is slightly less sharp the exponent increases.

The terminal velocity is dependent on the particle size. The terminal velocity only influences the overall time period over which the sedimentation process takes place as this parameter does not influence the relative velocity of the mixture.

4. How can the transition from a water-sand mixture to a solid sandy soil be best modelled?

   Theoretically, the water-sand mixture gains instant strength as the sand grains form a connecting network. The water-sand mixture is considered a sandy soil as the particle concentration exceeds 40%; which corresponds to a porosity of 0.6[-].

5. How can the inflow of sediment, both uniform and non-uniform, be best modelled?

   Modelling the inflow with a dummy reservoir is considered to be the best option, in particular in case the inflow concentration is not constant over time. The dummy reservoir has some limitations of which the most important are: no direct control over the inflow concentration and inflow velocity (only via several parameters) and it is not possible to model a turning point, after which the inflow concentration decreases over time. Modelling uniform flow can be done with the dummy reservoir or with a Dirichlet boundary condition.

7.1.2. General conclusions

The numerical model proposed is suitable for the modelling of (buoyant) plume behaviour. Moreover, the numerical model is able to simulate the inflow of material with a constant particle concentration over time as well as an increasing particle concentration over time. Overall, the development of the concentration water-sand mixture resulting from the numerical model is well in line with the small-scale experimental data. With the force balance suggested, it can be reasonably well predicted if and when pipeline flotation occurs.

The analyses on the more realistic scenario indicate that the thickness of the transition layer is independent of the numerical domain. The thickness of this transition layer is to a large extent influenced by the artificial diffusion and varies between 0.5[cm] and 2.0[cm]. In addition, the analyses confirm the hypothesis that a large diameter pipe is less susceptible for the exact phase transition concentration. The exact thickness of the transition layer and the exact phase transition concentration impact the buoyancy force acting on the pipe to a larger extent in case the pipe diameter is relatively small. Therefore it is suggested to consider, besides the weight of the pipe, also the diameter of the pipe when assessing the flotation potential.

A major limitation regarding the numerical model is the inability to add an initial discharge velocity to the discharged mixture. Further research is needed to investigate the possibility of adding an initial velocity or impulse to the discharged mixture.

With the simplified model proposed, the buoyancy force acting on the pipe can be calculated. The advantage of this simplified method is that it considers three phases in the model: the water-sand mixture, a more dense slurry and the soil. The model also considers the diameter of the pipe. The model is able to provide an estimate of the buoyancy force acting on the pipe at different embedment rates. The main assumption and also limitation of this model is that the domain concentration is implemented as a constant over time and space. An accurate prediction of this parameter is difficult and results in a significant uncertainty in the results obtained.

7.2. Recommendations

Further development of the numerical model is advised, in particular with respect to modelling with a larger discharge concentration and discharge velocity. Implementing a impulse acting on the discharged mixture might be considered in future work. When this is implemented, the effect of certain discharge parameters on the buoyancy- and concentration development can be investigated in more detail. In addition, scaling to a two dimensional model is interesting to investigate the effects of discharging under an angle. When this can not be implemented in the COMSOL interface considered in this study, it might be required to consider a more complex Multiphase Flow finite element model.

Improvements can be made with respect to the simplified model proposed in this study. Especially with regards to the considered constant domain concentration. More information on accurate determination of this parameter can be linked to the suggested improvements regarding the numerical model. With a numerical model in which the discharge velocity and discharge concentrations can be increased, a more complete relationship between the discharge parameters and a constant domain concentration can be assessed.

In order to experimentally improve the small-scale experimental model it is suggested to discharge downward from a distance of 50[cm] (5 times the pipe diameter). This is expected to improve the understanding of the discharge parameters in respect to the domain concentration measurements. Moreover, discharging downward is easier to implement and replicate in future numerical studies. Additionally, it is suggested to increase the number of measurement points along the height of the pipe, preferably to one point every centimetre or less. By doing so, more detailed information on the thickness and location of the transition layer can be obtained, as well as a more precise information on the location of the sedimentation front over time.

Eikhout (2021) performed pull-out experiments in order to gain more insight in the friction- and pull-out forces in case of partial embedment of the pipe. However, Eikhout (2021) had to conclude that the forces measured were unrealistically large for the small-scale set-up. It is suggested to perform additional, more controlled, pull-out tests to quantify the friction force and overall break-out forces at certain degrees of embedment. In addition, pressure sensors could be added at the bottom of the pipe in order to obtain more insights into the drainage conditions and potential suction effects that might be of influence at the moment the pipe starts to float.

Bibliography

Baldock, T. E., Tomkins, M. R., Nielsen, P., & Hughes, M. G. (2004). Settling velocity of sediments at high concentrations. *Coastal Engineering*, *51*, 91–100.

Biemans, S. (2012). Prevention of pipeline floatation during dredge-based backfilling. *Delft University of Technology*.

Bizzotto, T., Brown, M. J., Brennan, A., Powell, T., & Chandler, H. (2017). Modelling of pipeline and cable flotation conditions. *Offshore Site Investigation and Geotechnics: Smarter Solutions for Future Offshore Developments*, *1*(2), 865–871. https://doi.org/10.3723/OSIG17.865

Bürger, R., Bustos, M. C., & Concha, F. (1999). Settling velocities of particulate systems: 9. phenomenological theory of sedimentation processes: Numerical simulation of the transient behaviour of flocculated suspensions in an ideal batch or continuous thickener. *International Journal Of Mineral Processing*, *55*, 267–282.

Bürger, R., Evj, S., Karlse, K. H., & Lie, K. A. (2000). Numerical methods for the simulation of the settling of flocculated suspensions. *Chemical Engineering Journal*, *80*, 91–104. https://doi.org/10.1016/S1383-5866(00)00080-0

Bürger, R., & Tory, E. M. (2000). On upper rarefaction waves in batch settling. *Powder Technology*, *108*, 74–87.

Burgmans, S. H. (2005). Backfillen met de volvox asia. *Van Oord, Technical Report*.

Bustos, M. C., Concha, F., Bürger, R., & Tory, E. M. (Eds.). (1999). *Sedimentation and thickening. phenomenological foundation and mathematical theory* (8th ed.). Kluwer Academic Publishers.

COMSOL-Multiphysics. (2019). *Comsol multiphysics reference manual*. COMSOL Inc.

Dankers, P. J. T. (2006). On the hindered settling of suspensions of mud and mud-sand mixtures. *Delft University of Technology*.

de Nijs, M. A. J., van der Hout, R., Peters, J., & Haverkamp, J. (2009). Laboratory experiments on the effect of suction head modifications on spill of backfill. *Van Oord, Technical Report*.

Eikhout, P. M. A. (2021). Offshore pipeline flotation during sand backfilling with a tshd. an experimental study. *Delft University of Technology*.

Ferguson, R., & Church, M. (2004). A simple universal equation for grain settling velocity. *Journal of sedimentary Research*, *74*(6), 933–937.

Finch, M. (1999). Upheaval buckling and floatation of rigid pipelines : The influence of recent geotechnical research on the current state of the art. *Offshore Technology Conference*, 1–10.

Finch, M., & Machin, J. B. (2001). Meeting the challenges of deepwater cable and pipeline burial. *Offshore Technology Conference*, 1–6.

Hernández, H., Massart, T. J., Peerlins, R. H. J., & Geers, M. G. D. (2018). A stabilization technique for coupled convection-diffusion-reaction equations. *International Journal for Numcerical Methods in Engineering*, *116*(1), 43–65. https://doi.org/10.1002/nme.5914

Kynch, G. J. (1951). A theory of sedimentation. *Transactions Faraday Society*.

Latsa, M., Assimacopoulos, D., Stamou, A., & Markatos, N. (1999). Two-phase modeling of batch sedimentation. *Applied Mathematical Modelling*, *23*, 881–897.

Li, Z., Guo, L., Zhao, Y., Peng, X., & Kyegyenbai, K. (2022). A particle size distribution model for tailings in mine backfill. *Metals*, *12*(594).

Maude, A. D., & Whitmore, R. L. (1958). A generalized theory of sedimentation. *Br. J. Appl. Phys.*, *9*, 477–482.

Mehta, A. J. (1986). Characterisation of cohesive sediment properties and transport processes in estuaries. *Estuarine Cohesive Sediment Dynamics, Lecture Notes in Coastal and Estuarine Studies*, 290–325.

Minico, M. D. (2020). Finite element analysis of sedimentation and consolidation of soils. *Politecnico Di Milano*.

Palmer, A. C., & King, R. A. (Eds.). (2008). *Subsea pipeline engineering* (2nd ed.). Tulsa :PennWell.

Pane, V., & Schiffman, R. L. (1985). A note on sedimentation and consolidation. *Geotechnique*, *35*(1). https://doi.org/10.1680/geot.1985.35.1.69

Randolph, M. F., & Gourvenec, S. (Eds.). (2011). *Offshore geotechnical engineering*. Oxon:Spon,

Richardson, J. F., & Zaki, W. N. (1954). Sedimentation and fluidisation: Part i. *Trans. Inst. Chem. Eng.*, *32*, 1339–1360.

Rowe, P. N. (1987). A convenient empirical equation for estimation of the richardson-zaki exponent. *Chemical Engineering Science*, *42*(11), 2795–2976.

Salsa, S. (Ed.). (2008). *Partial differential equations in action. from modelling to theory*. Springer.

Shamsai, A., Pak, A., Bateni, S. M., & Ayatollahi, S. A. H. (2007). Geotechnical characteristics of copper mine tailings: A case study. *Geotechnical and Geological Engineering*, *5*(25), 591–602. https://doi.org/10.1007/s10706-007-9132-9

Spearman, J., & Manning, A. J. (2017). On the hindered settling of sand-mud suspensions. *Ocean Dynamics*, *67*, 465–483. https://doi.org/10.1007/s10236-017-1034-7

Stamatakis, K., & Tien, C. (1992). Batch sedimentation calculations - the effect of compressible sediment. *Powder Technology*, *72*, 227–240.

Tiller, F. M. (1981). Revision of kynch sedimentation theory. *AIChE*, *27*(5), 823–829.

Tomkins, M. R., Baldock, T. E., & Nielsen, P. (2005). Hindered settling of sand grains. *Sedimentology*, *52*, 1425–1432. https://doi.org/10.1111/j.1365-3091.2005.00750.x

Uesugi, M., Kishida, H., & Uchikawa, Y. (1988). Behavior of sand particles in sand-steel friction. *Soils and Foundations*, *28*(1), 107–118.

White, D. J., & Randolph, M. F. (2007). Seabed characterisation and models for pipeline-soil interaction. *International Journal of Offshore and Polar Engineering*, *17*(3), 193–204.

Winterwerp, J. C. (2002). On the flocculation and settling velocity of estuarine mud. *Continental Shelf Research*, *22*, 1339–1360.

Yang, K. (2020). Physical modelling of offshore pipeline flotation during tshd sand backfill. *Delft University of Technology*.

Zijlema, M. (2015). Computational modelling of flow and transport. *Educational resource Delft University of Technology*.

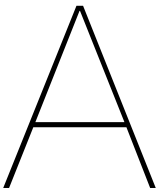

Appendix A

In this appendix all the results from the modelled small-scale experiments are displayed.

Test VNL12		
Parameter	Experimental data	Numerical implementation
Flotation	Yes	Yes
T_{dis}	60[s]	60[s]
C_{dis}	25%	7.2%
H_{sol}	0.0355 [m]	0.0348[m]
H_{sed}	5.0-7.5[cm]	6.2[cm]

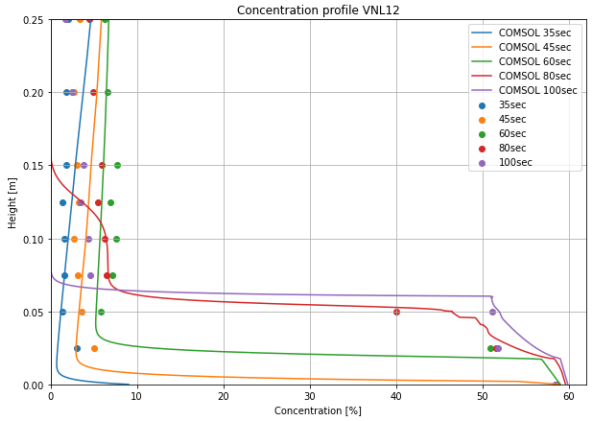

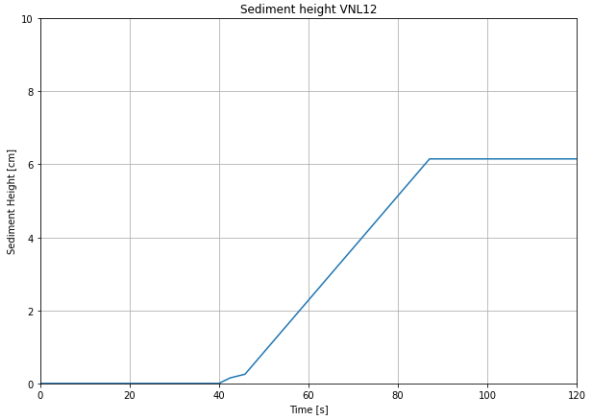

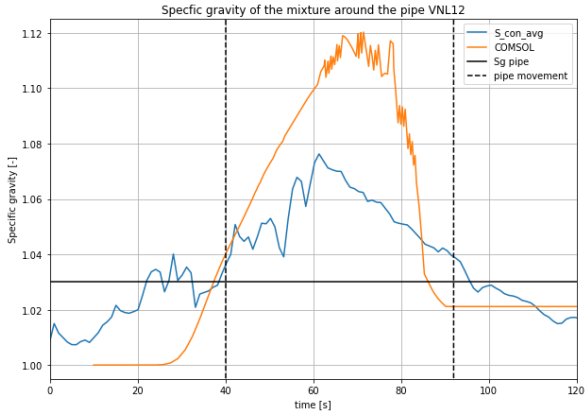

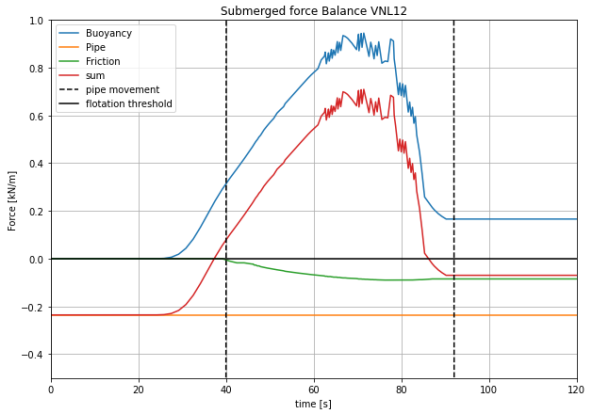

Test VML30		
Parameter	Experimental data	Numerical implementation
Flotation	Yes	Yes
T_{dis}	49[s]	55[s]
C_{dis}	27.5%	9.0%
H_{sol}	0.0404[m]	0.040[m]
H_{sed}	7.5-10[cm]	7.4[cm]

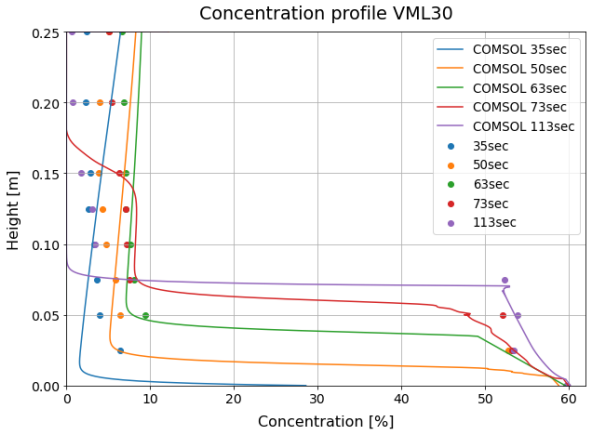

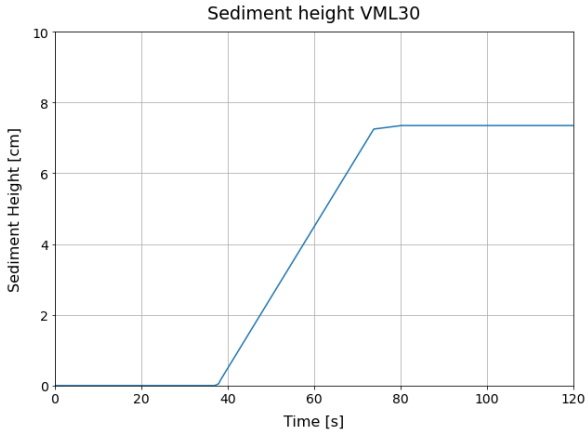

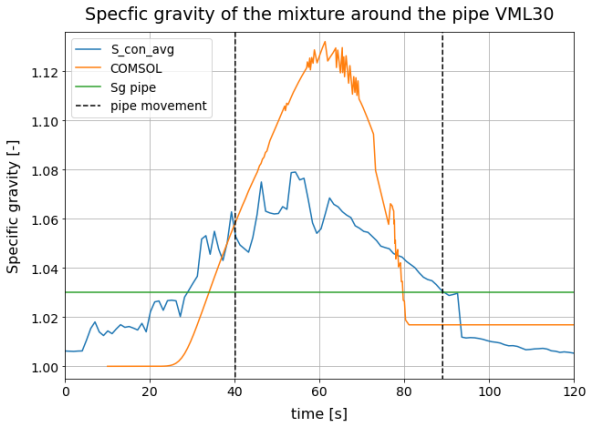

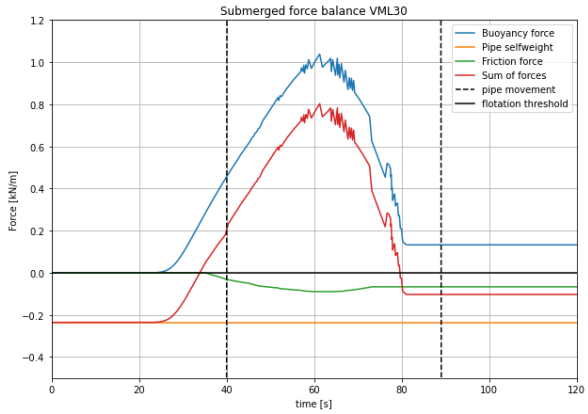

Test VML33		
Parameter	Experimental data	Numerical implementation
Flotation	Yes	Yes
T_{dis}	38[s]	68[s]
C_{dis}	27.0%	7.5%
H_{sol}	0.0361[m]	0.0462[m]
H_{sed}	7.5-10[cm]	8.4[cm]

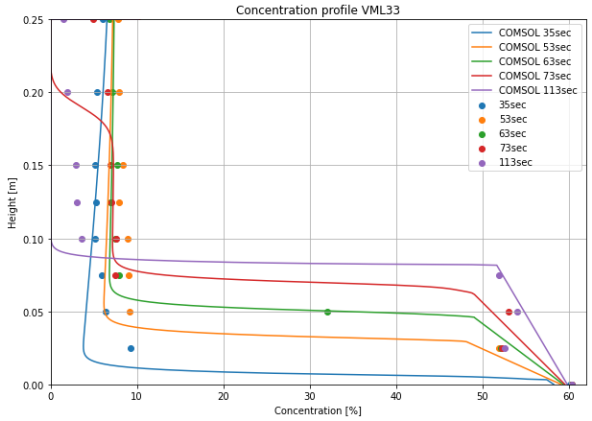

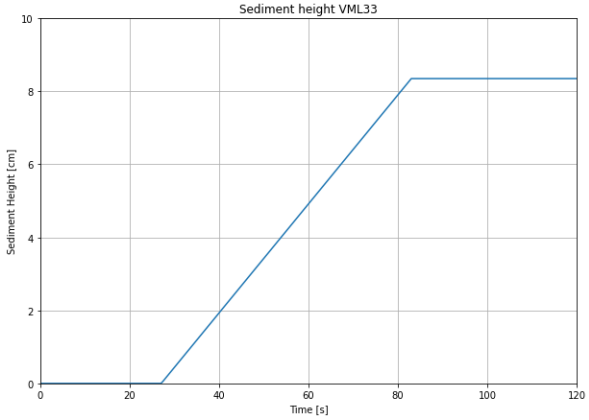

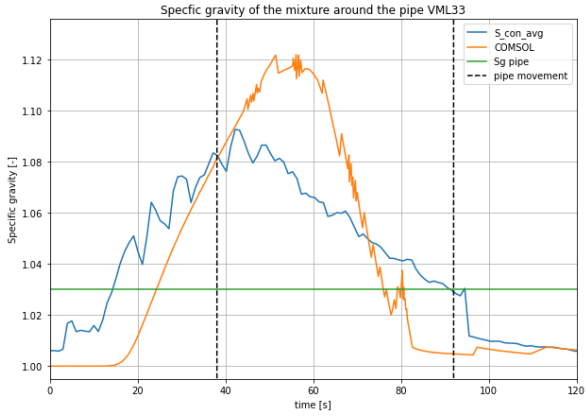

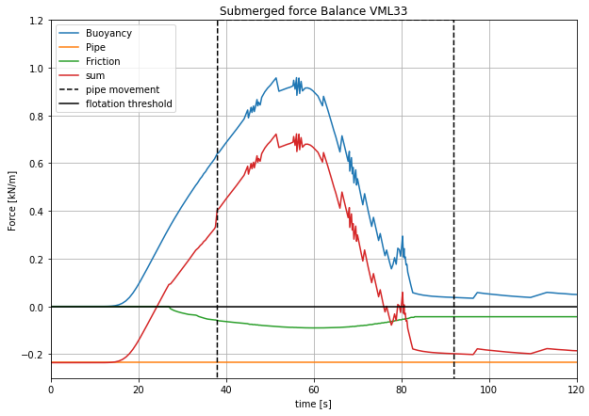

Test VVL39		
Parameter	Experimental data	Numerical implementation inflow
Flotation	Yes	Yes
T_{dis}	67[s]	75[s]
C_{dis}	24.7%	6.7%
H_{sol}	0.0383[m]	0.042[m]
H_{sed}	7.5-10[cm]	7.5[cm]

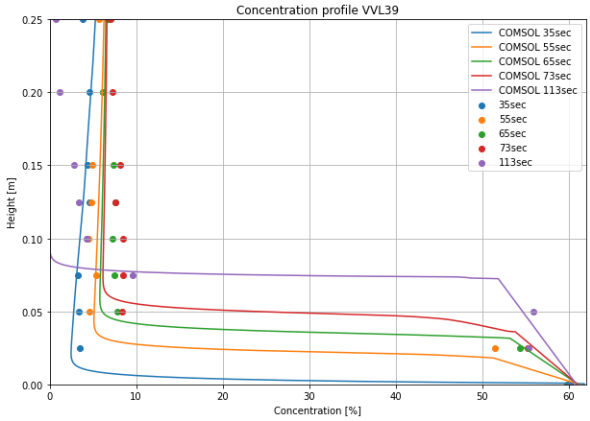

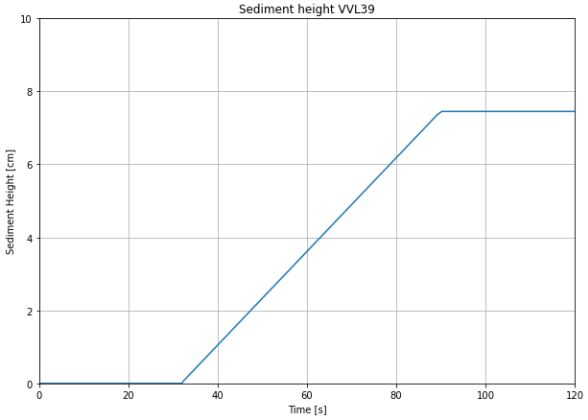

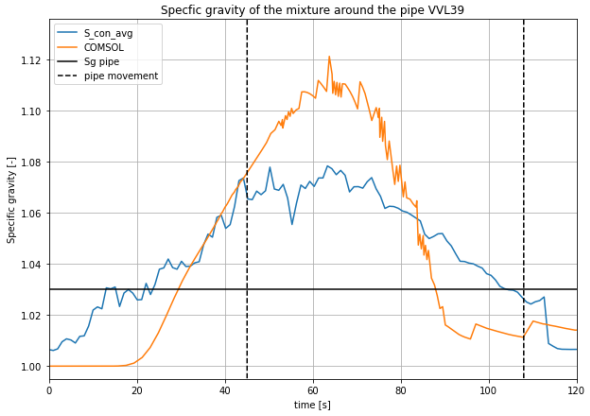

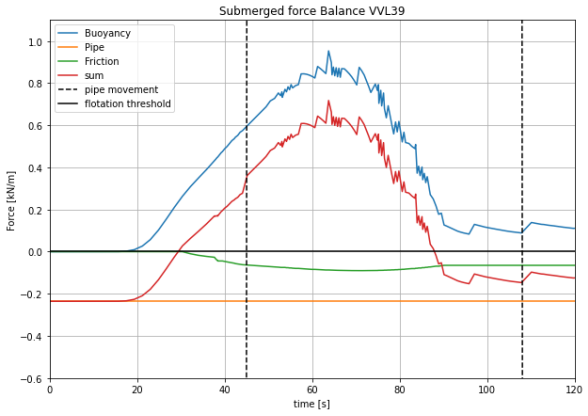

Test VNH47		
Parameter	Experimental data	Numerical implementation
Flotation	No	No
T_{dis}	26[s]	48[s]
C_{dis}	24.0%	7.0%
H_{sol}	0.0241[m]	0.030[m]
H_{sed}	5.0-7.5[cm]	5.4[cm]
SG_p	1.12[-]	1.12[-]

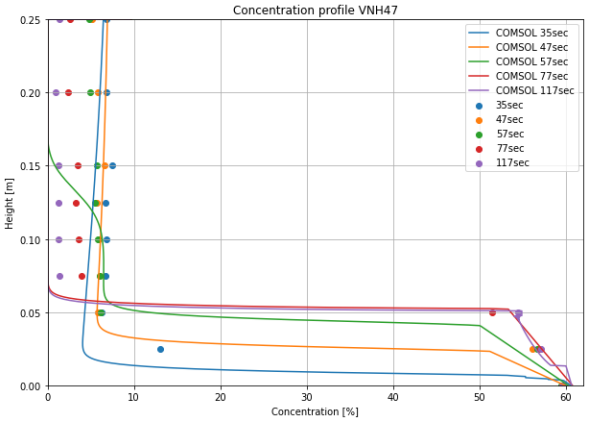

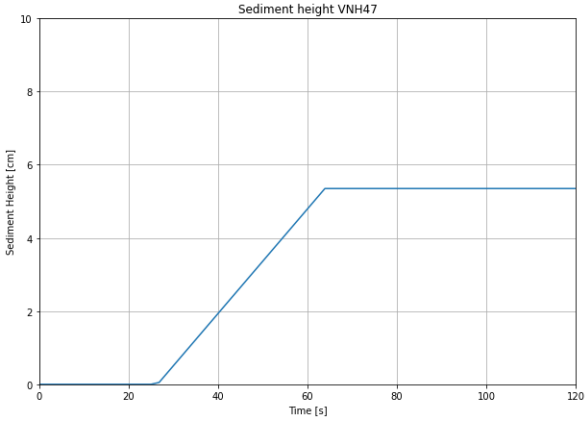

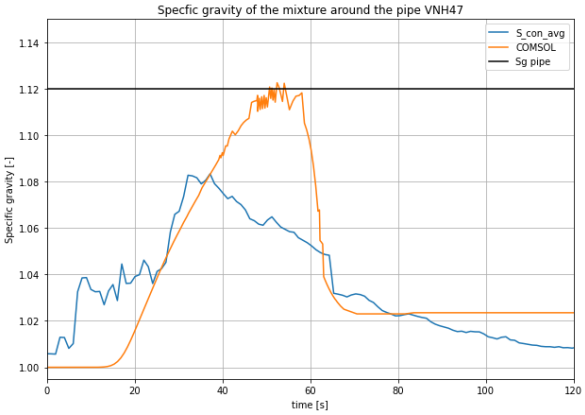

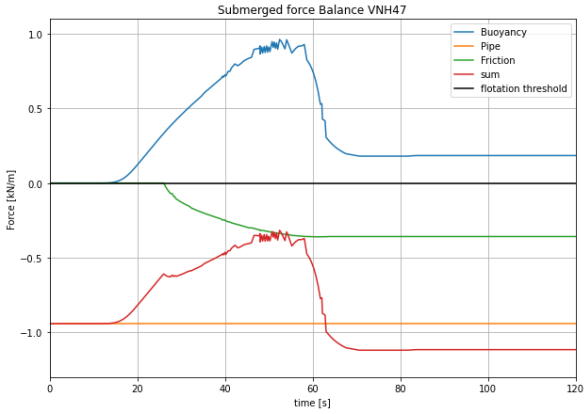

Test VNH50		
Parameter	Experimental data	Numerical implementation
Flotation	No	No
T_{dis}	44[s]	54[s]
C_{dis}	26.4%	7.5%
H_{sol}	0.0265[m]	0.315[m]
H_{sed}	5.0-7.5[cm]	5.5[cm]
SG_p	1.12[-]	1.12[-]

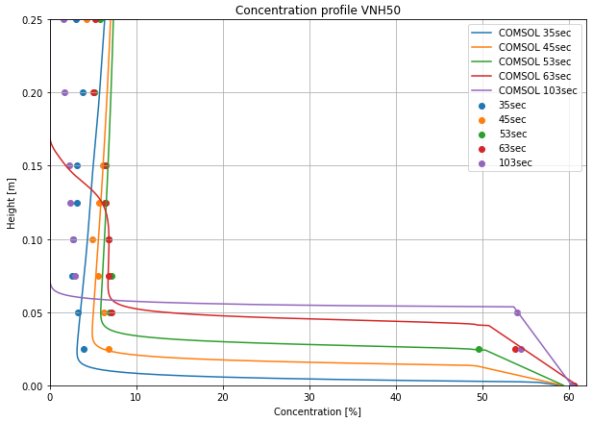

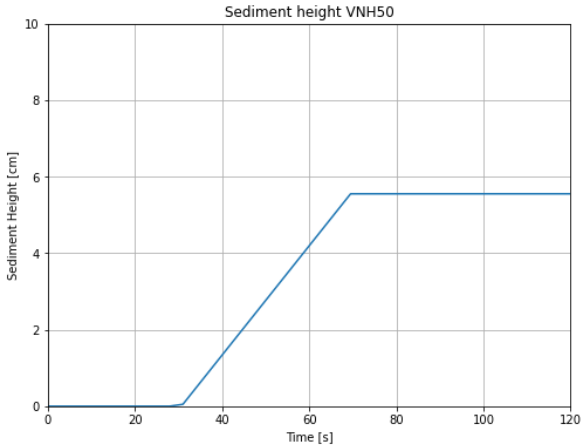

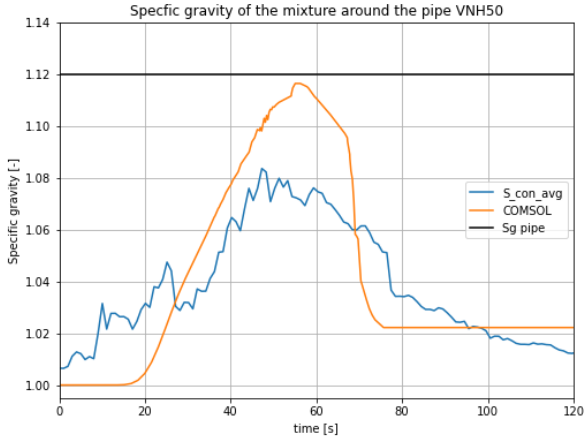

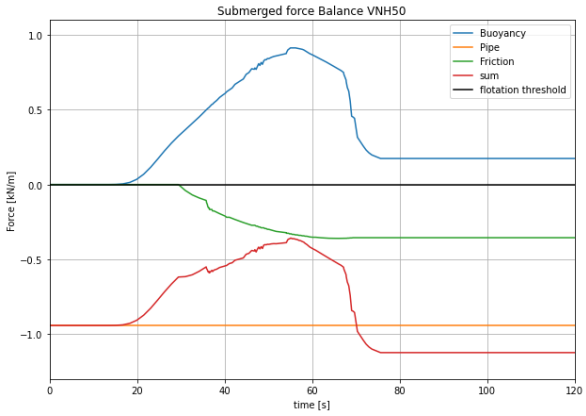

B

Appendix B

In this appendix all the concentration profiles with different hindered settlement exponents are displayed. This analysis has been projected on experiment VML30.

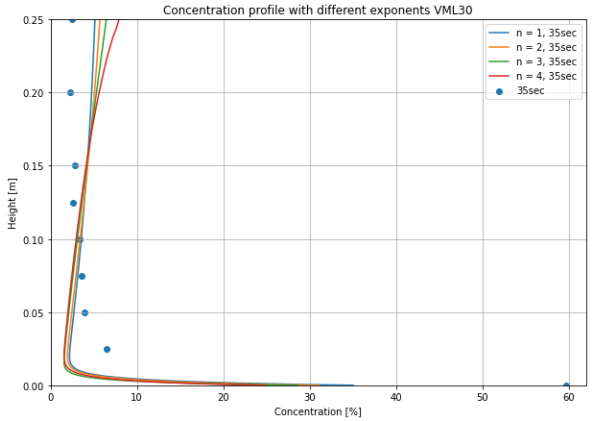
Concentration profile with different exponents VML30
n = 1, 35sec
n = 2, 35sec
n = 3, 35sec
n = 4, 35sec
35sec
Height [m]
Concentration [%]

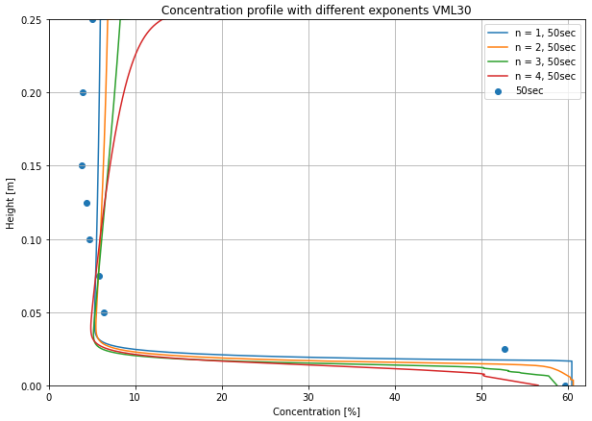
Concentration profile with different exponents VML30
n = 1, 50sec
n = 2, 50sec
n = 3, 50sec
n = 4, 50sec
50sec
Height [m]
Concentration [%]

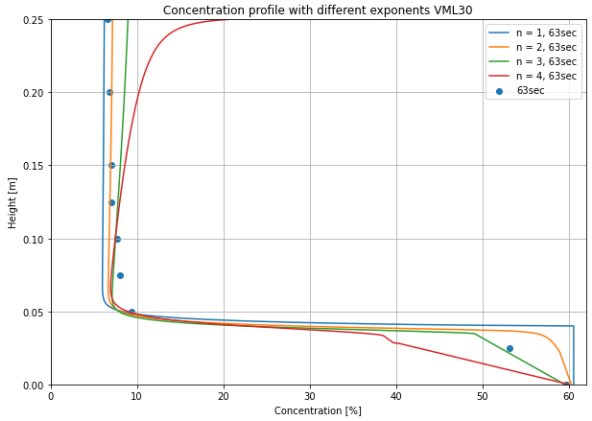
Concentration profile with different exponents VML30
n = 1, 63sec
n = 2, 63sec
n = 3, 63sec
n = 4, 63sec
63sec
Height [m]
Concentration [%]

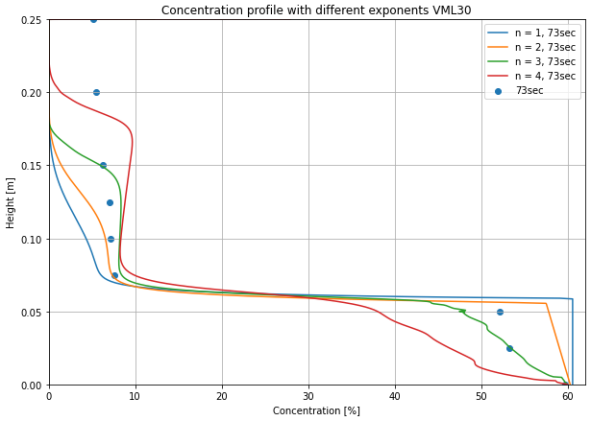
Concentration profile with different exponents VML30
n = 1, 73sec
n = 2, 73sec
n = 3, 73sec
n = 4, 73sec
73sec
Height [m]
Concentration [%]

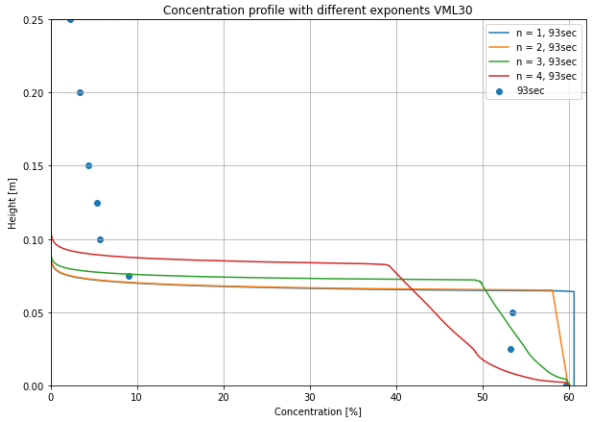
Concentration profile with different exponents VML30
n = 1, 93sec
n = 2, 93sec
n = 3, 93sec
n = 4, 93sec
93sec
Height [m]
Concentration [%]

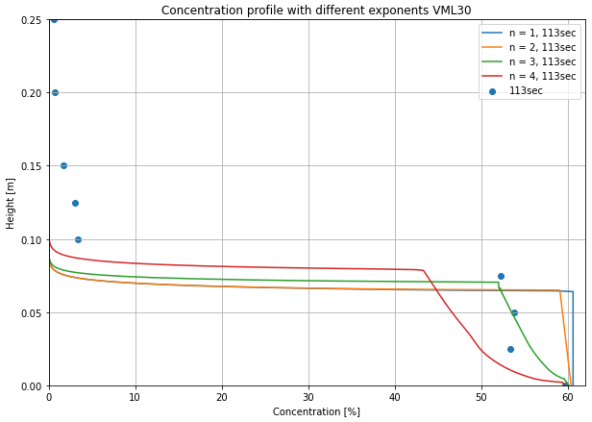
Concentration profile with different exponents VML30
n = 1, 113sec
n = 2, 113sec
n = 3, 113sec
n = 4, 113sec
113sec
Height [m]
Concentration [%]

C

Appendix C

In this appendix results of modelling of the more realistic scenario has been displayed.

C.1. Realistic case, exponent equals 1.0

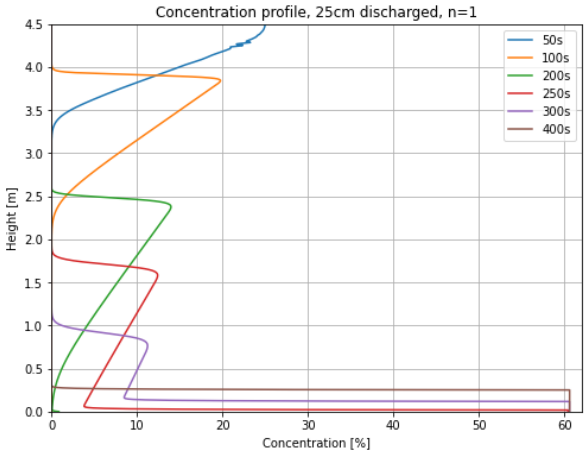

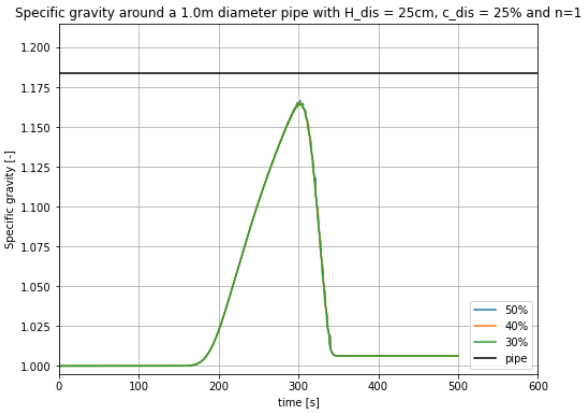

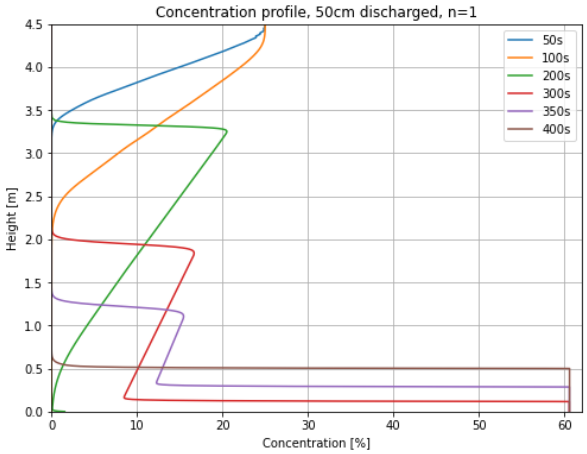

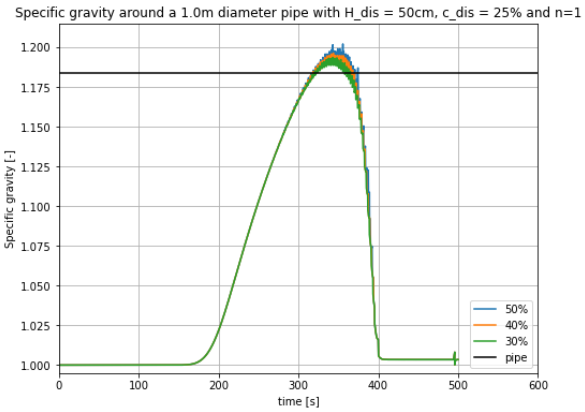

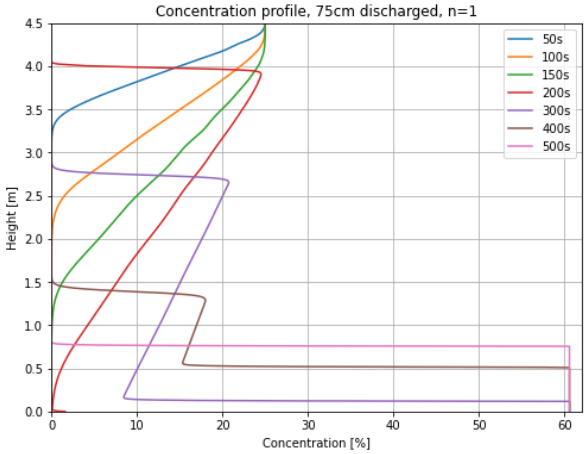

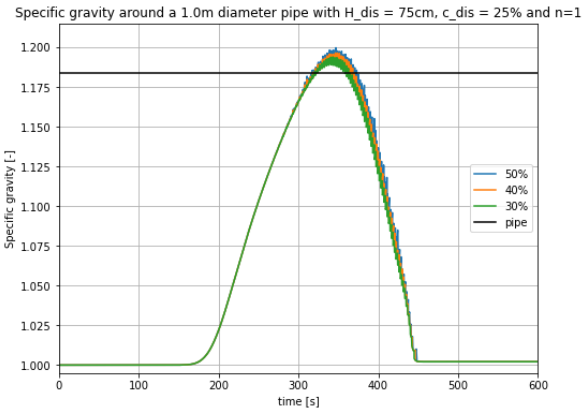

C.2. Realistic case, exponent equals 3.0

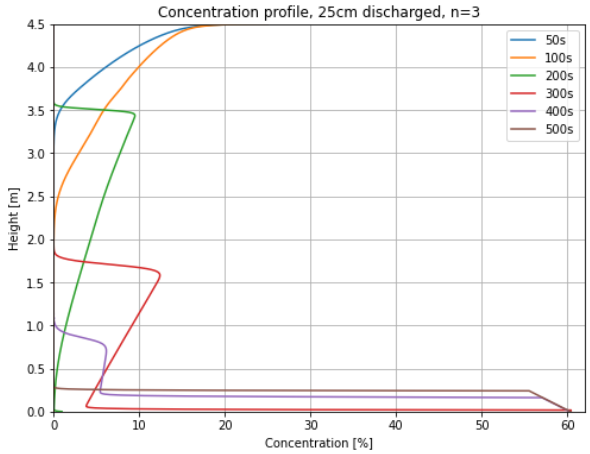

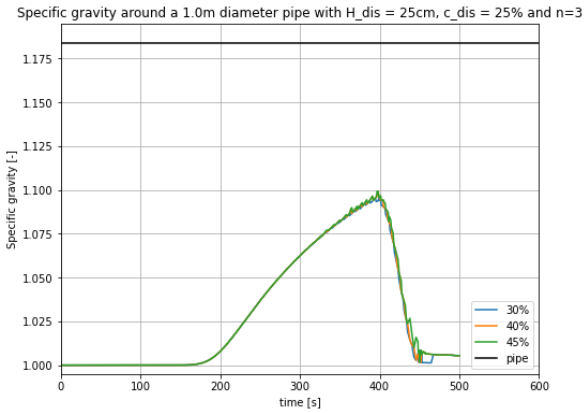

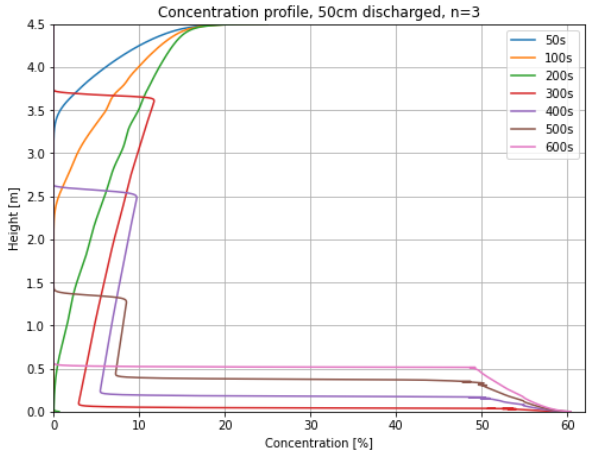

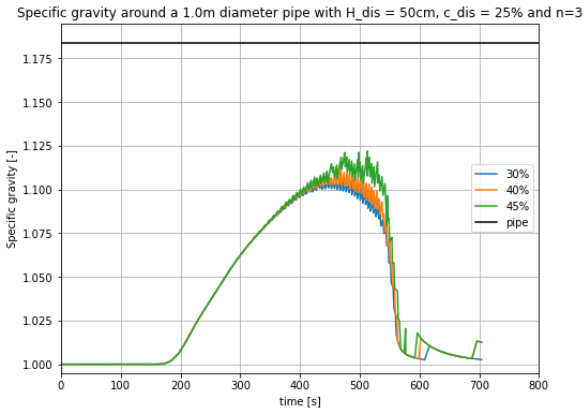

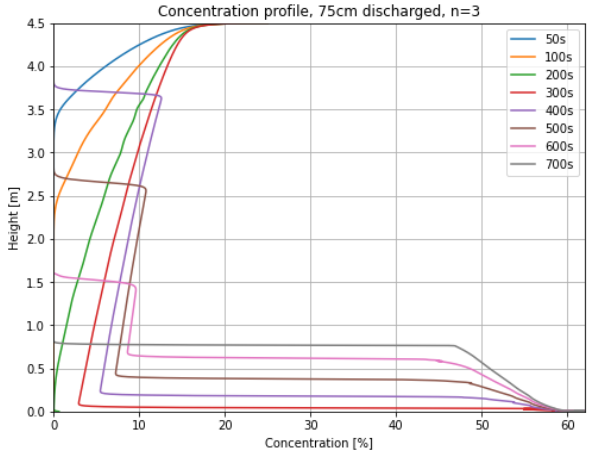

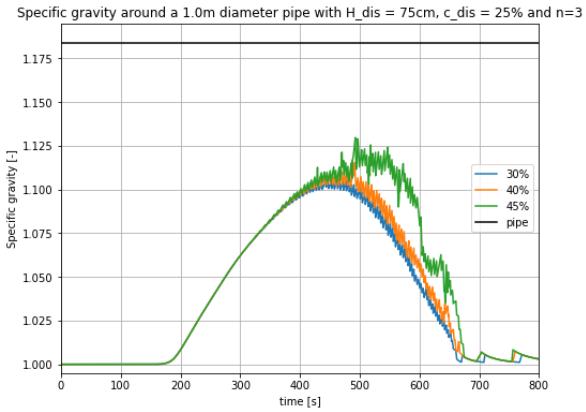

Appendix D

In this appendix the python code for the simplified calculation method is listed. For practical use the segment on experimental data is not relevant.

```
# -*- coding: utf-8 -*-
"""
Created on Tue Oct  4 09:18:30 2022

@author: lennart Stelling
"""

import numpy as np
import math
import matplotlib.pyplot as plt
from collections import namedtuple
import scipy.integrate as spint
from scipy.integrate import odeint
import pandas as pd

# ------- input parameters -----------------------------------------------------
D =0.1                          # Diameter pipe [m]
H_trans = 0.02           # Thickness transition layer [m]
c_domain = 0.04              # Domain concentration
c_phase = 0.40               # Phase transition concentration
vs = 0.018                   # Terminal velocity single grain [m/s]
Max_embedment = 0.075        # Maximum embedment concidered [m]
rho_p = 2650                 # Density particles [kg/m3]
rho_w = 1000                 # Density water [kg/m3]
g = 10                       # Gravitational acceleration
z = 0.25                     # Domain [m] from discharge point to top sand bed

#--------------- Calculation before embedment --------------------------------

vc = vs*(1-1.65*c_domain)**3    # Hindered settling velocity [m/s]
T_top = (z-D)/vc                # time dis_mixture to reach top of the pipe [s]
T_bottom = z/vc              # time dis_mixture to reach bottom of the pipe [s]

fluid = np.linspace(0,D,num=101)
r = D/2
a = (r-fluid)/r
Angle=2*np.arccos(a)
A_tot = np.pi*r**2

Seg_fluid = 0.5*r**2 * (Angle - np.sin(Angle))
Seg_notyet = A_tot - Seg_fluid
rho_fluid = rho_w*(1-c_domain)+ rho_p*(c_domain)
B_fluid = (g*rho_fluid*Seg_fluid) +(Seg_notyet* rho_w * g)
SG_fluid = (B_fluid/A_tot)/(1000*g)
Mix_pipe = (Seg_fluid/A_tot)*100

plt.figure(num=10,figsize=(8,6))
```

```
plt.plot(Mix_pipe,SG_fluid, label='Simplified calculation')
plt.title("Specific gravity as slurry covers the pipe")
plt.xlabel('percentage of the pipe covered by the discharge mixture [%]')
plt.ylabel('Specific gravity [-]')
plt.ylim(1.0,1.08)
plt.xlim(0,100)
plt.grid()
plt.legend()

# ------------ Calculation: SG over embedment ----------------------------------------
c_trans = (c_domain+c_phase)/2
h = np.linspace(0,Max_embedment,num=101)
r = D/2
a = (r-h)/r
P=2*np.arccos(a)
A_tot = np.pi*r**2

Seg_embed = 0.5*r**2 * (P - np.sin(P))
Trans = h + H_trans
a_trans = (r-Trans)/r
P_trans=2*np.arccos(a_trans)
Seg_Trans= 0.5*r**2 * (P_trans - np.sin(P_trans)) - Seg_embed

Seg_rest = A_tot - Seg_Trans- Seg_embed

rho_trans = rho_w*(1-c_trans)+ rho_p*(c_trans)
rho_domain = rho_w*(1-c_domain)+ rho_p*(c_domain)


B_embed = Seg_embed* rho_w * g
B_Trans = Seg_Trans * rho_trans*g
B_domain = Seg_rest * rho_domain * g

B_tot = B_embed + B_Trans + B_domain

SG = (B_tot/A_tot)/(1000*g)

embedment_rate = (h/D)*100

plt.figure(num=1,figsize=(8,5))
plt.plot(embedment_rate,SG, label='Simplified calculation')
plt.title("Specific gravity varying over embedment")
plt.xlabel('percentage of the pipe embeded [%]')
plt.ylabel('Specific gravity [-]')
plt.ylim(1.0,1.14)
plt.xlim(0,80)
plt.grid()
plt.legend()


# ------------ Experimental data ------------------------------------------

path1 =r'C:\Users\lenna\Pipefloatation1\Test33\Concentration_over_time_Test33.xlsx'
Raw_Data_T = pd.read_excel(path1, sheet_name='Sheet1')
T8 = pd.DataFrame(Raw_Data_T, columns=['T'],)
path2 = r'C:\Users\lenna\Pipefloatation1\Test33\Specific_gravity_Test33.xlsx'
Raw_Data_G = pd.read_excel(path2, sheet_name='Sheet1')
Average = pd.DataFrame(Raw_Data_G, columns=['A'],)

path7 = r'C:\Users\lenna\Pipefloatation1\Sediment_Height.xlsx'
Sed_H = pd.read_excel(path7, sheet_name='Height')
SG_VML30 = pd.DataFrame(Sed_H, columns=['SG39'],)
H_VML30 = pd.DataFrame(Sed_H, columns=['H39'],)*0.01
H_real = pd.DataFrame(Sed_H, columns=['Hr'],)*0.01
SG_real = pd.DataFrame(Sed_H, columns=['SGr'],)


SG0 = [1.0,1.0]
Time_offset = 6
T0 = [0, T_top+Time_offset]
T1 = np.linspace(T_top+Time_offset, T_bottom+Time_offset, num=101)
```

```
T2 = np.linspace(T_bottom + Time_offset , 27+ Time_offset, num=2)
T3 = np.linspace(27+ Time_offset, 83, num=101)
T4 = np.linspace(83,101, num=2)
Y2 = [1.066,1.1083]
Y4 = [1.0654, 1.0]


path3 = r'C:\Users\lenna\Pipefloatation1\COMSOL_VML33_2.xlsx'
COMSOL_Data_SG = pd.read_excel(path3, sheet_name='SG')
Time = pd.DataFrame(COMSOL_Data_SG, columns=['T'],)
SG_Comsol = pd.DataFrame(COMSOL_Data_SG, columns=['Sg40'],)

plt.figure(num=11,figsize=(9,7))
plt.plot(T0,SG0, c='k')
plt.plot(T1,SG_fluid, c='k', label = 'Simplified calculation')
plt.plot(T2,Y2,linestyle='dashed', c='k')
plt.plot(T3,SG, c='k')
plt.plot(T4,Y4,linestyle='dashed', c='k')
plt.plot(T8, Average, label='Experimental data')
plt.plot(Time, SG_Comsol, label='COMSOL calculation')
#plt.plot(H_VML30,SG_VML30, label='Numerical Model')
plt.title("Specific gravity of the mixture around the pipe VML33")
plt.xlabel('Time [sec]')
plt.ylabel('Specific gravity [-]')
plt.ylim(0.995,1.150)
plt.xlim(0,120)
plt.grid()
plt.legend()
```